

CONTROLLING THE BEHAVIOUR OF  
QUARTZ SURFACES: USING SILANE  
COUPLING AGENTS TO MINIMIZE  
SURFACE FOULING

**CONTROLLING THE BEHAVIOUR  
OF QUARTZ SURFACES:  
USING SILANE COUPLING AGENTS  
TO MINIMIZE SURFACE FOULING**

By

**AMRO M. RAGHEB**

A thesis

Submitted to the School of Graduate Studies  
in partial fulfillment of the requirements  
for the degree  
Master of Science

McMaster University

©Copyright by Amro Ragheb, April 2001

MASTER OF SCIENCE (2001)	McMASTER UNIVERSITY
(CHEMISTRY)	Hamilton, Ontario

**TITLE:** Controlling the Behaviour of Quartz Surfaces: Using Silane Coupling Agents to Minimize Surface Fouling

**AUTHOR:** Amro M. Ragheb, B.Sc. (Ain-Shams University, Cairo, Egypt)

**SUPERVISOR:** Professor Michael A. Brook

**Number of Pages:** 137

## **Abstract**

UV radiation disinfection technology is an advantageous method of wastewater disinfection as it avoids the formation of chemical by-products typically found from chlorination. One challenge with this technology is avoiding fouling on the quartz sleeves in which the UV lamps are housed. In this study, using a model fouling system, the roles in fouling of light, and the constitution of the fouling media, are examined. The systematic determination of fouling by various mixtures of human serum albumin, humic acid,  $\text{Ca}^{2+}$ , and  $\text{Fe}^{3+}$  was carried out on quartz slides in the presence and absence of UV (254nm) light. Fouling was assessed by the reduction in transmission of UV light through the quartz slides over time. It was determined that the most important factors were the concentration of iron and protein, which apparently act synergistically to foul the surface. Other contributing factors to the magnitude of fouling include the flow rate and the age of the fouling solution. Most important was the presence of UV light. In all solutions examined, fouling was observed to a lower degree when the system was exposed to light. On the other hand, XPS analysis has demonstrated differences in the nature of the fouling layer on the surface exposed to UV light compared to that in the dark.

It is generally accepted that low energy surfaces are less easily fouled than polar surfaces. Therefore, hydrophobic modification of the quartz by a series of different silane coupling agents was undertaken. Irrespective of the nature of the coating (alkylamine, alkyl, aryl, fluorocarbon, silicone), the rate and magnitude of fouling on the surface were comparable to the unmodified quartz. However, the more hydrophobic surfaces were easier to clean.

## **Acknowledgements**

I would like to express my gratitude to my parents and family, who supported me along the road, and have been always a sparking light in my life with their love and deep understanding and sacrifice. I also owe my friends a lot for their support and their faith in me, even when it seems that I have lost that faith. Their support, tenderness, understanding and help will never be forgotten.

Special thanks should go for my supervisor, Dr. Brook, who taught me how a man can provide a limitless understanding and patience and how the energy would be generated to extend the mind horizon toward exploring the unknown and hidden knowledge. His efforts will be always alive in my mind no matter how far my life trip would go. I also would like to acknowledge all my professors in McMaster University, who provided me with a tremendous support, help and understanding that I will always remember. Mrs. Dada deserves a special gratitude for her deep support and all the help that she provides to the graduate students' community that I was lucky to belong to.

I also will never forget my colleagues who were able to provide a supportive environment, with a special thank goes for Jannine Crowley for her valuable help to bring this work alive and for her patience during her work under my command, which was indeed a hard mission. Finally, I will always be grateful for those who gave me the chance to learn, explore the unknown and go beyond limits. I promise them not to let them down, ever.

## Table of Contents

Abstract	iii
Acknowledgements	iv
Table of Contents	v
Figures	ix
Schemes	xi
Tables	xi
<b>1. INTRODUCTION</b>	<b>1</b>
<b>1.1. Fouling phenomena</b>	<b>1</b>
<b>1.2. Fouling Types</b>	<b>2</b>
1.2.1. Biofouling	3
1.2.2. Crystallization fouling	8
1.2.3. Particulate fouling	10
<b>1.3. Interactive effects of different fouling types</b>	<b>13</b>
<b>1.4. Mitigation methods for fouling</b>	<b>14</b>
1.4.1. Physical mitigation methods	14
1.4.2. Chemical Mitigation	15
1.4.3. Chemical Modification of Surfaces	17
<b>1.5. Siliceous surfaces</b>	<b>19</b>
1.5.1. The Nature of Siliceous Surfaces	19
1.5.2. The isoelectric point of siliceous surfaces.	20
1.5.3. Physical Adsorption on siliceous surface	21
1.5.3.1. Absorption of Ions	21
1.5.3.2. Adsorption of organic cations and bases on silica	22
1.5.3.3. Adsorption of organic polymers on siliceous surface	23
1.5.3.4. Protein adsorption	24

1.1.1.5. Methods for siliceous surface modification	26
1.1.4. Silane coupling agents in surface modification	27
<b>1.6. UV Disinfection of Water</b>	<b>30</b>
<b>1.7. Objectives</b>	<b>31</b>
<b>1.8. References</b>	<b>32</b>
<b>2. THE ROLE OF UV LIGHT IN THE FOULING OF QUARTZ SLEEVES USED IN WATER DISINFECTION</b>	<b>39</b>
<b>2.1. Abstract</b>	<b>39</b>
<b>2.2. Introduction</b>	<b>39</b>
<b>2.3. Experimental section</b>	<b>41</b>
2.3.1. Chemicals	41
2.3.2. Equipment	42
2.3.2.1. Fouling Reactor	42
2.3.2.2. Fouling Protocol: Measuring UV Transmittance	44
2.3.2.3. X-ray Photoelectron Spectroscopy (XPS) of Fouled Surfaces	45
2.3.2.4. Foulants Examined	46
<b>2.4. Results</b>	<b>48</b>
2.4.1. Fouling Experiments	49
2.4.1.1. Individual Contaminants	49
2.4.1.2. Mixtures of Foulants	50
2.4.2. Visualization of Fouled Slides	54
2.4.3. Characterization of Fouled Slides	57
2.4.3.1. Aged Solution Experiment	59
2.4.4. Effect on of Flow Rates on Fouling	60
<b>2.5. Discussion</b>	<b>61</b>
2.5.1. Mitigating Effect of $\text{Ca}^{2+}$ in $\text{Fe}^{3+}$ / $\text{Ca}^{2+}$ Mixtures	62
2.5.2. Interactions of Humic Acid with Multivalent Ions Including Iron and Calcium	62

2.5.3. Complementary Interactions of Fe <sup>3+</sup> and HSA	64
2.5.4. Fe/HSA/humic acid	65
2.5.5. Nature of the Fouling Layer	65
2.5.6. Aging	67
2.5.7. Temporal Dependence of Fouling	68
2.5.8. Flow Rate	69
<b>2.6. Conclusions</b>	<b>70</b>
<b>2.7. Acknowledgments</b>	<b>70</b>
<b>2.8. References</b>	<b>71</b>
<b>3. THE ROLE OF HYDROPHOBIC COATINGS ON QUARTZ SLEEVES IN THE MITIGATION OF FOULING BY WASTEWATER STREAMS</b>	<b>75</b>
<b>3.1. Abstract</b>	<b>75</b>
<b>3.2. Introduction</b>	<b>76</b>
<b>3.3. Experimental section</b>	<b>78</b>
3.3.1. Surface modification protocol	78
3.3.1.1. Preparation of the Quartz Slides	78
3.3.1.2. Surface Modification by Coupling Agents	78
3.3.2. Silicones Crosslinked on the Surface	79
3.3.3. Fouling experiments	81
3.3.4. Cleaning of Fouled Slides	82
3.3.5. Optical Microscopy	83
3.3.6. X-ray Photoelectron Spectroscopy (XPS) of Fouled Surfaces	83
<b>3.4. Results</b>	<b>84</b>
3.4.1. Surface Modification and Fouling Experiments	84
3.4.2. Surface Characterization of Fouled Slides	91
3.4.3. Cleaning of Fouled Slides	96
<b>3.5. Discussion</b>	<b>97</b>
3.5.1. Temporal Dependence of Fouling: Interfoulant Adhesion	97

3.5.2. Cleaning and Drying: Fouling Layer/Surface Adhesion	98
3.5.3. Implications of these Studies on Fouling of UV-Reactors	100
<b>3.6. Conclusions</b>	<b>101</b>
<b>3.7. Acknowledgment</b>	<b>101</b>
<b>3.8. References</b>	<b>102</b>
<b>4. CONCLUSIONS AND FUTURE WORK</b>	<b>106</b>
<b>5. APPENDIX (OXIDIZABLE COUPLING AGENTS: INTRODUCTION OF SURFACE FUNCTIONALITY)</b>	<b>109</b>
<b>5.1. Abstract</b>	<b>109</b>
<b>5.2. Introduction</b>	<b>110</b>
<b>5.3. Experimental Section</b>	<b>112</b>
5.3.1. Materials	112
5.3.2. Instrumentation	113
5.3.3. Preparation of Coupling Agents	114
5.3.3.1. Synthesis of 2-(Phenyldimethylsilyl)ethyltriethoxysilane	114
5.3.3.2. Synthesis of bis(trimethylsiloxy)-methyl-(3-triethoxysilylpropyl)silane	115
5.3.3.3. Synthesis of 1,1,3,3-Tetramethyl-1((2-triethoxysilyl)ethyl)disiloxane	116
5.3.3.4. Synthesis of Methyl(2-triethoxysilyl-ethyl)siloxane Homopolymer	118
5.3.3.5. Synthesis of Methyl(2-triethoxysilyl-ethyl)dimethylsiloxane Copolymer (30-35%):	118
5.3.3.6. Hydrosilylation of Squalene	119
5.3.3.6.1. By $\text{HMe}_2\text{SiOSiMe}_3$	119
5.3.3.6.2. By $\text{HSi(OEt)}_3$	121
5.3.3.6.3. By $\text{HMe}_2\text{SiO(CH}_2)_3\text{Si(OEt)}_3$	121
5.3.3.6.4. Oxidation Experiments: Reactions on 4-grafted quartz slides	122
5.3.3.6.4.1. Ozonization	122
5.3.3.6.4.2. Reduction and coupling with DNPH:	122

5.3.4. Modification of the slides – Application of the coupling agent.	123
5.3.4.1. Hydrosilylated squalene	124
<b>5.4. Results</b>	<b>125</b>
<b>5.5. Discussion</b>	<b>132</b>
<b>5.6. Future Work</b>	<b>135</b>
<b>5.7. Conclusions</b>	<b>136</b>
<b>5.8. References</b>	<b>137</b>
<b>6. Appendix ii anticipated publication and co-authors</b>	<b>138</b>

## Figures

Figure 1: Microbial Biofouling Mechanism: (1) Surface Conditioning, (2) Bacteria Cells Attachment And (3) Exopolymer Formation	6
Figure 2: Energy-Distance Curves	12
Figure 3: The Effect Of Solution Concentration On The Adsorption Of Cationic Species On Siliceous Surfaces	23
Figure 4: Modification Of Siliceous Surface Using Octanol	26
Figure 5: Applying Silane Coupling Agents From Organic Solvent To Modify The Surface.	29
Figure 6: Simplified Diagram For Uv Wastewater Disinfection System.	31
Figure 7: Fouling Reactor	43
Figure 8: Individual Fouling Experiments In The Presence And Absence Of UV Light Using A: $Fe^{3+}$ (10 Mg/L), $Ca^{2+}$ (140 Mg/L), And B: HSA (100 Mg/L) And Humic Acid (50mg/L).	50
Figure 9: $Fe^{3+}$ (10 Mg/L) And A: Humic Acid (50 Mg/L); B: HSA (50mg/L).	52
Figure 10: Ternary And Quaternary Mixtures Of $Fe^{3+}$ (5 Mg/L), HSA (50 Mg/L), Humic Acid (50 Mg/L) And $Ca^{2+}$ (100 Mg/L)	53
Figure 11: $Fe^{+3}/Ca^{+2}$ A: In The Dark And B: UV	55
Figure 12: $Fe^{3+}$ /Humic Acid A: In The Dark And B: Under UV	56
Figure 13: $Fe^{3+}$ (10 Mg/L) / HSA (100mg/L) A: In The Dark And B: UV	57

Figure 14: Raw And Normalized (Norm) XPS Data From Dark And UV-Exposed Quartz Slides Exposed To The Quarternary Mixture (Fe/Ca/Humic Acid/Hsa).	58
Figure 15: Fouling Of Quartz By An Fe/Ca/Humic Acid/Hsa Mixture As A Function Of Fouling Solution Age	59
Figure 16: Fouling By Several Different Foulants Fouling At Solution In Two Different Flow Rates	60
Figure 17: Modification Of Quartz Slides	80
Figure 18: Fouling Reactor	86
Figure 19: Transmittance% <i>Versus</i> Time For Fouling By Fe <sup>3+</sup> (10 Mg/L), And Humic Acid (50 Mg/L) In The Absence And Presence Of Uv Light (254 Nm).	87
Figure 20: Transmittance % <i>Versus</i> Time For Fouling Of A: 3-5-Modified Slides By Fe <sup>+3</sup> (10 Mg/L), Hsa (100 Mg/L), And B: 6-Modified Slides By Fe <sup>+3</sup> (5 Mg/L), Hsa (50 Mg/L), Humic Acid (50 Mg/L) In The Absence And Presence Of Uv (254 Nm)	87
Figure 21: Transmittance% <i>Versus</i> Time For Fouling By Fe <sup>3+</sup> (5 Mg/L), Hsa (50 Mg/L), Ca <sup>2+</sup> (100 Mg/L) In The Absence And Presence Of Uv (254 Nm). A: 7-9, Quartz; B: 10, Quartz.	89
Figure 22: Modified Slides Tested In Fe <sup>+3</sup> (5 Mg/L) / Ca <sup>+2</sup> (100 Mg/L) / Humic Acid (50 Mg/L) / Hsa (50 Mg/L) Solution. A: 11,12,Quartz; B: 9a, 13, 14, Quartz.	91
Figure 23: Micrographs Of Partially Dried Fouled Films (Fe/ Hsa) A: Quartz – Uv; B: Quartz.	92
Figure 24: Micrographs Of Partially Dried Fouled Films (Fe <sup>+3</sup> / Hsa) A: 5-Uv; B: 5-Uv.	92
Figure 25: Micrographs Of Partially Dried Fouled Films (Fe <sup>+3</sup> / Hsa) A: 3-D; B: 5-D.	93
Figure 26: A: Slides Fouled By Fe <sup>3+</sup> And Humic Acid. A: 2-Uv; B: 2-D.	93
Figure 27: Low Resolution Xps Data Of Several Slides Fouled By Fe <sup>3+</sup> /Ca <sup>2+</sup> /Humic Acid/Hsa.	94
Figure 28: Xps Data Excluding Sio <sub>2</sub> (Quartz). Calcium Values Are Shown 10 Times Actual Value.	95
Figure 29: Effect Of The Cleaning Process On Slide Transmittance In Fe <sup>+3</sup> (10 Mg/L) / Hsa (100 Mg/L)	97
Figure 30 Cracking Process	100
Figure 31: Uv Spectra Of Dinitrophenylhydrazine, And Squalene After Ozonization/Reduction By Zn/Hoac And Dinitrophenylhydrazine.	130
Figure 32: Uv Transmittance Through A Quartz Slide Modified With 18, Ozonized And Reacted With 2,4-Dinitrophenylhydrazine.	131

Figure 4: UV Spectra Of A: Squalene And B: 4 Showing Presence Of Diene Fragments In The Latter Material.	133
--	-----

## Schemes

Scheme 1: Surface Modification With Chlorosilane	30
Scheme 2: Models Of Humic Acid Interaction With The Quartz Surface/Fouling Layer.	64
Scheme 3: Crosslinking Polydimethylsiloxane By Hydrosilylation On Functionalized Quartz Surface With Vinyltriethoxysilane	86
3.4.1.1. Scheme 4: Hydrosilylation Of Squalene Using Synthesis Of 1,1,3,3-Tetramethyl-1((2-Triethoxysilyl)Ethyl)Disiloxane	90
Scheme 5: Oxidation Reactions Of Squalene.	112
Scheme 6: Hydrosilylation Of Vinyltriethoxysilane With 1, 1, 2, 2 Tetramethyl-Disiloxane	116
Scheme 7: Synthesized Silane Coupling Agents.	126
Scheme 8: Hydrosilylation Of Squalene Using Pentamethyldisiloxane.	127
Scheme 9: Hydrosilylation Of Squalene Using 1,1,3,3-Tetramethyl-1((2-Triethoxy-Silyl) Ethyl) Disiloxane.	128
Scheme 10: Oxidation For Introducing New Functionality To Squalene Molecule.	129
Scheme 11: Ozonization/Reduction Reaction Of Grafted Quartz Surface With Squalene Followed By Coupling With Dinitrophenylhydrazine.	131
Scheme 12: Internal Bond In Hydrosilylation.	132
Scheme 13: Diene Formation In Squalene Hydrosilylation Reaction.	133
Scheme 14: Amine Reaction With An Epoxidized Squalene-Modified Surface.	136

## Tables

Table 1: Foulants Used In Fouling Experiments	47
Table 2: Chemical Modification Of Quartz Slides Surface Examined In Fouling Experiments.	80
Table 3: Chemical Composition Of Fouling Solutions In Fouling Experiments With Modified Slides.	82

Table 4: Commercial And Synthesized Silane Coupling Agents Used In Quartz And Glass Surface Modification.

# **1. Introduction**

## **1.1. Fouling phenomena**

Fouling phenomena are well known in various fields in our life. For example, fouling is found in heat exchange systems, cooling towers, water deionizers, pipelines, filters beds, calorimeters, the surfaces of ships' hulls, in food industries, domestic central heating systems, and even on our teeth.<sup>1,2</sup> Fouling is expected wherever an "interface" exists between two different phases. It is more pronounced at solid/liquid interfaces but also found, to a lesser degree, at solid/gaseous phase interfaces. The fouling of aqueous systems and the concomitant decrease of efficiency in energy utilization provides a major impetus for studying fouling processes. Most industries depend on water either as a chemical fluid in the reactions or alternatively as a heat exchange fluid that can be used in both cooling and heating systems. The limited resources of pure water and the growing demands for water have pushed forward the concept of "cycling" water in chemical processes. This term is not confined to waste-water treatment, but also relates to minimizing the amount of water used in industrial complexes. In order to achieve maximum efficiency from a process using water as a heat transfer fluid, there should be little resistance to heat exchange, flow rate, and clean surfaces should be maintained (this shall be dealt with in more detail below). This thesis will deal with understanding and controlling the nature of fouling on quartz surfaces.

The general definition of fouling is, “The process of gradual deposition of particulate material onto solid surfaces.”<sup>3</sup> This can include organic, inorganic and biofouling. The processes involved in fouling are discussed in more detail below. Two major approaches emerge in dealing with fouling phenomena. One strategy focuses on understanding fouling phenomena in a chemical sense through adhesion and adsorption. The other trend deals only with the symptoms of the problem and attempts to minimize the negative effects of fouling.

The study of fouling is complicated by the number of parameters involved. Different industrial sites have different types of foulants, and thus, different experiences with fouling: foulants can interact synergistically. Many efforts have been made to mimic the fouling process under controlled conditions using laboratory scale models.<sup>4,5</sup> These studies provide valuable information about the processes involved if the models are developed in conjunction with good characterization methods for the fouled surface, especially online characterization methods.<sup>2</sup> The development of model fouling systems is one of the objectives of this thesis.

## **1.2. Fouling Types**

Fouling phenomena may be broadly categorized into several classes: “crystallization”<sup>6,7</sup> or “precipitation” is fouling due to the deposition or the formation of (usually inorganic) crystals from solution onto a surface; “particulate fouling” is the accumulation of suspended solid particles from the fluid stream on the surface;<sup>3</sup> “chemical reaction fouling” describes the formation of a surface deposit resulting from

one or more chemical reactions between reactants contained in the flowing fluid; “corrosion fouling” where the surface itself is the source of the foulant and, finally; “freezing or solidification fouling”, which is attributed to the freezing of the process fluid itself on the surface. A different, very important type of fouling is biological fouling or “biofouling”, defined as “the deposition or growth of materials of biological origins”<sup>1,2,8</sup> including the attachment and metabolism of microorganisms like algae, bacteria and fungi (microbial fouling) on surfaces<sup>9</sup> or higher organisms such as sea-weed and barnacles (macrobial fouling). This thesis focuses on three of these fouling processes: biofouling, crystallization and precipitation fouling. Note that two or more types of fouling can occur simultaneously with natural and process waters.<sup>6,10</sup>

### **1.2.1. Biofouling**

Biofouling is one of the most important types of fouling. There is some dissention in the literature regarding the limitations of this class of fouling. One of the definitions for biofouling is, “The development of a colony of microorganisms embedded in a matrix of an organic polymer film formed on the surface.”<sup>6</sup> A broader definition considers biofouling as, “The deposition or growth of materials of biological origins.”<sup>1,6</sup> In this definition both living and dead biological materials are considered biofoulants as long as their metabolism byproducts still exist at the interface of the phases. Thus, the deposited materials may include microorganisms (e.g., bacteria, algae, diatoms, and yeast) and their constituents and metabolic products. When developed, this usually will take the form of the film or layer termed a “biofilm”. When higher organisms such as water-weeds,

seaweed and barnacles are involved in forming such a film, the deposits are then known as “macrobial fouling”. If the film left long enough, both types of biofouling can exist on the fouled surface.

Many studies have been done to explore the nature of biofouling processes and also the nature of the resulting biofilm. In these studies, extensive efforts were devoted to studying the microbiological aspects of the process, and the factors that affect the viability of the organism(s) in such environments. The complex nature of biofilms may more properly be considered the key point in understanding the steps of biofouling.

One of the known constituents of the biofilm caused by bacteria is a highly hydrated polysaccharide-like slime, which is termed now as glycocalyx.<sup>11,12</sup> It is very important to realize that the adhesion of these polysaccharides is not always a result of bacterial adhesion on a surface. That is, these polysaccharides can be found on the surface even if the bacteria itself does not form colonies there.<sup>13</sup> As well, work done by McEldowney and Fletcher showed clearly that other materials, such as protein-containing materials, can work as mediators on the surface to assist the bacterial adhesion.<sup>14</sup> These studies indicate the importance of surface conditioning step in understanding biofouling and fouling phenomena in general.

The mechanism of biofouling was discussed by Characklis in detail and the proposed mechanism can be summarized as followed:<sup>15</sup>

- 1) Development of polymeric film on the surface over a short time, which is responsible for changing surface properties (conditioning of the surface, Figure 1).

- 2) Deposition of single-cell microorganisms (bacteria) with a transient state that involves the attachment and detachment of individual organisms at the interface. This transient state is considered a reversible process in which long-range forces hold the cells near the surface, but shear forces can easily remove the cells.<sup>16</sup>
- 3) Colonization of the surface by the deposited single-cell microorganism(s). This step is known as to be an irreversible step and usually characterized by the synthesis of the extra-cellular polymers that bind the cells to the surface.<sup>17</sup>
- 4) Secondary deposition of higher level of microorganisms, which now can find a suitable environment on the surface for adhesion and survival. In other words, the complex biofilm developed by the colonization of bacteria can act now as a precursor for the deposition of higher levels of microorganisms and submicron-size particulates.<sup>6</sup>
- 5) Sloughing off of the film from the surface as the growth of the biofilm further develops. This is affected mainly by the shear forces at the interface and depends upon the nature of the formed film on the surface.

Before further discussing some of the factors that affect biofouling, it is useful to point out that fouling process is considered to be the net result of deposition and removal processes of the materials on the surface as pointed out by Characklis.<sup>15</sup> That is, when one discusses factors affecting fouling, both processes must be considered. Some of these factors include surface and fluid temperature, fluid velocity, surface characteristics,

nutrient concentration, fluid pH and finally the presence of inorganic materials, especially inorganic suspended particles.

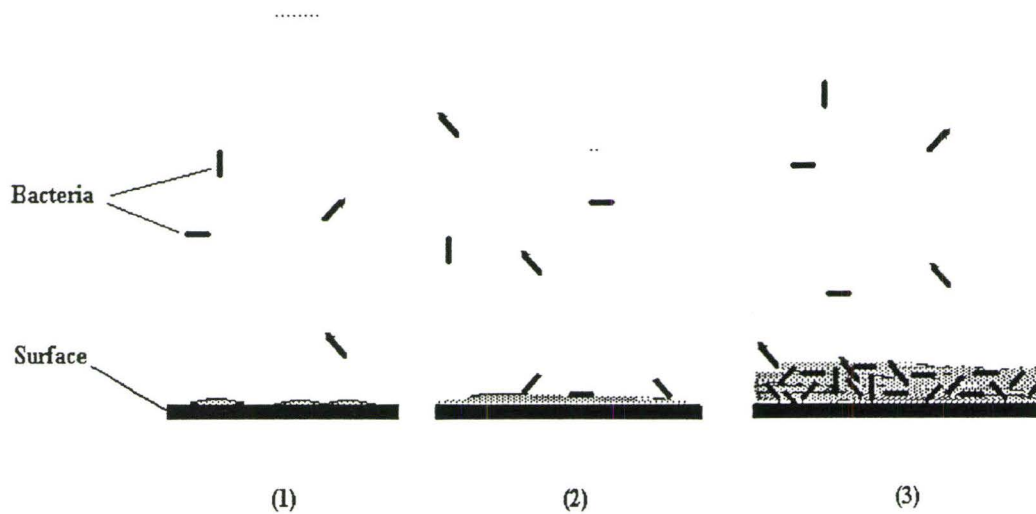


**Figure 1 Microbial biofouling mechanism: (1) surface conditioning, (2) bacteria cells attachment and (3) exopolymer formation**

Fluid temperatures can affect the growth of the living microorganisms in the fluid and on the surface as well; this will obviously impact on the extent of surface biofouling. Experiments done in evaluating the temperature effect on biofouling have revealed that there is an optimal range of temperature for the growth for every species of microorganism, and the thickness of the biofilm is sensitive to the temperature of both the fluid and the surface.<sup>18</sup> One of the expected results of the temperature variation is the concomitant variation in the production of exopolymers by the cells, which affects the nature of the formed biofilm and its detachment process.

Fluid velocity can impact biofouling through many ways. The fluid flow is considered important in terms of providing the bacterial colonies with the necessary nutrients and the removal of the metabolism by-products that can act as poisons,<sup>19</sup> hence increasing the extent of biofouling. On the other hand, high fluid velocity can enhance the sloughing process of the developed biofilm. Moreover, with very high fluid velocity, a compact deposited layer can be obtained that retards the diffusion of nutrients through the deposited layer, negatively affecting the growth of the organism. In other words, cell growth may be increased in presence of higher fluid velocities, but for much higher velocities the “active” layer becomes limited to the superficial layer of the deposit.<sup>20</sup>

Surface characteristics are important in the initial stage of fouling when the first layer of biofilm is established. In fact, the formation of the organic conditioning film, which starts the adhesion of the first layer of deposit on the surface, is indeed dependent on the critical surface tension of the surface<sup>20</sup> which can be defined as the energy required to form a unit area of the interface. Most engineering materials (including glass materials) demonstrate a high capacity for adsorbing the first layer of the biofilm.

Surface roughness is another property that can affect the adsorption process primarily at the initial stages. It is accepted that a high surface roughness favors the anchorage of microorganisms to the surface because of the higher contact area. However, this effect is less important once the surface is conditioned by the first layer.

The effect of pH on biofouling process is dual in nature. From the point of view of microorganism growth, there is an optimal pH value, generally at or near pH 7, at

which maximum growth and hence maximum extent of biofouling can be achieved. On the other hand, the pH of solution can affect the charge of the surface and its zeta potential. Most bacteria do possess negative electrical surface charges<sup>21</sup> and hence, the adhesion of these bacteria to positively charged materials is enhanced. In other words, the coating of solid surfaces with materials that increase surface negative charge would typically reduce the adhesion of bacteria to such surfaces.

The presence of inorganic species, especially divalent metal ions such as  $\text{Ca}^{+2}$  and  $\text{Mg}^{+2}$ , was reported to increase the extent of biofouling process.<sup>3,17</sup> This may be attributed to the bridging effect of the ions that could help in cross-linking fouling material layers.<sup>17</sup>

Finally, nutrient concentrations and oxygen content can play an important role in the biofouling process. The availability of both at the interface can enhance the bacterial growth and hence the formation of biofilms on the surface. The diffusional abilities of these nutrients through the biofilm can impact the process. With thick or compact films, through which oxygen diffusion is inefficient, anaerobic microorganisms are expected to dominate in the lower layers while aerobic organisms would prevail at the external layers. The deprivation of nutrients means simply that the growth process is strongly restricted.

### **1.2.2. Crystallization fouling**

Crystallization fouling, also known as “precipitation” or “scaling”, is defined as fouling caused by the deposition or the formation of crystals from solution onto the surface. This type can be found in industrial boilers, desalination systems, food processing, steam generators, cooling-water systems and many more. Crystallization

fouling depends on the salt type(s), concentration(s), and operating conditions present. Typical salts involved in such phenomenon are carbonate, sulfate, silicate, phosphates and hydroxides of calcium, barium, magnesium, sodium, and lithium.<sup>2</sup> Most of the bivalent salts are known to have inverse solubility in the range of cooling systems, which means they precipitate more efficiently as temperatures increase. In the following discussion, we focus on the available data taken from fouling of heat exchangers.

The crystallization process consists of two stages that usually take place simultaneously. The first stage involves the creation of small particles, usually termed nuclei. The second stage is the growth of the crystalline structure around the formed “nucleus”. Obviously, the number of nuclei present in a solution will control the ultimate size of the crystals formed. In general, pure salts form very hard, compact deposits while in the case of a mixture of salts, the deposit is usually very soft and flaky; it maybe even be easy to remove by the shearing action of the flowing fluid.

Spontaneous nucleation is associated only with clean conditions using pure solutions. In industrial conditions, this is highly unlikely; impurities generally provide the primary heterogeneous nucleation.<sup>7</sup> This is followed by secondary heterogeneous nucleation, which is a complicated process and covers a wide range of situations. For instance, collision breeding is believed to be widespread whenever high fluid shear conditions exist, which may favor crystal to crystal or crystal to wall collisions.<sup>7</sup> The mechanism of fouling at the wall is primarily particulate deposition instead of crystallization at the heat exchange wall itself. In this case, the formed deposit can be a loose aggregate of particles rather than crystals formed directly on the surface. The latter

have stronger structure and are more difficult to remove compared to the deposits formed by secondary heterogeneous nucleation.

The mechanism of crystallization fouling is summarized as followed:<sup>7</sup>

1. Nucleation phenomena at the surface and in solution as described above.
2. Diffusional phenomena, which involve the transport of ionic species, molecules and crystalline particles from the bulk of solution to the surface.
3. Deposition phenomena occurring at the interface that result in wall crystallization.
4. Removal phenomena occurring during the deposition stage, which opposes the effect of the deposition stage.
5. Change of the nature of the deposit over time. This may be hardening due to re-crystallization and crystal transformation, or softening (weakening) due to the lack of cohesion as the deposit grows as well as the production of planes of weakness.

### **1.2.3. Particulate fouling**

This type of fouling can be defined as “the accumulation of the solid particles from one phase onto the interface with another phase” such as the accumulation of solid particles from the fluid stream onto the surface of the solid phase. In water, for instance, the source of particulate material is quite varied and may include clay, dead shells, iron oxides, deposits of sloughed off materials, particles crystallized in the bulk of flowing water and corrosion products, among others.

When the particle size is equal to or smaller than  $1 \mu\text{m}$ , fouling phenomena can be handled and described in terms of colloidal chemistry. Since the nature of solid surfaces is usually different from the nature of the deposited particles, heterocoagulation is the appropriate term to describe the initial stage of the fouling process. Once the first layer is formed and established on the surface, the process becomes a homocoagulation in which subsequent particles of the same type are deposited and coagulated with the deposited layer on the surface.

The principal interaction forces between colloidal particles are van der Waal's forces and electrostatic double layer forces. In addition, steric hindrance effects due to polymer adsorption on the particle surface and ion bridging effects can also play roles in the process. It is clear that the net interactions determine whether the adhesion is promoted or depressed. In all cases, adhesion is expected only if the flow of fluid that contains the particles is not providing a shear force strong enough to overcome the net attractive force.

Van der Waal's forces in binary systems are attractive in nature. The mathematical formula for solid particle adhesion,<sup>3</sup> postulated initially by London and later on modified by Hamaker,<sup>3</sup> indicates that as the distance between the two particles or between the particle and the surface decreases, the attraction force increases as a consequence. Furthermore, Langbein<sup>22</sup> has indicated that as soon as the thickness of the surface layers of the two interacting solids becomes larger than the separation distance between them, their interaction is determined by the properties of the layer and not by the material underneath. This provides the principal for the usage of surface modification as

an antifouling technique: the active layer can be used to reduce the adhesion to the surface.

Electrostatic double layer forces, on the other hand, are considered to be repulsive forces and are well described through DLVO theory. Colloidal particles of similar natures are expected to have the same type of surface charge; hence, repulsion due to charge is expected. As the separation distance decreases, the repulsive force increases. It is clear here that the isoelectric point of the particle (solid) surface is an important factor in the magnitude of these forces and the pH affects the adhesion processes.

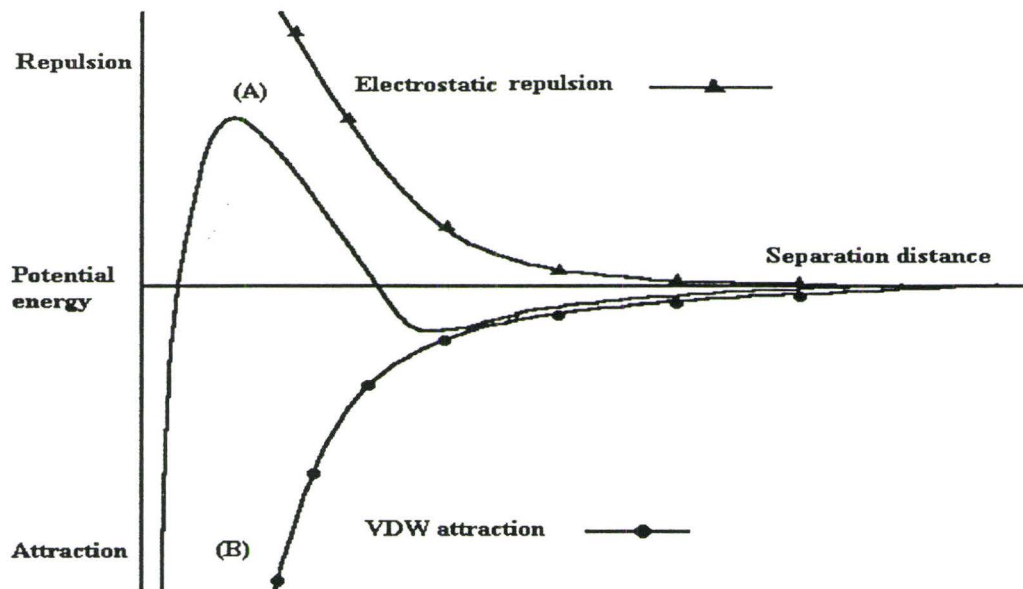


**Figure 2** Energy-distance curves

It is clear that we have two major forces that compete with each other. As the separation distance decreases, the attractive force due to van der Waal's forces will increase and the repulsion forces due to electrostatic double layer will increase too. At a certain point, the net result would be a high-energy barrier for which a net repulsive force

exists (Figure 2. A). As the separation distance further decreases, the attractive forces become higher than the electrostatic repulsion forces and net attraction force will result in particle adhesion (Figure 2. B). That is, the particle adheres once it has passed the net repulsive maximum point described in DLVO theory. In the case of solids of different charges, both van der Waal and electrostatic interactions are attractive and adhesion is further enhanced (Figure 2). This is believed to be the case at the initial stages of fouling when the particles adhere to the surface to form the first layer of the deposit.

In practice, other interactions can take place that further complicate the picture. Ions, for instance, can bridge two particles of similar electric charge. While polymers can also act as bridging agents between the two particles,<sup>23</sup> the aggregates formed by polymer adhesion may stimulate steric hindrance that could hinder further adhesion to the surface. Similarly, surface hydration of the particle surface can work to minimize the adhesion by creating a barrier that prevents a close approach of the hydrated surfaces. As a result, separation distances are insufficiently low to allow the dominance of the attraction forces.

### **1.3. Interactive effects of different fouling types**

As mentioned previously, it is rare to have a single fouling mechanism in processes involving water. It is expected in most cases that a given type of fouling will enhance other type(s) of fouling. For instance, it is difficult to mitigate biofouling in the presence of corrosion fouling, as the corrosion film may facilitate biofilm formation. In another example, living microorganism colonies on the surface may enhance the rate of corrosion, either by its metabolic by-products, such as in the case of SRB (sulfur reducing

bacteria) in MIC (microbial induced corrosion),<sup>1,2,6</sup> or by the depression of mechanical mitigation processes. Also, the formation of a biofilm on the surface may enhance particulate fouling once the surface nature has been changed or “conditioned” by biofouling; the attachment process is assisted by the new sticky properties of the surface.<sup>6</sup>

It is important to realize that the interdependency of fouling mechanisms does not always enhance each individual process. Sometimes the effect of one foulant suppresses other fouling mechanisms. For example, the corrosion of copper containing alloys may slow down the rate of biofouling mechanism, as the  $\text{Cu}_2\text{O}$  can affect the microorganisms<sup>20</sup> and hence retard the build up of the biofilm.

#### **1.4. Mitigation methods for fouling**

Several distinct approaches are utilized to mitigate fouling; no one method serves all fouling problems. For example, chlorine, which is known to be an oxidizing antifouling agent, is used to depress biofouling. However, iron hydroxide formed on the surface as a result of corrosion may react with chlorine and reduce the amount of chlorine available for breaking up the extracellular polysaccharide film.<sup>6</sup> Worse, the chloride exacerbates corrosion. Some of the methods that are applied to mitigate fouling will be described

##### **1.4.1. Physical mitigation methods**

Fouling layers can be removed abrasively by physical devices. Two on-line methods are known: sponge-ball cleaning<sup>24</sup> and reversing-flow shuttle brushes.<sup>25</sup> In the

first method, properly selected balls are circulated in the aqueous solution (responsible for fouling) and then collected downstream using a screen. These beads abrade the surface through collisions. In the case of the reversing flow shuttle brush, brushes are installed in each tube and cages are installed at both ends of the tube. At timed intervals, water flow is reversed to run the brushes through the tubes, cleaning the surfaces during the traversal.

In the case of biofouling, these physical methods are often inefficient because of the pseudoelastic nature of the biofilm; spiny balls and brushes seem to move through the film but do not remove it. However, physical cleaning works well when combined with chemical methods that can destroy the biofilm structure.

Other methods have been described, but are not yet in wide use. They include the use of magnetic fields, electric fields (both of which affect crystallization fouling), radio frequency (said to change the crystal morphology and size, hence retarding heterogeneous nucleation), ultraviolet light (to affect biofouling processes) and surface modification prior to fouling.

#### **1.4.2. Chemical Mitigation**

Chemical mitigation methods, as expected, are widely used in mitigating several types of fouling. For biofouling, many approaches exist. The nature of a deposited biofilm can be affected by factors that actually control bacterial growth on the surface and assist or suppress the processes described above. Agents that oxidize the group responsible for the formation of adenosine triphosphate (ATP), which is essential for the

microorganism survival, will act as a biocide. Oxidizing antifouling agents, such as chlorine, also have the ability to oxidize the extracellular film on the surface leading to its depolymerization. It is further advantageous to use wall shear produced by flowing fluid (see previous section), enough to remove the debris of the depolymerized biofilm.<sup>26</sup> If colonies of bacteria are well established and the thickness of the deposited layer acts as a barrier to prevent efficient penetration of the oxidizing chemical through it, the efficiency of the antifouling agent will be indeed diminished.<sup>6</sup>

Chlorine can be applied either continuously or periodically to the bulk fluid in order to depress biofouling. The application of chlorine in water treatment, however, is accompanied by the production of some undesirable by-products such as chloramines or carcinogenic hydrocarbons (disinfection byproducts DBPs).<sup>9</sup> Other oxidizing chemicals have been investigated, therefore, such as hydrogen peroxide and ozone gas.

For crystallization and corrosion fouling, chromate was once successfully used for both corrosion protection and crystal growth control. However, it was banned due to toxicity concerns and has not yet been replaced with a chemical agent that has a comparable performance. Polyphosphates are used to prevent scaling, but their utilization is limited to temperatures below 90°C; they are thus considered low temperature additives. Polyphosphates, however, are microorganism nutrients that may enhance biofouling process. More recently, membrane methods to control the composition of the fouling solution has been utilized to minimize fouling.<sup>27</sup>

### 1.4.3. Chemical Modification of Surfaces

An entirely different approach to decreasing problems due to fouling utilizes surface treatments that change the fouling behaviour of the surface. Although there are many types of surface treatments, in this thesis we focus on the use of very thin films of surface modifiers that change the inherent chemical and the physical properties of the substrate's surface. It is thus possible to render the surface hydrophobic or hydrophilic in nature, an electrical insulator or conductor, active or inert toward specific chemical environments, to control its adsorption properties, etc.

Successful surface modification is largely dependent on the suitable choice of surface modifier, which must be able to adhere to the surface via either physical or chemical adhesion forces, must further achieve the desired properties for the substrate and, finally, must have the necessary durability under the conditions of use. Thus, the surface of prosthetic devices, such as heart valves, must be the subject of surface modification to reduce the adhesion of blood materials on its surface; metal surfaces are commonly inactivated/passivated toward environmental conditions that cause corrosion by surface modification.

One of the important consequences of surface modification is the ability to change the adsorbability of the surface either in terms of selectivity for or quantity of adsorbed material. The validity of this approach to mitigating fouling is highly dependent on the criteria established for each individual case of fouling. The nature of the surface (chemical and physical), the nature of the adsorbate (chemical and physical), the

conditions of the process (pH, temperature, flow rate, etc.) and the nature of the proposed surface modifier all must be considered in a careful manner.

Surface modification is considered a safe tool to minimize fouling, as the modifying agent should, in principle, remain bound to the surface (this is important if the constituents have some toxicity associated with them). For instance, many attempts have been made to mitigate marine fouling using surface modification. In this case, reduced surface energy surfaces<sup>28</sup> result from modifications with materials such as silicone,<sup>29,30,31,32</sup> Teflon,<sup>®</sup> and epoxy.<sup>29,33</sup> Metal surfaces can be modified by electrofinishing, a commercial method that produces a very smooth surface. The effect of the method actually is to delay the initial deposition but it can't eliminate fouling problems. Ion implantation, which involves the bombardment of the surface with ions in the keV to MeV energy range, can work to minimize crystallization fouling over the metal surface.

In addition to modifying surface structure, one can incorporate chemicals in the surface. Biocides<sup>34</sup> based on tin and copper that can affect microorganisms found in vicinity to the interface act to reduce the rate of biofouling processes.<sup>1,6,9</sup> This biological effect, however, is thought to cease after several layers of deposits are formed on the surface. Under such cases, retardation of the process is likely to take place rather than complete elimination.

## 1.5. Siliceous surfaces

Silica and quartz are important types of siliceous surfaces that have many industrial applications including working as fillers and thickening agents in organic systems, including elastomers, ink and paints. The properties of these compounds depend largely on the surface chemistry of the solid phase. In the following discussion, we consider the nature of the silica surface, the nature of deposition on the surface and the efforts to modify the surface using silane coupling agents.

### 1.5.1. The Nature of Siliceous Surfaces

Kiselev postulated in 1936 that the surface of the amorphous silica is actually covered by OH groups bound to an  $\text{SiO}_2$  skeleton.<sup>35</sup> Later, in 1940, Carman recognized that water hydrates the surface of anhydrous  $\text{SiO}_2$  to create silanol groups.<sup>36</sup> Since then, many studies have focussed on how these hydroxyl groups can affect the adsorption phenomenon on the siliceous surface and, further, how the external environment affects the adsorption through changing the nature of those hydroxyl groups.

The OH groups on siliceous surfaces are important in controlling adsorption on such surfaces. Hydroxy groups can participate in the adsorption of many chemical species via hydrogen bonding between the hydrogen atom of the OH group and electronegative atoms or  $\pi$  electrons of adsorbate molecules, especially in the adsorption of such species from non-aqueous solutions.<sup>37</sup> Evidence for this role has been presented by many workers in the field. For example, Dubinin emphasized the importance of the SiOH group in adsorption of any material whenever a donor-acceptor match, particularly

hydrogen bonding, exists.<sup>38</sup> As early as 1950, dehydration studies demonstrated that absorption of methyl red from benzene solution is less efficient for dehydrated than hydrated silica gels.<sup>39</sup> It was also shown that water molecules are preferentially adsorbed on hydroxylated silica surfaces when compared to essentially hydrophobic siloxane surfaces (SiOSi) that don't have free SiOH groups, as is the case with quartz.<sup>40,41</sup>

The number of hydroxyl groups on a siliceous surface is affected by the thermal history of that surface. For example, heating silica particles in a vacuum to various temperatures can reduce the number of OH groups remaining on the surface.<sup>35,42</sup> Also, the number of hydroxyl groups is known to be greater for an amorphous silica surface than a crystalline quartz surface. Typical amorphous silica surfaces possess about 4-5 OH groups/nm<sup>2</sup>.<sup>43</sup>

The presence of adsorbed water on silica surface constitutes a real problem when attempting to estimate the concentration of OH groups on the siliceous surfaces. Most of the studies conducted to estimate the OH groups include desorption of adsorbed water first under vacuum and heat. Dehydration at higher temperatures can lead to the formation of Si-O-Si bonds as noted above. In surface modification of silica using alkoxy silanes, adsorbed water is believed to react first with alkoxy silanes and chlorosilanes to hydrolyze them and hydrogen bonding of the resulting silanol to the surface silanol can occur rather than covalent grafting to the surface (see below).<sup>44</sup>

### **1.5.2. The isoelectric point of siliceous surfaces.**

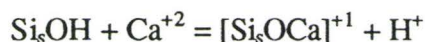
A siliceous surface has a point of zero charge (isoelectric point) at a pH of about 2. As the pH increases up to 6, the charges increase but are still very low; above that

value the surface charge will increase as the pH increases up to 10.7 at which, the surface would be extensively negatively charged.<sup>45</sup> Taking the OH group number as  $4.6 \text{ nm}^{-2}$ ,<sup>43</sup> it was shown that, at pH: 8, 9 and 10, the surface charge measured as  $\text{OH}^- \text{ nm}^{-2}$  was found to be 0.76, 1.45 and 2.52, respectively.<sup>46</sup>

### 1.5.3. Physical Adsorption on siliceous surface

#### 1.5.3.1. Absorption of Ions

Ions readily adsorb onto siliceous surfaces. The site-binding theory proposed by Yates, Levine, and Healy states that an adsorbed counterion forms an ion pair at or just within the surface;<sup>47</sup> the ionic sites are considered to be a two dimensional array of discrete positive, neutral and negative sites at the silica-water interface. Unlike other metal oxides, counterions, such as  $\text{Na}^+$ , are found almost in the same surface plane as the potential determining  $\text{SiO}^-$ . This can be attributed to the open network of oxygen ions at the surface that contains spaces large enough to accommodate the adsorbed cations. It was shown as early as 1954 that the order of ion adsorption follows  $\text{Ca}^{+2} > \text{Ba}^{+2} > \text{Sr}^{+2}$ .<sup>48</sup> When  $\text{Ca}^{+2}$  is adsorbed on siliceous surface, it displaces only one  $\text{H}^+$  ion,<sup>49</sup> rather than two as might be expected.<sup>50</sup> It was further shown that  $\text{Ca}^{+2}$  was adsorbed above pH 5 and that the amount adsorbed was proportional to the surface area.<sup>51,52</sup>



Siliceous surfaces also strongly adsorb certain polyvalent cations,<sup>53</sup> such as  $\text{Fe}^{+3}$ ,  $\text{Al}^{+3}$ ,  $\text{Cr}^{+3}$ , even at low pH where the magnitude of the negative charge on the surface is

fairly small. The behaviour of surface silanol groups as ligands for metal ions,  $\text{Fe}^{+3}$ ,  $\text{Cu}^{+2}$ ,  $\text{Cd}^{+2}$ , was tested by Schindler *et al.*<sup>54</sup>

### 1.5.3.2. Adsorption of organic cations and bases on silica

For organic bases such as amines, the mechanism of adsorption of ions on silica is dependent on the strength of the base and the pH of the solution. In neutral solution, the adsorption occurs via hydrogen bonding of the amine with a silica surface. Ionic bonds can be formed as well, providing that the pH of solution is high enough to allow negative charge formation on the silica surface.

The size and type of hydrocarbon group bound to nitrogen are also major factors in the adsorption processes of alkylamines and quaternary alkylammonium ions. Once the ion is bound to the surface, the surface can be rendered hydrophobic. Increased hydrophobicity accompanies an increase in the size of the hydrocarbon chain. Hydrophobic bonding with other hydrophobes, including other surfactant molecules, will favour their adsorption on the surface in such cases. The concentration of the depositing solution is a very important factor too. If the concentration is very low, a monolayer of the adsorbate can be adsorbed on the surface rendering it hydrophobic. When the concentration is increased, a double layer can be formed at the surface such that the hydrophobic hydrocarbon group will be physically bound to the hydrocarbon chain of the adsorbed mono-layer, leaving the hydrophilic termini of the compound pointing outward to the solution (Figure 3). This changeover in behaviour was confirmed to take place at concentrations near the critical micelle concentration (c.m.c.).<sup>55</sup>

The importance of the hydrophobic bonding in the adsorption of quaternary ammonium cations was indicated by Bresler *et al.*,<sup>56</sup> who showed that the adsorption of quaternary ammonium ions possessing long hydrophobic chains is higher than those of shorter chain length, especially at pH 3-6.

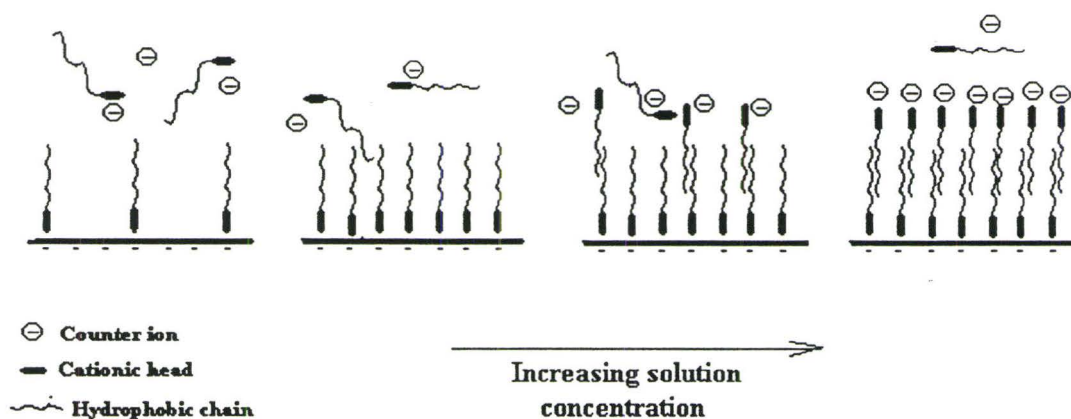


**Figure 3** The effect of solution concentration on the adsorption of cationic species on siliceous surfaces

#### 1.5.3.3. Adsorption of organic polymers on siliceous surface

The adsorption of polymers on siliceous surfaces is governed by several factors, including the nature of the polymer (chemical structure, functional groups, chain length, spatial arrangement, isoelectric point), the interaction forces between polymer chains, the solvent (aqueous/non aqueous) and the surface, the number of binding sites available both on the surface and the adsorbed polymer's chain, the pH of the solution, and the nature of the electrolytes present.<sup>57</sup>

#### 1.5.3.4. Protein adsorption

Proteins are a class of polymers that will be important in this thesis. The adsorption of proteins on siliceous surfaces is very complex. The diversity of protein functional groups and its multiconstituent structure give it peculiar position among the different classes of adsorbates. Protein adsorption can involve hydrogen bonding with OH, NH or COOH groups; ionic bonding can take place between charged sites on the surface and the charged quaternary ammonium cations found in some proteins; and, finally, hydrophobic bonding through the hydrophobic segments found in some proteins can occur with the surface. It was shown that proteins are adsorbed within sharp pH limits. For albumin, it was found the optimum pH to be 5, while it was 6 for  $\gamma$ -globulin. It was also found that proteins eluted from silica at sharply defined pH of about 7.5 and 8 for albumin and  $\gamma$ -globulin, respectively.

In more recent work, it was shown that the adsorption of bovine serum albumin BSA to silicon oxide surface is strongly dependent on the pH value; as the pH shifted away from the isoelectric point, the adsorption is reduced. It was also shown that the adsorption was irreversible; that is, the desorption of protein was unachievable by dilution. However, the adsorption was reversible with respect to solution pH at low BSA concentrations only.<sup>58</sup> In other words, desorption of protein can be achieved by changing the pH of dilute solutions. At high pH values, the negative charges that develop on the surface lead predominately to ionic bonding, while at low pH, hydrophobic bonding is expected to take place. This was shown in an interesting experiment<sup>59</sup> that compared the adsorption of protein from aqueous solution of pH 3 on three different macroporous silica

gels: fully hydroxylated, dehydroxylated by calcination at 750°C, and hydrophobed by trimethylchlorosilane. It was found that the adsorption on the chemically modified silica gel was the strongest while it was the weakest on the hydroxylated silica. With seven proteins (lysozyme, ribonuclease A, pepsin, lactoalbumin, ovalbumin, human serum albumin and  $\gamma$ -globulin), it was found that desorption is complete when the hydroxylated silica was treated with 20% isopropanol solution for all of the proteins except ovalbumin (90% desorption). In the case of dehydroxylated silica gel, three of these proteins only partially desorbed (lactoalbumin, ovalbumin and  $\gamma$ -globulin). In case of trimethylsilylated silica, the same three proteins demonstrated the smallest degree of desorption.

The deposition of albumin on a quartz surface at different potentials was examined using cyclic voltammetry and a quartz crystal microbalance.<sup>60</sup> The experiment demonstrated the dependence of the adsorption process on the potential of the electrode; the adsorption was highly accelerated by the application of positive potential to the electrode, indicating an electrostatic interaction between the positively polarized electrode and the negatively charged albumin molecules. It was also found that the adsorption of the albumin on the electrode is irreversible, as the dilution of the solution did not lead to desorption of protein molecules. As noted above with pH changes, protein can be desorbed from dilute solution by shifting the charge of the electrode to the negative direction.

The adsorption of proteins on siliceous surfaces is inevitable. Discussions of protein adsorption must consider not only the deposition of native protein, but also denatured proteins that frequently bind more tightly to the surface. Improved binding of

denatured proteins that frequently bind more tightly to the surface. Improved binding of the denatured protein can be understood in terms of the multiple binding sites on the siliceous surface that can interact with the protein through different types of attractive forces, hence facilitating the flattening of the protein molecule on the surface. As a consequence, the hydrogen-bonding coiled configuration of the protein is destroyed, usually irreversibly.

#### 1.5.3.5. Methods for siliceous surface modification

Although there are several methods of surface modification, we focus here on two major categories, which are differentiated by the nature of the bond created between the surface and the grafted alkyl group. The first category involves the formation of a surface Si-O-C bond sequence; the second a surface Si-O-Si sequence using silane coupling agents (see below). The former bonds can be formed by the direct condensation of an alcohol or acid with the silica surface (Figure 4).

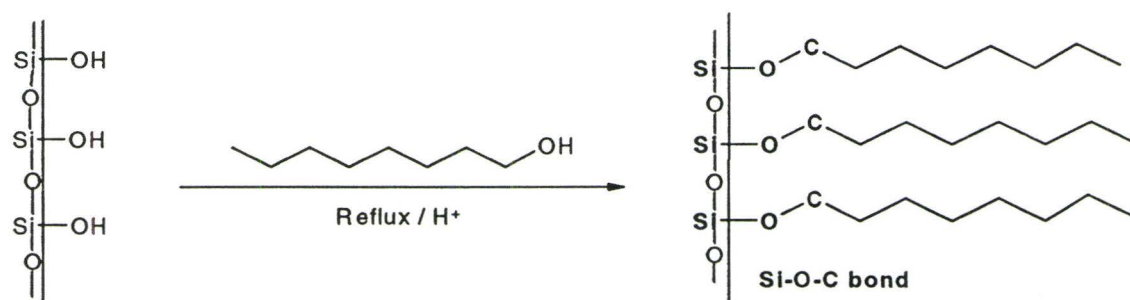


**Figure 4** Modification of siliceous surface using octanol

These reactions can only be performed at high temperatures (250°C) in an autoclave or under reflux at temperatures in excess of 150°C. It was shown that the

structure of different isomers could affect the rate of the process, and the activity decreases in the order normal, iso, neo and tertiary.<sup>61</sup> Such changes were found to render the hydrophilic surface of the silica hydrophobic, as discovered by Iler.<sup>62</sup>

The stability of these alkoxy silane surfaces was found to increase as the coverage of the surface by hydrocarbon groups approaches the close-packed state. In this case, no underlying silanol groups that can promote water adsorption are exposed, which minimizes or prevents hydrolysis. If such criteria are achieved, the coating becomes extremely stable to hydrolysis.<sup>63</sup>

#### **1.5.4. Silane coupling agents in surface modification**

Silane coupling agents are widely used to modify a wide variety of surfaces including metals, metal oxides, wood, and organic polymers.<sup>64</sup> More important than any of these, however, is the modification of silica and other siliceous surfaces. They were initially developed to improve bonding of organic resins to mineral surfaces. Thus, the first silane coupling agents contained organofunctional groups that could be used to link silica to organic resins.<sup>64</sup>

Theoretically, dispersion forces can work effectively to bind organic resins (polymers) to the oxide surface, if complete<sup>65</sup> “wetting” were achieved between the resin and substrate. However, in practice the resin has to compete with contaminants and surface water at the interface. Silanes, especially alkoxy silanes, were used as coupling agents, as they utilize surface water to generate silanol groups, which are believed to form strong hydrogen bonds to the hydroxylated surfaces. In addition, alkoxy silanes

themselves can form covalent bonds with the surface by reacting with surface hydroxyl groups to form covalent siloxane bonds.<sup>65</sup> These changes to surface energy permit wetting by hydrophobic materials such as polyesters and other organic polymers.

The major effect of the surface chemistry of the modified surface is indeed the nature of the alkyl or functional alkyl group bound to the silane coupling agent. Depending on the chemical and physical properties of alkyl group, the surface response to the surrounding environment can be greatly controlled. Film thickness, polarity, permeability, electrostatic charge, and wetting properties may be controlled by proper choice of the alkyl group. It is furthermore possible to use functional groups that can also chemically graft, by radical or ionic means. Silane coupling agents thus permit surface characteristics and thus adhesion of other materials to be controlled.

Silane coupling agents typically have the structures  $R_3SiX$ ,  $R_2SiX_2$ , and  $RSiX_3$  (where  $X = Cl, MeO, EtO, etc.$ ) can react with the silanol groups on the surface to form a physisorbed or chemisorbed layer of organosilyl groups (Figure 5).

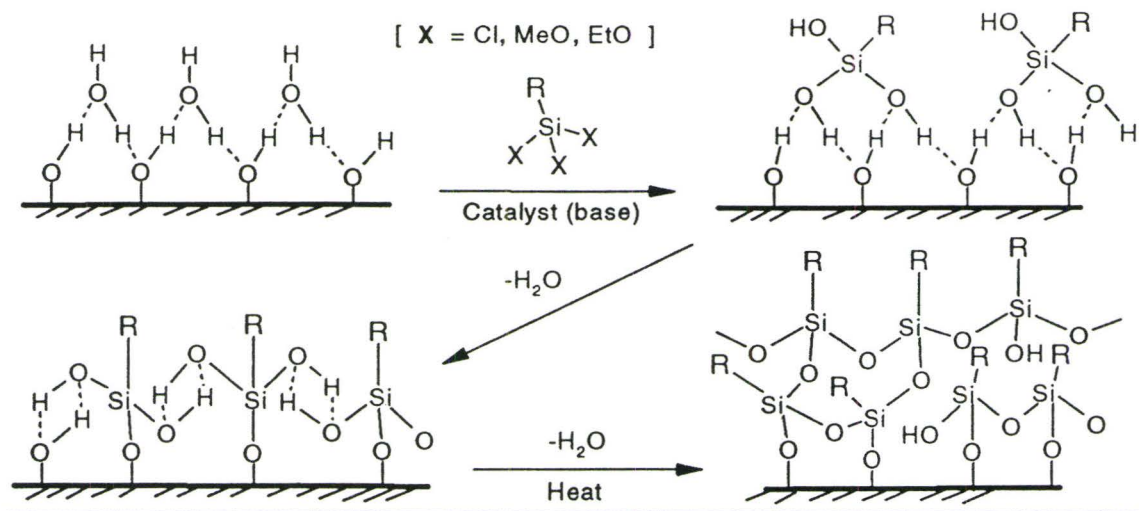
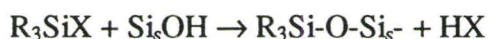


**Figure 5** Applying silane coupling agents from organic solvent to modify the surface.

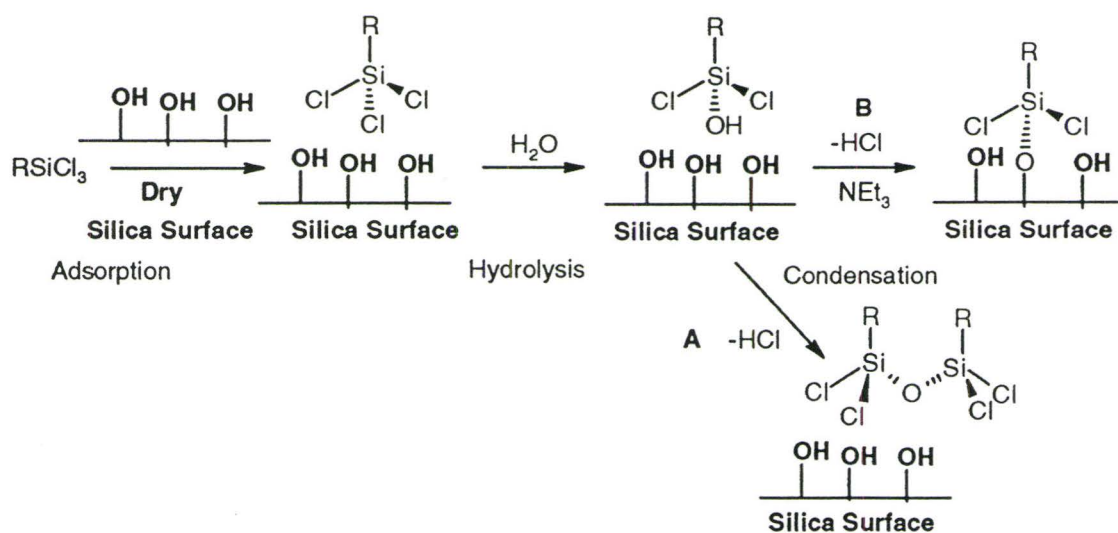
There is, however, evidence that efficient surface modification can also occur with adsorbed water, without the necessity to invoke a direct coupling agent/surface bond.<sup>66</sup>



Koenig and Shih<sup>67</sup> showed using Raman spectroscopy (absorption at 788 cm<sup>-1</sup> compared to 783 cm<sup>-1</sup> for the siloxane homopolymer) that vinyltriethoxysilane (VTES), for instance, condensed with the glass surface via a covalent siloxane bond across the interface. It was further demonstrated that the reaction was reversible when the surface was boiled in water (after drying 110°C, the siloxane bond absorption line at 788 cm<sup>-1</sup> was restored).

Alkoxysilanes are generally more useful coupling agents than the corresponding chlorosilanes as a consequence of the by-products of the reaction. In case of

alkoxysilanes, the by-product of the reaction is an alcohol (typically ethanol or methanol), which can be easily evaporated. This is not the case of chlorosilanes that leads to the formation of the undesirable by-product hydrochloric acid, especially in industry (Scheme 1).



**Scheme 1: Surface modification of silica using chlorosilane.**

### 1.6. UV Disinfection of Water

UV irradiation has been adopted as a reliable, environmentally safe tool for water disinfection. UV radiation was recognized earlier this century for its fatal effect on living organisms in water.<sup>33</sup> While chemical agents, such as chlorine, chlorine dioxide, sodium chlorate, sodium chlorite and ozone are still used for water disinfection, UV radiation disinfection has the advantage of avoiding potentially harmful by-products. In chemical disinfection, these by-products (known in the water treatment field as disinfection by-products DBPs) can impact the public health.

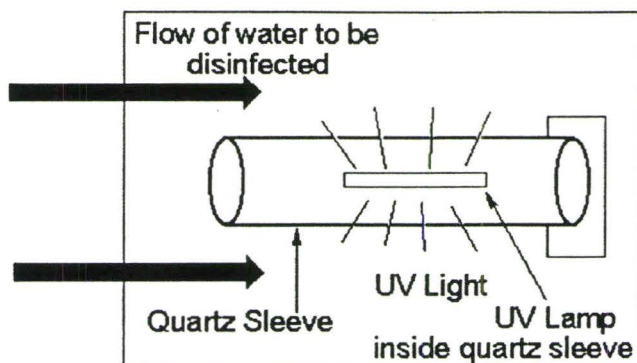


**Figure 6 Simplified diagram for UV wastewater disinfection system.**

The benefits of UV disinfection, however, are limited by some practical considerations. Fouling, particularly from (very dirty) wastewater streams is frequently very efficient, which compromises the disinfection efficiency. Thus, there is a need to develop an understanding of fouling processes from wastewater, particularly in the presence of UV light. Very little is known about such fouling processes on bare quartz. Similarly, the ability of silane coupling agents to mitigate fouling in the presence of UV light was almost unexplored.

### **1.7. Objectives**

In this thesis, our objectives are to better understand the chemistry of quartz surfaces, particularly in the presence of UV light. We have chosen to utilize the fouling as a metre by which we can measure the chemical changes at the interface. Therefore, in Chapter 2 we examine fouling phenomena on quartz surface by using model fouling system that was built to mimic the actual wastewater fouling both in the dark and in the

presence of UV light. In Chapter 3, based on the assumption that hydrophobic surfaces will foul less, quartz surfaces were modified with commercial coupling agents and those we synthesized. The effect of the coupling agent on the magnitude of surface fouling, both in the light and the dark, is examined. Finally, we summarize the relationship between the chemistry on the surface to the efficiency of fouling and nature of the fouling layer in the light and the dark. An appendix contains some of the experimental conditions used for synthesis of the coupling agents and, in the case of a squalene-modified coupling agent, some preliminary data on its sensitivity to oxidation.

## 1.8. References

- <sup>1</sup> Kent, C. A., "Biological Fouling: Based Science and Models" in *Fouling Science and Technology*, edited by Melo, L. F., Kluwer Academic Publishers: Dordrecht, 207 (1988).
- <sup>2</sup> Lappin-Scott, H. M. and Costerton, J. W., *Biofouling* 1, 323 (1989).
- <sup>3</sup> Vesser, J., "Adhesion and removal of particles I" in *Fouling Science and Technology*, edited by Melo, L. F., Kluwer Academic Publishers: Dordrecht, 87 (1988).
- <sup>4</sup> Lo, W., Nelson, Y. M., Lion, L. W., Shuler, M. L. and Ghiorse, W. C., *Water Res.* 30, 2413 (1996).
- <sup>5</sup> Hseih, K. M., Murgel, G. A., Lion, W. L. and Shuler, M. L., *Biotechnol. Bioeng.* 44, 219 (1994).

- <sup>6</sup> Panchal, C. B. and Knudsen, J. G., *Adv. Heat Transfer* 31, 431 (1998).
- <sup>7</sup> Bott, T. R., "Crystallization Fouling: Basic Science and Models" in *Fouling Science and Technology*, edited by Melo, L. F., Kluwer Academic Publishers: Dordrecht, 251 (1988).
- <sup>8</sup> Kent, C. A., Juddridge, J. E., "Microbial Fouling In Heat Transfer Surfaces In Cooling Water Systems" in *Harwell Report AERE-R 10065*, Harwell, U. K. (1981).
- <sup>9</sup> Hottinger, K. J., "Surface Bound Biocides-A Novel Possibility to Prevent Biofouling" in *Fouling Science and Technology*, edited by Melo, L. F., Kluwer Academic Publishers: Dordrecht, 233 (1988).
- <sup>10</sup> Bott, T. R., "General Fouling Problems" in *Fouling Science and Technology*, edited by Melo, L. F., Kluwer Academic Publishers: Dordrecht, 3 (1988).
- <sup>11</sup> Costetron, W. J., Gessey, G. G. and Cheng, K. G., *Sci. Amer.* 238, 86 (1978).
- <sup>12</sup> Sutherland, I. W., "Polysaccharides in the adhesion of marine and freshwater bacteria" in *Microbial Adhesion to Surfaces*, edited by Berkeley, R. C. W., Lynch, J. M., Melling, G., Rutter, P. R. and Vincent, B., Horwood: Chichester, 329 (1980).
- <sup>13</sup> Allison, D. G. and Sutherland I. W., *J. Gen. Microbiol.* 133, 1319 (1987).
- <sup>14</sup> McEldowney, S. and Fletcher, M., *J. Gen. Microbiol.* 132, 513 (1986).

- <sup>15</sup> Characklis, W. G., *Biofouling Biocorros. Ind. Water Syst.* (Proc. Int. Workshop Ind. Biofouling Biocorros.) 7 (1991); Characklis, W. G., *Biotechnol. Bioeng.* 23, 1923 (1981).
- <sup>16</sup> Harborn, R. S. and Kent, C. A., "Aspect Of Cell Adhesion" in *Fouling Science and Technology*, edited by Melo, L. F., Kluwer Academic Publishers: Dordrecht, 125 (1988).
- <sup>17</sup> Marshall, K. C., Stoute, R. and Mitchell, R., *Can. J. Microbiol.* 17, 1413 (1971).
- <sup>18</sup> Bott, T. R. and Pinheiro, M. M. V. P. S., *Can. J. Chem. Eng.* 55, 473 (1977).
- <sup>19</sup> Beal, S. K., *Nucl. Sci. Eng.* 40, 1 (1970).
- <sup>20</sup> Pinheiro, M. M. V. P. S, Melo, L. F., Bott, T. R. and Pinheiro, J. D., "Effect of Design and Operating Variables on Biofouling " in *Fouling Science and Technology*, edited by Melo, L. F., Kluwer Academic Publishers: Dordrecht, 223 (1988).
- <sup>21</sup> Harden, V. P. and Harris, J. O., *J. Bacteriol.* 65, 198 (1953).
- <sup>22</sup> Langbein, D., *J. Adhes.* 1, 237 (1969).
- <sup>23</sup> Fleer, G. J., "Polymer Adsorption and its Effect on Colloid Stability" Thesis, Agricultural University Wageningen, Netherlands (1971).
- <sup>24</sup> Kern, W. I., *Combustion* 18 (1975).

- <sup>25</sup> Webb, R. L. and Kim, N. H., "Particulate fouling in enhanced tube" in *Heat Transfer Equipment Fundamentals, Design, Application and Operating Problems*, ASME HTD 108, 315 (1989).
- <sup>26</sup> Taylor, R. J. and Bott, T. R., "Biofouling Prevention and Destruction Using Chemical biocides" in *Fouling Mitigation of Industrial Heat-Exchanger Equipment*, edited by Panchal, C., Begell House: New York, 163 (1997).
- <sup>27</sup> Baker, R. W., *Membrane Technology and Applications*, McGraw Hill: New York, 214 (2000).
- <sup>28</sup> Kerr, A., Hodgkiess, T., Cowling, M. J., Beveridge, C. M., Smith, M. J. and Parr, A. C. S., *J. Appl. Microbiol.* 58, 1067 (1998).
- <sup>29</sup> Swain, G.W., Nelson, W.G. and Preedeekanit, S., *Biofouling* 12, 257 (1998).
- <sup>30</sup> Swain, G.W., Nelson, W.G. and Preedeekanit, S., *Biofouling* 10, 187 (1996).
- <sup>31</sup> Nevell, T. G., Edwards, D. P., Davis, A. J. and Pullin, R. A., *Biofouling* 10, 199 (1996).
- <sup>32</sup> Edwards, D. P., Nevell, T. G., Plunkett, B. A. and Ochiltree, B. C., *Int. Biodeterioration & Biodegradation* 34, 349 (1994).
- <sup>33</sup> Oliver, B. and Carey, J., *J. Water Poll. Cont. Fed.* 48, 2619 (1976).
- <sup>34</sup> Marshall, A. and Bott, T. R., "Effectiveness of biocides" in *Fouling Science and Technology*, edited by Melo, L. F., Kluwer Academic Publishers: Dordrecht, 591 (1988).

- <sup>35</sup> Kiselev, A. V., *Kolloidn. Zh.* 2, 17 (1936).
- <sup>36</sup> Carman, P. C., *Trans. Faraday Soc.* 36, 964 (1940).
- <sup>37</sup> Iler, R., *The chemistry of silica*, John Wiley & Sons: New York, Chap. 6, 648 (1979).
- <sup>38</sup> Dubinin, M. M., *Bull. Acad. Sci. USSR, Eng. Trans.* 1620 (1960).
- <sup>39</sup> Shapiro, I. and Kolthoff, I. M., *J. Am. Chem. Soc.* 72, 776 (1950).
- <sup>40</sup> Young, G. J., *J. Colloid. Sci.* 13, 67 (1958).
- <sup>41</sup> Young, G. J. and Brush, T. P., *J. Colloid. Sci.* 15, 361 (1960).
- <sup>42</sup> Iler, R., *The chemistry of silica*, John Wiley & Sons: New York, Chap. 6, 639 (1979).
- <sup>43</sup> Iler, R., *The chemistry of silica*, John Wiley & Sons: New York, Chap. 6, 633 (1979).
- <sup>44</sup> Herzberg, W. J. and Erwin, W. R., *J. Colloid. Interface Sci.* 33, 172 (1970).
- <sup>45</sup> Iler, R., *The chemistry of silica*, John Wiley & Sons: New York, Chap. 6, 661 (1979).
- <sup>46</sup> Ahmed, S. M., *Can. J. Chem.* 44, 1663 (1966).
- <sup>47</sup> Yates, D.E., Levine, S. and Healy, T. W., *J. Chem. Soc. Faraday Trans. 1*, 70, 1807 (1974).
- <sup>48</sup> Carroll, B. and Freeman E., *J. Phys. Chem.* 58, 335 (1954).
- <sup>49</sup> Boehm, H. P. and Schneider, M., *Z. Anorg. Chem.* 301, 326 (1959).
- <sup>50</sup> Iler R. K., *J. Colloid. Interface Sci.* 53, 476 (1975).
- <sup>51</sup> Greenberg, S. A., *J. Phys. Chem.* 60, 325 (1956).

- <sup>52</sup> Tadros, E. and Lyklema, J., *J. Electroanal. Chem. Int. Electrochem.* 22, 1 (1969).
- <sup>53</sup> Santon, J. H., Maatman, R. W., *J. Phys. Chem.* 68, 757 (1964).
- <sup>54</sup> Schindler, P.W., Furst, B., Dick, R. and Wolf, P., *J. Colloid. Interface Sci.* 55, 469 (1976).
- <sup>55</sup> Bijsterbosch, B. H., *J. Colloid Interface Sci.* 47, 186 (1974).
- <sup>56</sup> Bresler, S.E., Kolikov, V. M., Katushkina, N. V., Ponomareva, R. B., Demin, A. A., Zhadanov, S. P. and Koromal'di, E. V., *Colloid. J. USSR Engl. Transl.* 36, 592 (1974).
- <sup>57</sup> Iler, R., *The chemistry of silica*, John Wiley & Sons: New York, Chap. 6, 702 (1979).
- <sup>58</sup> Su, T. J., Lu, J. R., Thomas, R. K. and Cui, Z. F., *J. Phys. Chem. B* 103, 3727 (1999).
- <sup>59</sup> Kholokhlova, T. D. and Nikitin Y. S., *Russ. J. Phys. Chem.* 67, 1892 (1993).
- <sup>60</sup> Guo, B., Anzal, J. and Osa, T., *Chem. Phar. Bull.* 44, 800 (1996).
- <sup>61</sup> Lambert, R. and Singer, N., *J. Colloid. Interface Sci.* 45, 440 (1973).
- <sup>62</sup> Iler, R. K., *US Patent* 2,657,149 (Dupont), *Chem. Abstr.*, 50, 11564 (1953).
- <sup>63</sup> Iler, R., *The chemistry of silica*, John Wiley & Sons: New York, Chap. 6, 694 (1979).
- <sup>64</sup> Pleuddeman, E. P., *Silane Coupling Agents*, Plenum Press, New York, Chap. 1 (1991).
- <sup>65</sup> Pleuddeman, E. P., *Silane Coupling Agents*, Plenum Press, New York, Chap. 4 (1991).
- <sup>66</sup> Pleuddeman, E. P., *Silane Coupling Agents*, Plenum Press, New York, Chap. 4, 101 (1991).

<sup>67</sup> Koenig, J. and Shih, P. K., *J. Colloid. Interface Sci.* 64, 565 (1978).

## **2. The Role of UV Light in the Fouling of Quartz Sleeves Used in Water Disinfection**

### **2.1. Abstract**

Wastewater disinfection using UV light is often compromised by fouling of the UV-lamp surface. To determine the most significant parameters in the fouling process, quartz surfaces were fouled by model fouling solutions containing individually or as mixtures  $\text{Fe}^{3+}$ ,  $\text{Ca}^{2+}$ , human serum albumin and humic acid. The most significant fouling was observed in solutions containing iron and protein; calcium exacerbated such fouling. The fouling could be reduced by aging the solution before exposing it to the quartz surface. The flow rate was also found to affect the fouling: very low and very high flow rates were accompanied by less fouling than intermediate rates. The most important observation was that the magnitude of the fouling was shown to be significantly less when the fouling took place in the presence of UV light. Fouling layers of different elemental composition were found on UV-exposed and dark slides. The origins of these observations are discussed.

### **2.2. Introduction**

Many pundits have begun to claim that the control of fresh water, as its availability decreases, is going to be one of the defining elements in the way in which the planet develops over the next decades. Common sense and, increasingly, legal requirements are mandating more stringent requirements for water purity both following

extraction from the environment, particularly when destined for human consumption,<sup>1,2</sup> and prior to reentry to the environment. In the latter case, major challenges continue to arise in the purification and disinfection of treated sewage prior to discharge into natural water environments.

Chemical agents, such as chlorine, chlorine dioxide, sodium chlorate, sodium chlorite and ozone are frequently used for disinfection during wastewater treatment. However, these compounds and their chemical by-products (known in the water treatment field as disinfection byproducts DBPs), resulting from their reaction with organic and inorganic materials contained in the effluent, can impact the public health and must thus be dealt with; an association has been made between DBPs and a negative impact on human health.<sup>3</sup>

It was recognized earlier this century that UV irradiation can act to disinfect harmful, waterborne biological entities.<sup>4</sup> The use of UV irradiation avoids the formation of chemical DBPs and has been widely adopted as a reliable, environmentally safe tool for water disinfection. UV systems typically contain an intense light source in a quartz sleeve, across or along which the water flows at relatively high speed. One practical problem associated with UV disinfection, in certain classes of waters, is the attendant fouling of the quartz sleeve, which reduces light transmission and thus disinfection efficiency.

In this work, we focus on trying to better understand fouling phenomena on quartz surfaces in aqueous solutions. To do so, using a model fouling reactor and fouling solution, several parameters were examined: the interdependency of different foulants on

total fouling,<sup>5,6</sup> the composition of the resulting fouled layer, the presence or absence of UV light, the age of the fouling solution and the flow rate. We note that there are other factors that can be expected to affect the rate and magnitude of fouling such as pH, temperature, and surface roughness. In the following work, the latter variables were held constant. From these studies, it should be possible to develop a model that will allow a prediction of the types of anti-fouling protocols that should be utilized at the different waters found at different treatment sites (it is known that fouling varies widely from site to site). By doing so, we hope to be able to extend the effective lifetime of the quartz surface, reduce the efficiency of fouling, and minimize the necessity for surface cleaning and the attendant costs.

## **2.3. Experimental section**

### **2.3.1. Chemicals**

Human serum albumin (HSA, Sigma), humic acid (Aldrich), ferric chloride hexahydrate  $\text{FeCl}_3 \cdot 6\text{H}_2\text{O}$  (BDH), calcium chloride dihydrate  $\text{CaCl}_2 \cdot 2\text{H}_2\text{O}$  (Fisher Chemicals), sodium hydroxide (BDH) and hydrochloric acid (BDH) were used without further purification. MilliQ water (distilled deionized water) was used to prepare the solution for each experiment (15 litres for each). The pH of each fouling solution was adjusted to pH 7 only at the beginning of the experiment using sodium hydroxide solution (1.0 M NaOH) or hydrochloric acid solution (1.0 M HCl).

The magnitude of fouling was determined on standard quartz microscope slides obtained from PSI<sup>®</sup> Supplies. They mimic the fused quartz sleeves on commercial UV lamps used in water disinfection.<sup>7</sup> All slides initially had at least 85% UV transmittance at 254nm. Prior to use, slides were dipped in 5M hydrochloric acid solution for at least 2 days, then cleaned thoroughly with distilled water and acetone, followed by a 20 min cleaning period using Argon plasma glow discharge system Picotron<sup>™</sup> (Park Dental Research Corp.) just before the launch of the experiment. The slides were removed from the plasma cleaning system to clean glass containers and then directly transferred to the reactor. Typical contact angles for the cleaned slides were in the range 2-3° using deionized distilled water (milliQ water). Contact angle measurements were carried out using an NRL contact angle goniometer (model 100-00), manufactured by Ramé Hart Inc.

### **2.3.2. Equipment**

#### **2.3.2.1. Fouling Reactor**

Fouling experiments were carried out using a special reactor designed and provided by Trojan Technologies (Figure 7). The reactor consisted of two adjacent channels of 103 cm length and 5 cm width, with one common inlet from which the solution streams diverge to provide each channel with an equal amount of fouling solution. The height of the fluid stream over the bottom surface of the reactor was adjusted and measured to be ~1.4 cm. At the terminus of one channel, a low pressure UV lamp with a primary output at 254 nm was mounted about 7 cm above the surface of the

fouling solution to illuminate the solution in this region (labeled the UV zone). The lamp was kept above the water to eliminate any thermal effects of the lamp (along the heated surface) and to maintain a constant amount of UV radiation to the surface to be fouled; as the surface of the UV lamp is not in contact with the fouling solution, fouling on the lamp surface is avoided.

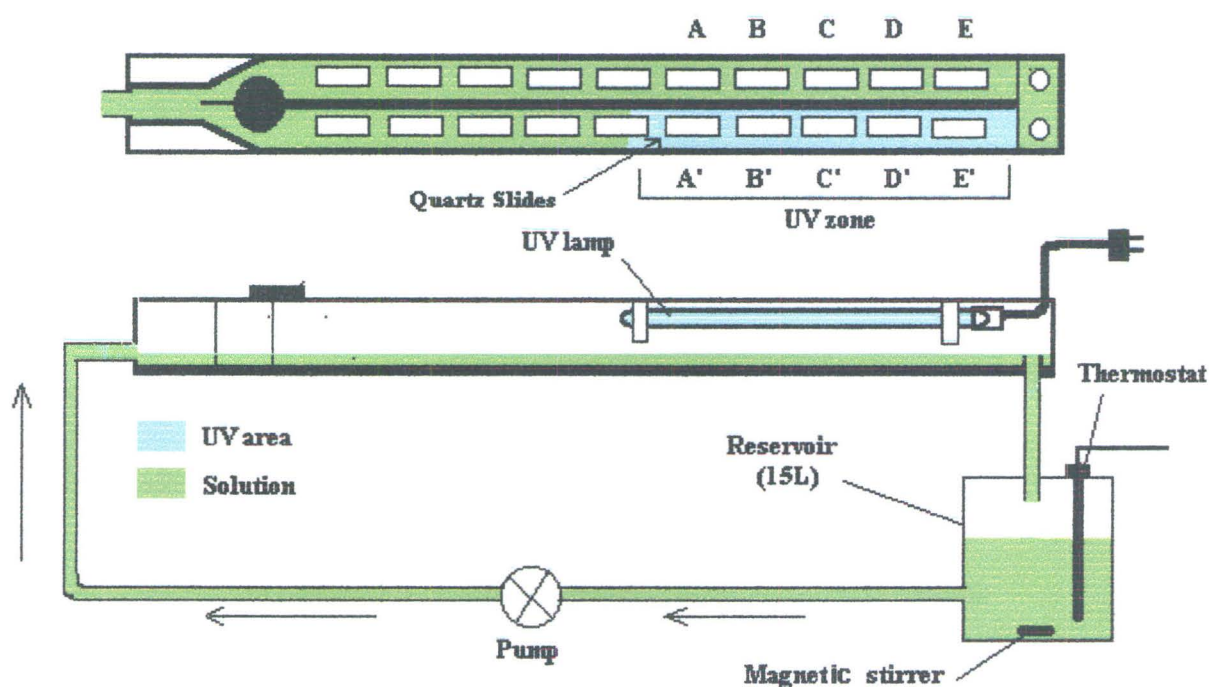


**Figure 7: Fouling Reactor**

Quartz slides (coupons, see below) were laid at the bottom of the channel in certain cavities at specific positions (A/A'-E/E', Figure 7). The exposed top surface of the slide was flush with the bottom of the reactor such that the fouling surface traversed as planar a surface as possible to minimize turbulent flow. Cavities not filled with quartz

sample coupons were filled with aluminum coupons. Each quartz slide exposed in the UV zone was twinned with another slide at the same position in the dark (e.g. B (dark) against B' (UV), Figure 7). In all cases, the slides were placed in positions closest to the reactor outlets, where the flow was the least turbulent. The flow rate was set at ~140 mL/min in each channel using the flow rate control knob of the pump and flow level knob in the reactor. This flow rate was used in all experiments. A magnetic stirrer was used to stir the 15 litre solution reservoir. A thermostatted water bath adjusted the temperature of the solution to 32 °C for all experiments.

#### **2.3.2.2. Fouling Protocol: Measuring UV Transmittance**

The UV transmittance of the quartz slides was measured using Varian Cary-300 and Cary-50 instruments, respectively. The transmittance of each clean quartz slide over 340-200 nm was taken as a reference line to which all successive measurements were normalized. Each slide was removed at certain times from the reactor then gently dipped in MilliQ water to remove the unbound fouling solution; the pH of the solution was noted when slides were removed. The slides were left to dry for about five minutes (until fluid water could no longer be seen) at room temperature, examined by the UV instrument using a special slide holder designed to fit the microscopic slide inside the Cary instrument, then placed back in their original positions in the reactor.

The transmittance of each slide was scanned over the range of 340-200 nm. This facilitates the comparison of different slides; the different foulants used in these experiments absorb over various UV ranges. The magnitude of the transmittance at 254 was used to quantitate fouling: the average of 8 positions over 2 slides was taken for each

side. The transmittance at 254 nm was used because it is an efficient wavelength at which UV light disinfects water and it is the primary wavelength used in commercial UV lamps.

Microscope images of some of the fouled slides were obtained using an optical microscope (Carl Zeiss Axiovert 25 CA, Empix Imaging Inc.). After removal from the reactor, the slides were allowed to dry at the end of the experiments at ambient temperature and kept in a capped glass container (~3-4 weeks) until they were imaged. The images were obtained in the polarized inverse (reflected) mode in the dark field.

#### **2.3.2.3. X-ray Photoelectron Spectroscopy (XPS) of Fouled Surfaces**

Quartz surfaces fouled with the quaternary mixture (see below) were characterized by XPS (Leybold MAX 200 XPS). Slides were broken/cut into pieces less than 1 cm<sup>2</sup>. Unmonochromatized Al K<sub>α</sub> (15 kV and 25 mA) X-ray radiation was used as the excitation source. Features in the resultant low resolution spectra due to excitation from the weaker X-ray satellite lines, which are also present in the non-monochromatic source, were subtracted by use of an algorithm supplied with the instrument.<sup>8</sup> Atomic percentages of the elements present were derived from spectra run in a low-resolution mode (pass energy=192 eV), which were normalized to unit transmission of the electron spectrometer by means of a routine provided by the manufacturer.<sup>9</sup> The sensitivity factors used (O 1s = 0.78, N 1s = 0.54, C 1s = 0.34, Si 2p =0.40) were empirically derived by Leybold for the normalized spectra. Binding energies and peak areas were obtained by the use of the standard provided with the spectrometer. The energy scale of the spectrometer was calibrated to the Cu 2p<sub>3/2</sub> (932.7 eV) and Cu 3p (75.1 eV) peaks,

respectively, and the binding energy scale was then shifted to place the C 1s feature present at 285.0 eV.<sup>10</sup> Large-area analysis (2x4 mm or 4x7 mm) was performed so that exposure of the samples to the X-ray would be minimized, while sufficient signal to noise ratios could be obtained for the spectral features.

#### **2.3.2.4. Foulants Examined**

Four foulants were examined individually and in combination (reasons for choosing these specific compounds are noted in the results section). The solution concentrations used for each chemical foulant were a compromise between the concentrations of analogous reagents in natural waters and the expediency of the experiment. It was initially necessary to ensure that the instruments to be utilized for analysis were sufficiently sensitive for the experiments. Thus, the first set of experiments used concentrations of  $\text{Fe}^{3+}$  and  $\text{Ca}^{2+}$  comparable to the maximum levels normally found in wastewater treatment plants. Subsequent experiments were done with the much lower concentrations found in most treated waters.<sup>11</sup> There are no reference concentrations in natural waters for humic acid and HSA specifically, so a balance was made between sensitivity of the instrument and the use of a reasonable amount of the chemical agent, based on total organics found in treated waters. The concentration of chemical agents in each experiment and the duration time of each experiment are listed in (Table 1).

**Table 1: Foulants Used in Fouling Experiments**

Exp	Fouling agents	Dura- tion (days)	Fe <sup>3+</sup> (mg/L)	Ca <sup>2+</sup> (mg/L)	Humic acid (mg/L)	HSA (mg/L)
1	Fe <sup>3+</sup>	6	10	-	-	-
2	Ca <sup>2+</sup>	6	-	140	-	-
3	Humic acid	6	-	-	50	-
4	Human serum albumin (HSA)	6	-	-	-	100
5	Fe <sup>3+</sup> / Ca <sup>2+</sup>	7	10	140	-	-
6	Fe <sup>3+</sup> / Humic acid	6	10	-	50	-
7	Fe <sup>3+</sup> / HSA	7	10	-	-	100
8	Fe <sup>3+</sup> / HSA	6	5	-	-	50
9	Fe <sup>3+</sup> / HSA / Ca <sup>2+</sup>	6	5	100	-	50
10	Fe <sup>3+</sup> / HSA / Humic acid	6	5	-	50	50
11	Fe <sup>3+</sup> / Ca <sup>2+</sup> / HSA / Humic acid	7	5	100	50	50
13	Fe <sup>3+</sup> (High flow rate)	4	10	-	-	-
14	Fe <sup>3+</sup> / Ca <sup>2+</sup> / HSA / Humic acid (aging)	4	5	100	50	50

## 2.4. Results

Model fouling solutions were created from mixtures of up to four contaminants: iron, calcium, humic acid and human serum albumin (HSA). Iron was chosen because it is often found in natural waters, it is commonly used as a flocculating agent in waste treatment plants, and, moreover, because of its (problematic) ability to absorb UV light.<sup>12</sup> Calcium was selected because it is a known variable in fresh waters (hardness) and because multivalent ions such as calcium and iron are able to act as bridge/crosslinking sites between hydrophilic organic functional groups such as carboxylic acids.<sup>13</sup> A typical surface-active protein, HSA, was chosen because materials of this type are typical constituents of biological broths derived from lyzed cells. Finally, humic acid compounds are well known as constituents of natural water, and can be found in soil as well. Humic acids can bind metals and act as detergents.<sup>11</sup> We were intrigued to learn whether such surfactant-like molecules mitigate fouling on quartz surfaces.

In the following sections, fouling experiments involving the four contaminants, individually and in mixtures, are described. Quartz slides were fouled in two separate streams, one of which was subjected to UV light (Figure 7). The degree of fouling was judged by changes in light transmission through the quartz slide at 254 nm, and fouling on the analogous “UV” and “dark” slides were compared. Experiments were carried out over several days, with changes in transmission through the slide measured approximately each 24 hours.

## 2.4.1. Fouling Experiments

### 2.4.1.1. Individual Contaminants

Quartz slides were exposed to each one of the four foulants; the loss of UV transmission in all cases can be seen in Figure 8. In all the Figures, thick lines refer to slides that were not exposed to UV light and thin lines to UV-exposed samples. Several factors are noteworthy: i) fouling was always more pronounced in the absence of UV light; ii) of the two ions,  $\text{Fe}^{3+}$  is much more opaque to UV light at the concentrations used than  $\text{Ca}^{2+}$  - indeed,  $\text{Ca}^{2+}$  is not a significant contributor to loss of UV transmission; and, iii) protein is a more severe foulant than humic acid at the concentrations used. The relationship between the magnitude of fouling with mixtures of foulants will comprise much of the remainder of the results section.

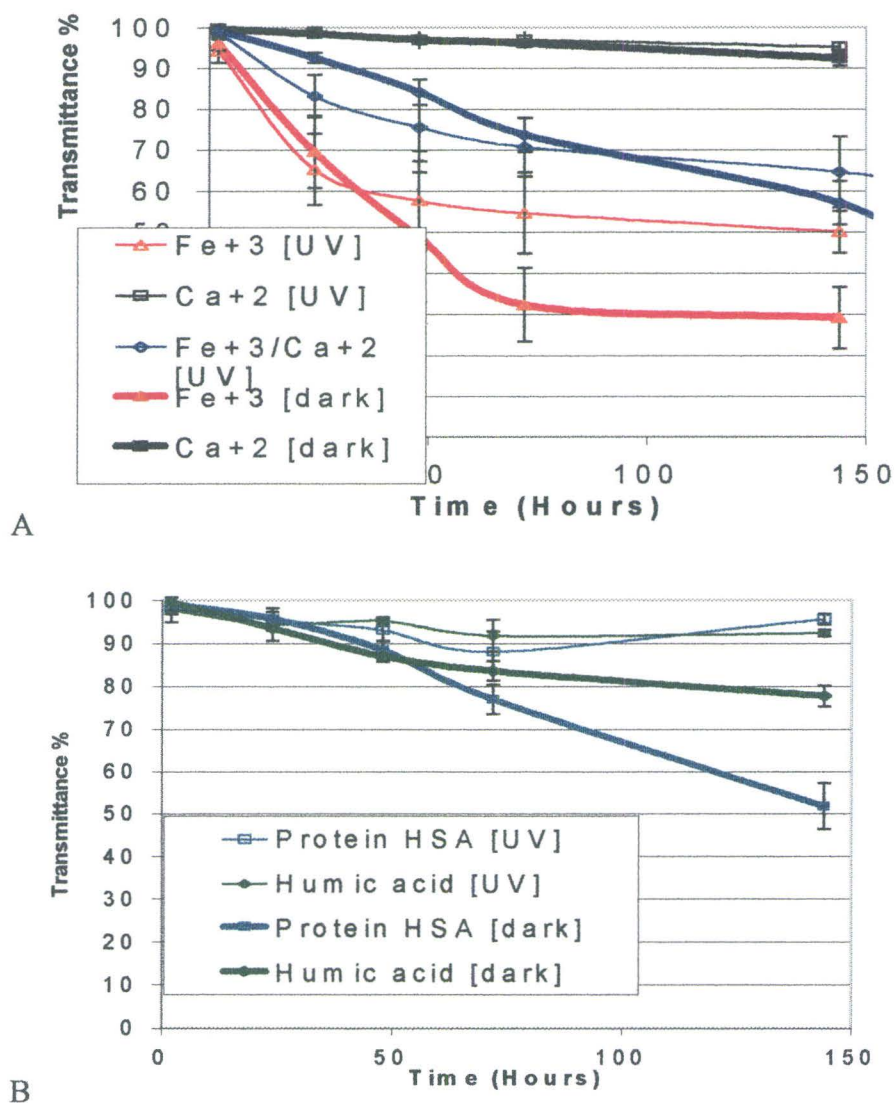


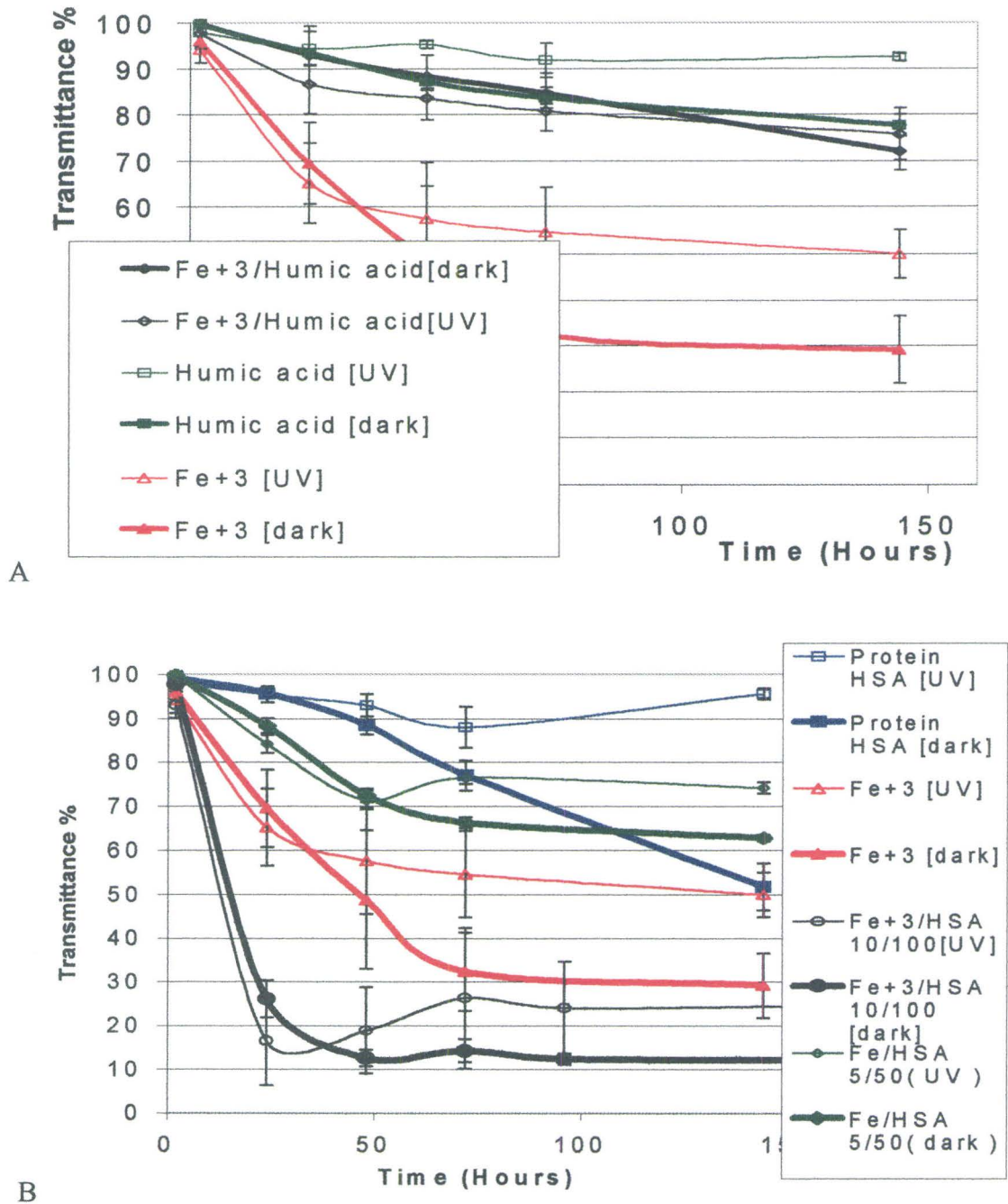
**Figure 8: Individual fouling experiments in the presence and absence of UV light using A: Fe<sup>3+</sup> (10 mg/L), Ca<sup>2+</sup> (140 mg/L), and B: HSA (100 mg/L) and humic acid (50mg/L).**

#### 2.4.1.2. Mixtures of Foulants

HSA and Fe<sup>3+</sup> led to the largest decrease in UV transmission of the individual foulants tested. Various binary mixtures of each of these compounds with the other

foulants were first examined, followed by ternary and quaternary mixtures. The decrease in transmission was very severe at higher concentrations of iron and HSA. Therefore, some of these experiments were reproduced at lower concentrations. The results include:  $\text{Fe}^{3+}$  (10 mg/L) +  $\text{Ca}^{2+}$  (140 mg/L) (Figure 8A);  $\text{Fe}^{3+}$  (10 mg/L) + humic acid (50 mg/L) (Figure 9A);  $\text{Fe}^{3+}$  (5 mg/L) + HSA (50 mg/L) (Figure 9B); ternary and quaternary mixtures of  $\text{Fe}^{3+}$  (5 mg/L), HSA (50 mg/L), humic acid (50 mg/L) and  $\text{Ca}^{2+}$  (100 mg/L) (Figure 10); a comparison of fouling from “fresh” and “aged” solutions (Figure 15); and, fouling as a function of flow rate (Figure 16).

Several features are apparent from comparing these graphs. The most significant observation is that fouling in the dark is always more problematic than in the UV-exposed samples, as determined by a reduction in transmittance. Other observations are noted on a mixture by mixture basis: i)  $\text{Fe}^{3+}$  and  $\text{Ca}^{2+}$ : The graph indicates that fouling caused by  $\text{Fe}^{3+}$  /  $\text{Ca}^{2+}$  mixture solution was less than that caused by  $\text{Fe}^{3+}$  solution alone (Figure 8). That is, when examining only these two foulants, the calcium mitigates fouling by iron; ii)  $\text{Fe}^{3+}$  and humic acid: When examined in this binary mixture, humic acid leads to a reduction of fouling by iron in both the UV and dark regions (Figure 9); and, iii)  $\text{Fe}^{3+}$  and HSA: The presence of HSA amplifies significantly the fouling of the quartz slide. In this case, at the concentrations used ( $\text{Fe}^{3+}$  10 mg/L, HSA 100 mg/L), fouling is so severe that the slide became almost opaque, irrespective of the presence of UV light. The experiment was thus repeated at lower concentrations by half and demonstrated the expected correlation between fouling efficiency and foulant concentration (Figure 9B).



foulants found in waste streams. The comparison of two ternary mixtures:  $Fe^{3+}$ ,  $Ca^{2+}$  and HSA; and  $Fe^{3+}$ , HSA and humic acid; and the quaternary mixture  $Fe^{3+}$ ,  $Ca^{2+}$ , HSA and humic acid suggests that humic acid, as noted above, mitigates fouling both in the UV and dark regions. By contrast,  $Ca^{2+}$  exacerbates fouling from these mixtures. As before, the presence of UV is an important factor in reducing fouling (Figure 10). Unlike the simple mixture of iron and calcium, the effect of calcium is overpowered by the effect of protein in these more complex mixtures.

In many of the fouling mixtures containing both iron and HSA, a temporal trend for fouling is observed that is quite different from the other mixtures. There is a decrease to a minimum transmittance at about 24 hours, following which the UV transmittance improves. This phenomenon will be discussed below.

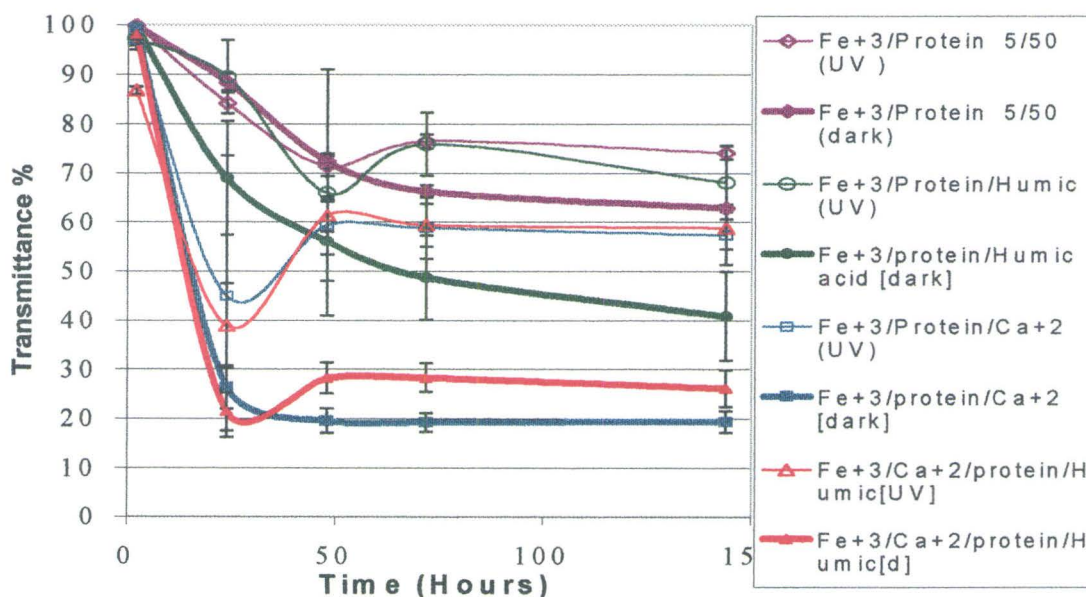


**Figure 10: Ternary and quaternary mixtures of  $Fe^{3+}$  (5 mg/L), HSA (50 mg/L), humic acid (50 mg/L) and  $Ca^{2+}$  (100 mg/L)**

#### 2.4.2. Visualization of Fouled Slides

In addition to determining the factors important in the evolution of fouling on quartz in wastewater treatment under intense UV irradiation, an ancillary objective was to determine if any factors associated with the fouling broth facilitate the cleaning of the quartz slide: cleaning is frequently a “necessary evil” in actual waste water disinfection using UV irradiation.<sup>7</sup> Optical microscopy of some selected fouled slides, using dark field microscopy, shed some light on the level of adhesion of the fouling layer to the quartz. The magnitude of fouling can be judged by two criteria: total light transmission which reflects the magnitude of fouling, and defects in the fouling that, as described below, may reflect adhesion of the fouling layer to the quartz and, thus, ease of cleaning.

A comparison of light transmission, by optical microscopy, was undertaken of the quartz slides fouled by the  $\text{Fe}^{3+}/\text{Ca}^{2+}$  mixture. As seen in Figure 11, the fouling layer is thicker in the absence of UV irradiation (less black area); patchy, particulate islands of foulant characterized the UV-irradiated slide. The iron/humic acid mixture showed more fouling than  $\text{Fe}^{3+}/\text{Ca}^{2+}$ , although it was also of a particulate nature (Figure 12). The iron / HSA mixture was much more heavily fouled in both the UV and dark slides, the latter were completely obscured (Figure 13) with a thick coherent film; the UV slide, while heavily fouled, had both transparent and translucent areas. The particulate nature of the other mixtures noted is not seen, suggesting a very different foulant lies on the surface. Quaternary mixtures behaved in a similar manner (figures not shown).

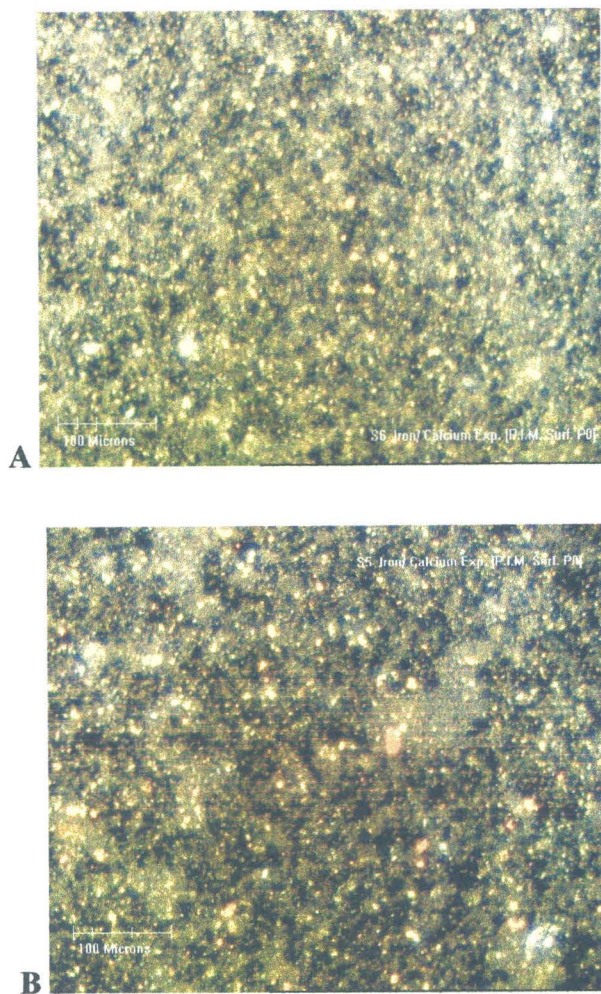


**Figure 11:  $\text{Fe}^{+3}/\text{Ca}^{+2}$  A: in the dark and B: UV**

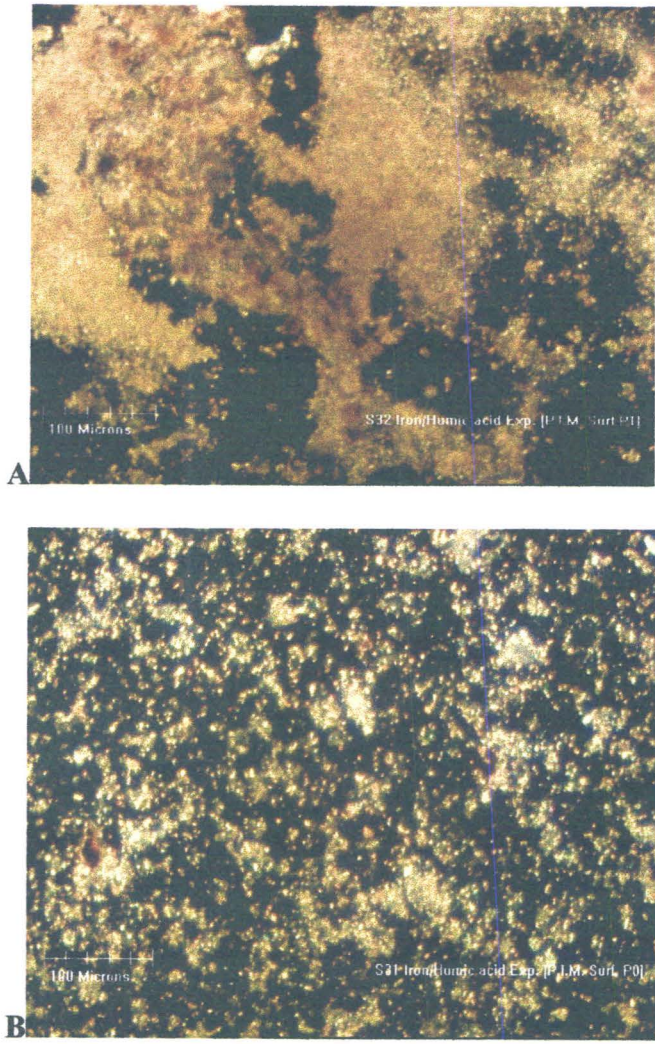


**Figure 12: Fe<sup>3+</sup>/humic acid A: in the dark and B: under UV**

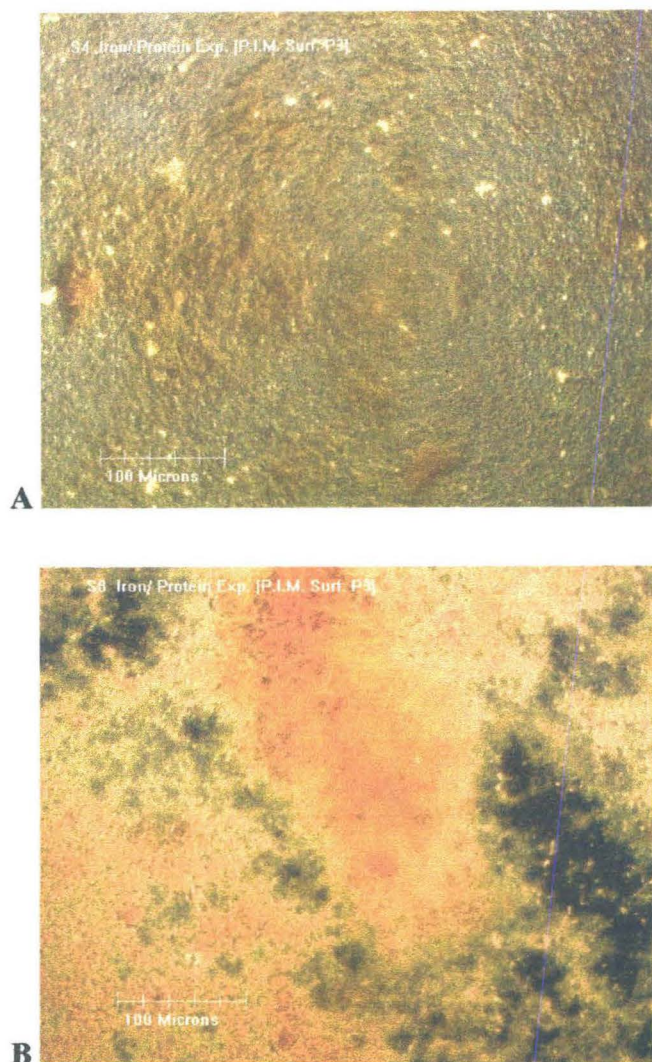


**Figure 13:  $\text{Fe}^{3+}$  (10 mg/L) / HSA (100mg/L) A: in the dark and B: UV**

### **2.4.3. Characterization of Fouled Slides**

X-ray photoelectron spectroscopy was used to provide some insight regarding the chemical nature of the fouling on the dark and UV-exposed slides. Slides fouled by the quaternary mixture (Fe/Ca/humic acid/HSA) in the dark and exposed to UV were shown to be quite distinct in their fouling patterns. The fouling layer on the UV slide was

sufficiently thin (XPS penetrates about 70-100Å<sup>14</sup>) that the underlying silicon signal from SiO<sub>2</sub> could be seen (41atom% SiO<sub>2</sub> present). By contrast, the dark slide showed only a small quantity of silicon, indicating the thickness of the fouling layer was almost at the maximum penetration depth of the instrument (7atom% SiO<sub>2</sub>). To more easily compare the nature of the two films, the results were normalized to 100% after removing contributions from SiO<sub>2</sub> (Figure 14). Two features are immediately apparent: there is much more nitrogen (attributed to the protein) on the dark slides and much more iron on the UV slides in both an absolute and relative sense. This indicates very different fouling films in the two cases. In both cases, there remains significant amounts of both carbon and oxygen, which may be attributed to humic acid constituents.

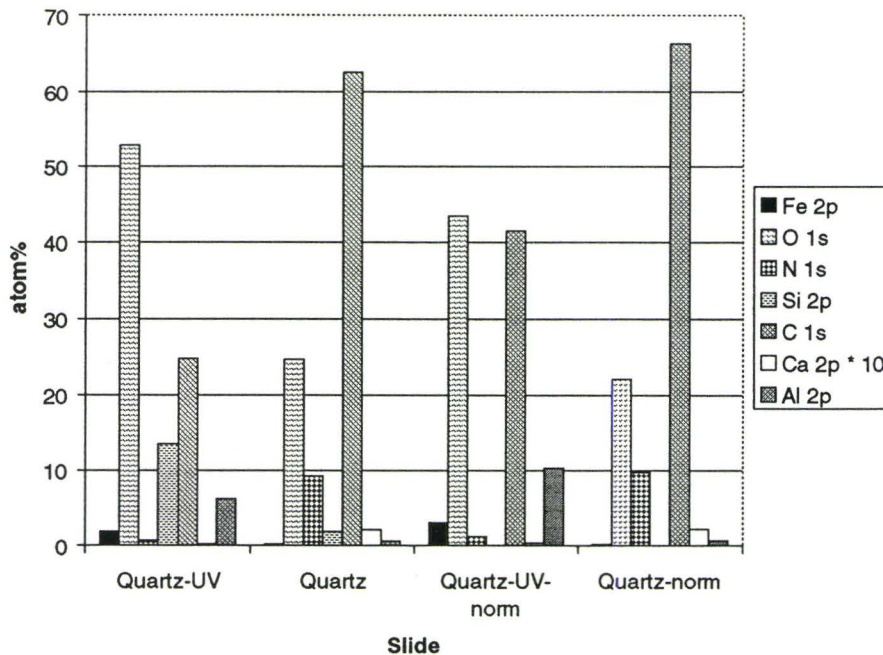


**Figure 14: Raw and Normalized (norm) XPS data from dark and UV-exposed Quartz Slides Exposed to the Quarternary Mixture (Fe/Ca/humic acid/HSA).**

### 2.4.3.1. Aged Solution Experiment

A minimum in UV transmittance through slides was observed after about 24 hours in solutions that contained both proteins and iron (e.g., Figure 10). The subsequent improvement in transmittance could arise from sloughing of the fouling layer from the substrate, a change in the nature of the fouling solution as a function of age or a change in the surface-bound layer. In an attempt to discriminate between these possibilities, a comparison was made between the fouling of a fresh solution of  $\text{Fe}^{3+}$  / HSA /  $\text{Ca}^{+2}$  / humic acid and an identical solution that had been aged a day before coming in contact with the quartz. It can be clearly seen from Figure 15 that the older solution fouled to a significantly lower degree.

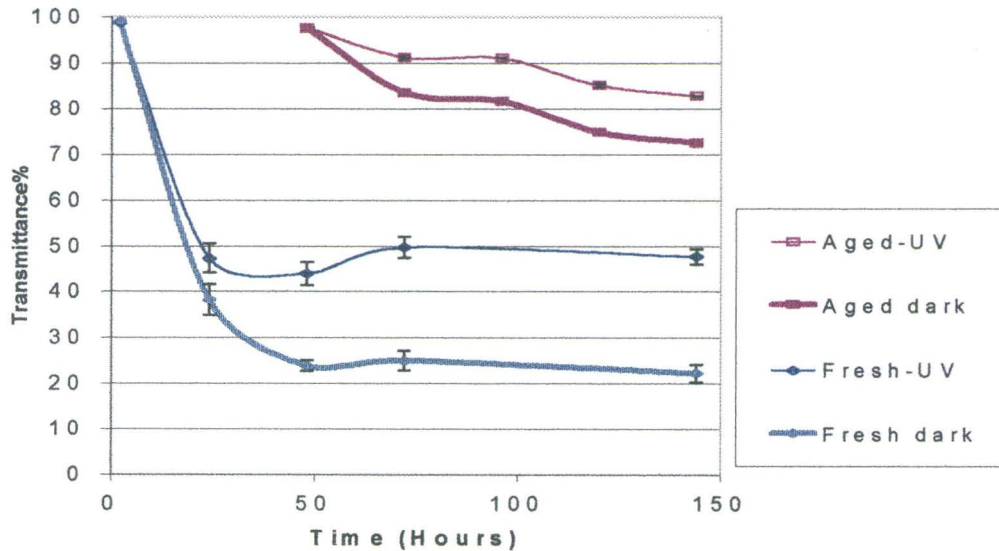


**Figure 15: Fouling of quartz by an Fe/Ca/humic acid/HSA mixture as a function of fouling solution age**

#### 2.4.4. Effect on of Flow Rates on Fouling

The final parameter to be examined in the study of fouling was the flow rate of the solution. Typically, wastewater streams have a relatively high velocity (approximately  $0.1-1 \text{ m/s}^{15}$ ), such that the exposure time of the sample to the disinfecting UV light is approximately 1-10 s. To examine the effect of flow rate, experiments were conducted at three different velocities in the reactor: 0 mL/min, 140 mL/min and 500 mL/min. These data demonstrated that fouling is reduced at stagnant and higher flow rates (500 mL/min, which corresponds to approximately  $1.2 \times 10^{-2} \text{ m/s}$ ), but is much worse at 140 mL/min ( $\approx 3.3 \times 10^{-3} \text{ m/s}$ ). This clearly points to an optimal flow rate at which fouling is minimized, either in the presence of UV light of the dark.

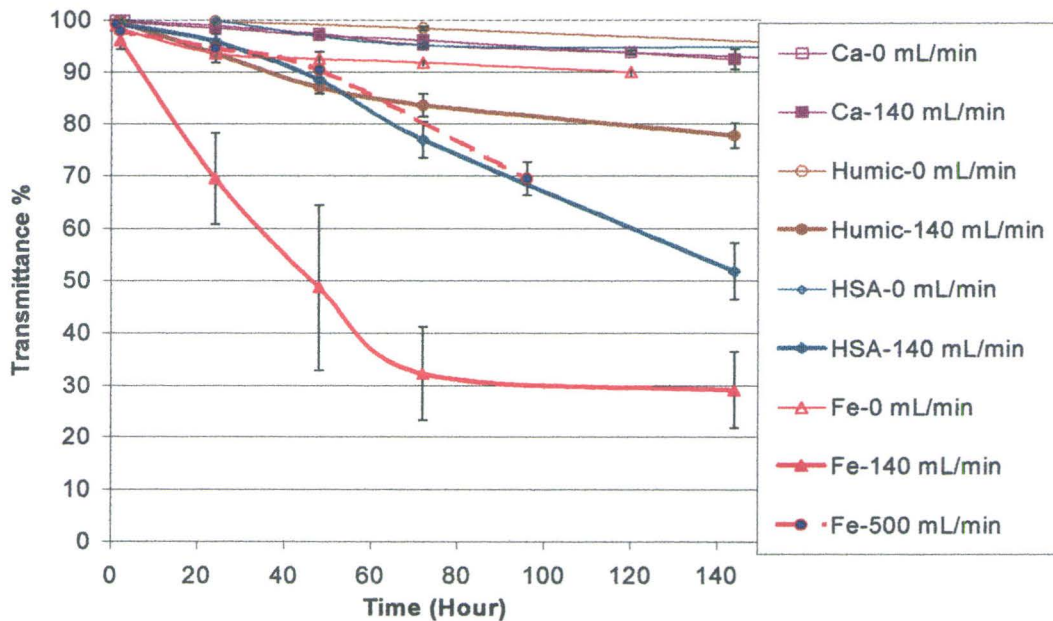


**Figure 16: Fouling by several different foulants fouling at solution in two different flow rates**

## 2.5. Discussion

$\text{Fe}^{3+}$  is well known to those who disinfect wastewater by UV to be a problematic foulant due to its opacity to UV light. In this work, the deposition on quartz of iron and three other typical fouling agents was studied individually and in combination. Individually, neither calcium nor humic acid compounds were significant fouling problems, at least when judged by UV transmittance through the quartz slide at 254 nm; both can act to mitigate fouling by other contaminants. By contrast, HSA and particularly iron foul significantly in their own right and work cooperatively to facilitate deposition on the quartz surface. In the following discussion, several of the results above will be examined in turn. These include consideration of the interplay between foulants that facilitates fouling, the nature of the fouling layer, the events leading to fouling and finally, of most importance, we examine the role of UV light in reducing the fouling.

Iron oxide forms a slimy, adhesive film on surfaces, including quartz. This is difficult to remove mechanically when hydrated, and extremely difficult to remove once the film has dried.<sup>16</sup> Chemical means may be used to clean iron-fouled surfaces in practice.<sup>17</sup> Due to the high extinction coefficient of iron and iron oxides, the quartz surface dramatically reduces disinfection ability in wastewater treatment by UV as seen in Figure 8.

Proteins, particularly globular proteins such as albumin, are surface active materials. Removal of protein films is frequently more difficult once denaturation has occurred because of favorable protein/surface interactions.<sup>18</sup> The relatively minor loss of

transmittance through protein-fouled surfaces may be ascribed to the surface adsorption by the UV-active moieties, such as tryptophan, in the protein (Figure 8).

### **2.5.1. Mitigating Effect of $\text{Ca}^{2+}$ in $\text{Fe}^{3+}$ / $\text{Ca}^{2+}$ Mixtures**

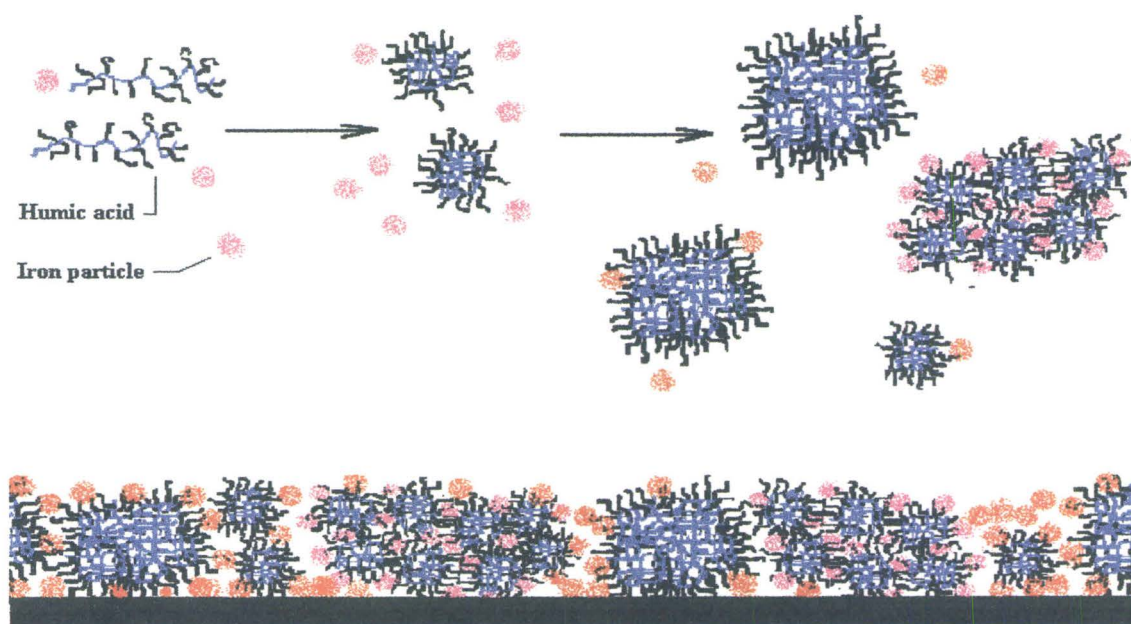
The level of fouling caused by the  $\text{Fe}^{3+}$  /  $\text{Ca}^{2+}$  mixture solution was found to be less than that caused by  $\text{Fe}^{3+}$  solution alone. Furthermore, the deposition on the surface consisted of small particulate domains (Figure 11). In crystallization fouling, it is known that pure salts usually form hard, compact deposits that bind tightly to the surface, while mixture of salts usually form soft and removable layers of the deposited materials.<sup>19</sup> This may be attributed to “primary heterogeneous nucleation,” a process in which spontaneous nucleation is readily achieved in the presence of trace impurities leading to the formation of small crystals instead of large crystals. Due to their larger surface area, the small crystals are more soluble. In addition, the presence of small crystals may favor “secondary heterogeneous nucleation”,<sup>20</sup> a process that usually takes place whenever fluid shear conditions exist. Under such conditions, the fouling mechanism can change to particulate (crystals) deposition rather than crystallization; crystal to crystal and crystal to surface collisions can take place, leading to more weakly bound deposits.

### **2.5.2. Interactions of Humic Acid with Multivalent Ions Including Iron and Calcium**

Humic acid is an ill-defined mixture of oxygenated organic materials. The carboxylate groups in humic acid can behave as ligands to multivalent metals that act as bridges.<sup>13,21</sup> Thus, as with the proteins (see below), high molecular weight aggregates

held together by iron ions or complexes can deposit on the quartz films. Because of the chelation of the humic acid, the iron is unable to form coherent iron oxide films.

Humic acid is also able to form “pseudomicelles” similar to those formed by synthetic detergents,<sup>22</sup> having non-polar cores and polar surfaces that make them water compatible. Such micelles can have detergent-like behavior at concentrations as low as 5-10 ppm. Due to variations in molecular size and composition of humic acids, a broad dispersity in micelle size and properties is generally observed. These micelles, and the humic constituents, compete with iron for the available surface area on the quartz slide. This can mitigate fouling by changing the effective character of the deposition surface, interfering with the coherence of an iron oxide film and providing a surface-active underlayer that facilitates removal of iron oxide films by mechanical/chemical means (Scheme 2); fouled materials can slough off the surface. The small particulate nature of the fouling deposit, clearly seen in Figure 12, is consistent with deposition and partial loss of humic acid/Fe aggregates, but is not consistent with a homogenous coherent film of iron oxide bridged by humic acid.



**Scheme 2: Models of humic acid interaction with the quartz surface/fouling layer.**

### 2.5.3. Complementary Interactions of $\text{Fe}^{3+}$ and HSA

Proteins possess a variety of ligands (carboxylates, thiols, imidazole groups) that can bind effectively to multivalent ions such as  $\text{Fe}^{3+}$ . It is, therefore, not unexpected to see enhanced fouling, as judged by opacity of the fouling layer to 254 nm light, over their individual fouling behaviors, when  $\text{Fe}^{3+}$  and HSA are mixed together. In the dark zone, the deposition of the material was quite heavy. Thick coherent films, rather than small, unassociated particulates, characterize the fouling. The differences in the presence of UV light, both the magnitude (Figure 9, Figure 10) and nature of fouling (Figure 13), are discussed below.

#### 2.5.4. Fe/HSA/humic acid

When humic acid is added to the iron/protein solution, its ligand character is manifested more than its surfactant behavior: fouling is exacerbated in both UV and dark films (Figure 10). Even thicker coherent films formed when humic acid was added to the  $\text{Fe}^{+3}$ /protein mixture, especially in the dark zone. The addition of calcium, another multivalent metal, in ternary or quaternary mixtures similarly aggravates fouling in both the UV and dark zones. In both cases, this is consistent with metals bridging the biopolymers. This facilitates aggregation of protein and humic acids in solution, their deposition on the surface, and leads to an improved stability of the resulting biofilm (Figure 10).<sup>23,24</sup>

While it is true that chelation would take place between protein molecules and the metal ions, still though the process of binding through ligand formation can take place as well and this will enhance the aggregation of the biopolymer molecules in general.

#### 2.5.5. Nature of the Fouling Layer

The UV transmittance data through the slides (Figure 8-Figure 13) provides a single value that provides no molecular insight into the nature of the fouling layer. The XPS data is more revealing. With a take-off angle of  $90^\circ$ , XPS can measure the top 70-100Å of a surface.<sup>14</sup> It is apparent from the data shown in Figure 14 that much less silicon from the underlying quartz is observed in “dark” slides than the UV-exposed slides; this is consistent with much thicker layers.

The elemental composition of the layers in the dark slides is also quite different from the UV-exposed slides. Much more iron is present in the UV-exposed slides in both an absolute and relative sense. While both the dark and UV-exposed slides have significant quantities of carbon and oxygen, only the dark slides are rich with nitrogen. These data are consistent with fouled layers of humic acid and iron in the UV slides and both protein and humic acid, bridged with iron and calcium (where present), on the dark slides.

In the presence of UV light, one must address that fact that protein-containing solutions foul more effectively than protein-free solutions, yet the resulting fouling films contain very little (protein-derived) nitrogen. One must further account for an enhanced absolute quantity of iron on the surface, when compared to the analogous dark slides. Finally, one must explain the observation that reduced fouling is associated with the  $\text{Fe}^{3+}$ /humic acid mixtures, but that enhanced fouling is observed from  $\text{Fe}^{3+}/\text{Ca}^{2+}$ /humic acid/HSA mixtures and that, on the UV slides, the resulting fouling film is mostly comprised of iron/humic acid (derivatives). These observations must be associated with the mechanism of deposition and/or subsequent reactions that differ between the UV and dark slides.

Iron and humic acid, when present, form complexes that foul the surface. For the reasons already noted, simple mixtures of iron and humic acid foul to a relatively low degree due to the surfactancy of the humic acid. However, when both protein and iron are present, aggregation in solution is followed by deposition on the quartz surface. Humic acid, when also present, can further facilitate the formation and deposition of aggregates.

In the absence of UV light, complex thick, coherent (Figure 13) biofilms, crosslinked with iron and calcium<sup>23</sup> (where present), build up. It should be noted that these sequestering events lead to prevention of well-defined iron oxide films or aggregates on the surface. These films comprise protein, humic acid, iron and calcium, as shown by XPS, but are primarily iron/protein mixtures.

In the UV-exposed slides, there is little evidence for nitrogen and thus for protein, yet the presence of protein greatly facilitates the fouling process. This phenomenon can be explained by considering the stability of proteins to UV light. Proteins undergo photodegradation,<sup>25</sup> leading to the formation of soluble organic fragments. This provides a mechanism to account for the near absence of nitrogen on the slides. Once deposited, the protein preferentially undergoes photoerosion into smaller, soluble fragments. Their departure disrupts the fouling matrix, leaving behind primarily iron and humic acid. The sequence of deposition/photoerosion further provides a route to large iron oxide aggregates. These account for the higher iron content, yet higher transmittance, found on the UV-exposed slides (Figure 14).

#### **2.5.6. Aging**

UV light is an important factor in reducing the magnitude of fouling as noted above. However, other factors are also clearly significant. "Day-old" solutions fouled far less efficiently than fresh solutions (Figure 15). Visual inspection the aged solutions showed heterogeneous iron oxide particulate of at least 100 microns in diameter. These

flocculated particles either don't efficiently deposit on the quartz surface, or are readily abraded from the surface by the flow of the solution.

### **2.5.7. Temporal Dependence of Fouling**

Two different fouling profiles were observed with all the slides; either there was a continuous decrease in transmittance to some minimum, after which no further fouling was noted, or, following a decrease in transmittance, there was an improvement to a new plateau (Figure 10). Dark slides, in particular, followed the latter profile after 24-48 hours, when the foulants included both protein and iron. This temporal dependence can be ascribed both to changes in the properties of the fouling solution and to the changes that occur on the fouled surface.

As noted above, aged solutions are able to foul less efficiently than fresh solutions. Thus, after approximately 24-36 hours, further fouling does not occur for the most part. Indeed, the particulate materials formed may aid in cleaning the surface by abrasion. This would account for the increase in transmittance after about a day. In addition, amelioration of the fouled surface results from protein degradation.

The fouling and photodegradation processes operate against each other. Initially, with a fresh solution, fouling occurs more rapidly than photodegradation of the fouled layer. However, the photodegradation continues to counteract fouling which, with time, becomes less efficient as the solution ages. The changeover point, when the photodegradation has the upper hand, occurs at about one to two days. While the photodegradation can improve the transmittance by removing proteinaceous material,

apparently it cannot assist in the removal of iron oxides, in spite of the ability of iron to undergo photoreduction to more soluble  $\text{Fe}^{2+}$  species.<sup>26,27</sup>

### 2.5.8. Flow Rate

The final factor examined in these studies was the effect of flow rate on fouling. The data in Figure 16 demonstrates that there is a fouling “sweet spot”. In the absence of flow, and at higher flow rates, the magnitude of fouling is much lower than at intermediate flow rates. Since the sequence of fouling has not been explicitly determined in these studies, one can only speculate the reasons for this dependence on fouling, particularly for soluble foulants. For particulate matter, however, these data suggest at high flow rates that particulate/surface collisions are too energetic to favor deposition. By contrast, at low flow, the electrostatic repulsion of the surface is sufficient to overcome attractive forces. Support for this proposition would require a study of deposition as a function of solution ionic strength.

These studies reveal some of the important factors in controlling the fouling of quartz surfaces by wastewater. The interaction of protein with iron, exacerbated by calcium, leads to the most profound fouling. Such constituents in a fouling solution cannot be avoided in practice. However, the studies suggest that design of treatment plants should extend, to the extent practically possible, the lifetime of the solution as much as possible before exposure to the quartz: aged solutions foul less. Furthermore, careful cleaning of the quartz sleeves is required following any “dark” cycle, as such surfaces are expected to be extensively fouled. Finally, reactor design must incorporate

considerations of flow to avoid the high fouling domain noted above at intermediate flow rates. With the information provided above, the control of fouling moves to surface cleaning and modification, which forms the basis of the following paper.<sup>28</sup>

## **2.6. Conclusions**

The examination of the deposition on quartz of four prototypical foulants found in wastewater surfaces has shown that the interaction of proteins with multivalent metals, particularly iron, is the most significant fouling problem for UV wastewater disinfection systems: fouling causes dramatic loss of UV transmission through quartz. The presence of UV light during the fouling process reduces the magnitude and changes the nature of the fouling layer; the deposition of the foulant is much less coherent in the presence of UV. This is attributed to the photodegradation of the protein components of the fouling layer, which allow for partial recovery of the transmittance. Other contributing factors to the magnitude of fouling were shown to be the flow rate, the dependence of which follows a parabolic function, and the age of the fouling solution; older solutions foul quartz much less severely.

## **2.7. Acknowledgments**

We acknowledge with gratitude financial support for this work from Trojan Technologies and Materials and Manufacturing Ontario. We further thank Trojan Technologies for providing access to fouling reactors of three different geometries and to their instrumentation, including the optical microscope.

## 2.8. References

- <sup>1</sup> Even in developed countries, problems with water purity can have disastrous consequences. Seven people died and hundreds were made sick by *E. coli* in drinking water in Walkerton, Ontario, Canada in May 2000. Improper water purification following heavy rains in an intensive agricultural area has been accepted as the cause of this tragedy.
- <sup>2</sup> <http://www.walkertoninquiry.com/index.html>.
- <sup>3</sup> Cohn, P. D., Cox, M. and Berger P. S., "Health and Aesthetic aspects of water quality" in *Water quality and treatment: a handbook of community water supplies*, American Water Works Association, edited by Letterman, R. D., McGraw Hill: New York, Chap. 2, 254 (1999).
- <sup>4</sup> Oliver, B. and Carey, J., *J. Water Pollution Control Fed.*, 48, 2619 (1976).
- <sup>5</sup> Lappin-Scott, H. M. and Costerton, J. W., *Biofouling*, 1, 323 (1989).
- <sup>6</sup> Meyer, A. E., Baier, R. E. and King, R. W., *Can. J. Chem. Eng.* 66, 55 (1988).
- <sup>7</sup> Maarschalkerweerd, J. M., *US Patent 5,504,335* (to Trojan Tech.), 1996;  
Maarschalkerweerd, J. M., *US Patent 4,482,809* (to Trojan Tech.), 1984;  
Maarschalkerweerd, J. M., *US Patent 4,872,980* (to Trojan Tech.), 1989;  
Maarschalkerweerd, J. M., *US Patent 5,590,390* (to Trojan Tech.), 1996.
- <sup>8</sup> Van Attekum, P. M. T. and Trooster J. M., *J. Electron. Spectrosc. Relat. Phenom.* 11, 363 (1977).

- <sup>9</sup> Berresheim, K., Mattern-Klossen, M. and Wilmers, M., *Fresenius J. Anal. Chem.* 341, 121 (1991).
- <sup>10</sup> Seah, M. P., *Surf. Interface Anal.* 14, 488 (1989).
- <sup>11</sup> Blatchley III, E. R., Johnston, C. T. and Lin, L., *Water Res.* 33, 3330 (1999).
- <sup>12</sup> Letterman, R. D., Amiratharajah A. and O'Melia, C. R., "Coagulation and Flocculation" in *Water quality and treatment: a handbook of community water supplies*, American Water Works Association, edited by Letterman R. D., McGraw Hill: New York, Chap. 6 (1999).
- <sup>13</sup> Cotton, F. A., Wilkinson, G., *Advanced Inorganic Chemistry*, 3<sup>rd</sup> Ed., Wiley: New York, Chap. 35, pp. 855-868 (1972).
- <sup>14</sup> Andrade, J. D., *X-ray Photoelectron Spectroscopy, Surface and Interfacial Aspects of Biomedical Polymers*, Plenum: New York, Vol. 1, pp 105-195 (1985).
- <sup>15</sup> William Cairns, Trojan Technologies, personal communication.
- <sup>16</sup> Ketelson, H. and Brook, M. A., *US Provisional Patent Application*, T8465796 (to Trojan Technologies), 2000.
- <sup>17</sup> Maarschalkerweerd, J. M., *US Patent* 5,418,370 (to Trojan Tech.), 1995.
- <sup>18</sup> Norde, W., *Adv. Colloid Int. Sci.* 25, 267 (1986).
- <sup>19</sup> Panchal, C. B. and Knudsen, J. G., *Adv. Heat Transfer* 31, 431 (1998).

- <sup>20</sup> Bott, T. R., "Crystallization Fouling: Basic Science And Models" in *Fouling Science and Technology*, edited by Melo, L. F., Kluwer Academic Publishers: Dordrecht, pp. 251-260, (1988).
- <sup>21</sup> Characklis, W. G., *Biofouling Biocorros. Ind. Water Syst.* (Proc. Int. Workshop Ind. Biofouling Biocorros.) 7 (1991); Characklis, W. G., *Biotechnol. Bioeng.* 23, 1923 (1981).
- <sup>22</sup> Wandruszka, R. V. "The Secondary Structure of Humic Acid and its Environmental Implications", EPA report, R82-2832-010 (1999).
- <sup>23</sup> Norde, W. and Fabier, J. P., *Colloids Surf.*, 87, 64 (1992); Arntfield, S. D., *ACS Symp. Ser.* 650(Macromolecular Interactions in Food Technology), 82 (1996); Magdassi, S. and Garti, N., *Surfactant Sci. Ser.* 39(Interfacial Phenom. Biol. Syst.), 289 (1991).
- <sup>24</sup> Lappin-Scott, H. M. and Costerton J. W., *Biofouling* 1, 323 (1989); Vesser, J., "Adhesion and removal of particles I" in *Fouling Science and Technology*, edited by Melo, L. F., Kluwer Academic Publishers: Dordrecht, pp. 87-104, (1988).
- <sup>25</sup> Soltermann, A. T., Biasutti, M. A., Senz, A. and Garcia, N. A., *Amino Acids* 9, 123 (1995).
- <sup>26</sup> Faust B. C., "A Review of the Photochemical Redox Reactions of Iron(III) Species in Atmospheric, Oceanic, and Surface Waters: Influence on Geochemical Cycles and Oxidant Formation" in *Aquatic and Surface Photochemistry*, edited by Helz, G. R., Zipp, R. G. and Crosby, D. G., Chap.1, p.14, Lewis Publishers: London, (1994).

<sup>27</sup> Waite, T. D. and Szymczak, R., 'Photoredox Transformation of Iron and Manganese in Marine Systems: Review of Recent Field Investigations" in *Aquatic and Surface Photochemistry*, edited by Helz, G., R., Zipp, R. G. and Crosby D. G., Chap. 2, 51, Lewis Publishers: London, (1994).

<sup>28</sup> Subsequent chapter in this issue.

### **3. The Role of Hydrophobic Coatings on Quartz Sleeves in the Mitigation of Fouling by Wastewater Streams**

#### **3.1. Abstract**

Wastewater disinfection using UV light is often compromised by fouling of the quartz surface of the UV-lamp. To determine if such fouling could be mitigated by low energy surfaces, quartz surfaces were rendered hydrophobic using a series of silanes based on alkanes, alkenes, fluoroalkanes, and silicones. The modified surfaces were fouled with a model fouling solutions containing individually or as mixtures  $\text{Fe}^{3+}$ ,  $\text{Ca}^{2+}$ , human serum albumin and humic acid. The most significant fouling was observed in solutions containing iron and protein; calcium exacerbated such fouling. Essentially no difference between the quartz and modified-quartz slides with respect to the magnitude of the fouling, the physical appearance of the fouled surfaces using optical microscopy, nor the elemental composition of the films by XPS could be observed. However, there was lower adhesion, as expected, between the fouling layer and the underlying surface in the case of hydrophobically-modified quartz. Extensive cracking of the fouled layer took place only on the modified surfaces, which were also more amenable to cleaning by pressurized water. These results suggest that while mitigation of fouling by mechanical or chemical cleaning is easier with modified surfaces, a reduction in the magnitude of the fouling does not accompany such modifications.

### 3.2. Introduction

UV radiation has been adopted as a reliable, environmentally safe tool for water disinfection.<sup>1</sup> As noted in the accompanying paper,<sup>2</sup> one of the practical problems associated with water treatment systems of this type is the occurrence of fouling on the external surface of the quartz sleeves that surround the UV lamps. Such fouling reduces the transmission of light into the water to be treated and, thus, the efficiency of disinfection.

Many types of fouling<sup>3,4</sup> are known, including crystallization or precipitation fouling,<sup>5,6</sup> particulate fouling, fouling due to chemical reactions, and corrosion fouling. The deposition of iron oxide films, which on quartz sleeves are known to be very opaque to UV irradiation at the operating wavelength of 254 nm, fall into one or more of these classifications. An important additional fouling mechanism in wastewater reactors is biofouling, in which biological materials are deposited or grow on surfaces.<sup>7,8,9</sup> These can include biomolecules, such as proteins, or living microorganisms including algae, bacteria and fungi (microbial fouling) on surfaces.<sup>10</sup> Both bio/organic and inorganic fouling are problematic in wastewater disinfection by UV.

In an attempt to minimize fouling phenomena on surfaces, many different chemical modification processes have been examined in detail, especially in the case of marine fouling. Traditional methods for the mitigation of fouling include lowering the surface energy to minimize adhesion (using materials such as silicone,<sup>11-15</sup> epoxy and Teflon,<sup>® 11,12</sup>), changing the surface potential,<sup>16</sup> or even grafting the surface with biocides or polymer layers that leach biocides,<sup>10</sup> such as copper<sup>17</sup> or tributyltin compounds,<sup>18</sup> to

affect the bacterial activity at the interface, which is believed to have a major role in biofouling processes.<sup>5,7,8,19</sup> Clearly, the leaching of biocidal materials from surfaces is not a viable option in applications involving water treatment, particularly the treatment of drinking water. However, it was of interest to determine if surface modifications that change surface activity on quartz surfaces would: i) mitigate fouling on quartz sleeves in UV water disinfection systems, and, ii) survive the intense UV irradiation associated with these reactors.

Any study of surface fouling must begin with a clear definition of the specific fouling system and the mechanism of fouling. Both fouling and biofouling processes are very sensitive to the nature of the surface, as well as to the chemical and biological composition of the solution<sup>2,8,20</sup> that constitutes the liquid phase at this solid/liquid interface. They can further depend upon temperature, flow rate, nature of the surface and finally, any specific chemical, biochemical, or physical interactions with the surface.

In previous work, we examined the fouling of quartz using an artificial fouling system containing  $\text{Fe}^{3+}$ ,  $\text{Ca}^{2+}$ , human serum albumin (HSA) and/or humic acid. The effect of UV light on fouling processes was also established and shown to decrease the magnitude of fouling. In those studies, the combination of protein and iron was most effective at fouling quartz surfaces. In this paper, we extend these studies to organically-modified quartz surfaces, using the same fouling mixtures. The objectives of the study were to determine whether such modifications can help reduce fouling and/or facilitate cleaning of the quartz surface.

### **3.3. Experimental section**

#### **3.3.1. Surface modification protocol**

A protocol involving three separate stages was developed to reproducibly modify the quartz coupons used in the fouling experiments: cleaning of the slide, application of the coupling agent or other surface treatment, and, the removal of any excess physically bound materials.

##### **3.3.1.1. Preparation of the Quartz Slides**

Quartz Slides (PSI<sup>®</sup> Supplies) of at least 85% UV transmittance at 254 nm were utilized. Slides were thoroughly cleaned by soaking in 5M hydrochloric acid solution for at least 2 days then rinsed thoroughly with distilled water and acetone, followed by 20 min oxidative cleaning using an Argon plasma glow discharge system Picotron<sup>™</sup> (Park Dental Research Corp.) immediately before the launch of the experiment. Contact angles (sessile drop, water) were recorded after removal from the plasma cleaning system. Measurements of the contact angle were carried out using NRL contact angle goniometer (model 100-00, Ramé Hart Inc.) using deionized distilled water (milliQ water). The slides were removed to a clean glass container and transferred to an oven where they were heated for 30 min at 110 °C, before being transferred to the modification apparatus. Contact angles measured for the clean slides were in the range of 2-3°.

##### **3.3.1.2. Surface Modification by Coupling Agents**

A novel silane coupling agent **10** was prepared as described elsewhere.<sup>21</sup> Silane coupling agents were applied in a special apparatus designed to maximize coating efficiency.

The apparatus (Figure 17) was constructed of Pyrex and designed to accommodate a standard microscope slide (upper part), with a magnetic stir bar to permit stirring during the surface modification process (lower part, Figure 17). The tube, containing the quartz slide and solution, was attached to a condenser and solution of the silane coupling agent in acetone (~ 4 % by weight) was refluxed at 56 °C for 24 h. The slide was removed, rinsed with acetone, and then dried in an oven at 110 °C for 3 h. The slide was finally cleaned by Soxhlet extraction using dried cyclohexane under nitrogen for 24 h. In case of multi-step modifications, such as hydrosilylation of a vinylsilane-modified surface (see next section), an additional Soxhlet step was used at each reaction step. Contact angles were measured for all the modified slides.

For the modification by Teflon<sup>®</sup>, drops of Teflon<sup>®</sup> AF 1601S (an amorphous fluoropolymer based on 2,2-bis(trifluoromethyl-4,5-difluoro-1,3-dioxole)) were wiped on the clean slide surface, after which the slide was incubated at 100 °C for 20 min and at 200 °C for a further 20 min.

### 3.3.2. Silicones Crosslinked on the Surface

For multiple-step modifications, the quartz slide was first refluxed in a ~4% solution of a small functional coupling agent, vinyltriethoxysilane (VTES) or vinyltrimethoxysilane (VTMS) in acetone for 24 h at 56 °C followed by Soxhlet extraction. In the second step, the surface-bound double bond was hydrosilylated in the usual apparatus with 4 wt% of the Si-H-containing silicone and 1-2 drops of Karstedt's catalyst (Pt divinyltetramethyl-disiloxane complex, Gelest) in either hexane or pentane, previously dried over anhydrous MgSO<sub>4</sub>. The solution was stirred overnight under

nitrogen, then the slide was rinsed with hexane and cleaned by Soxhlet extraction using dried cyclohexane for 24 h.

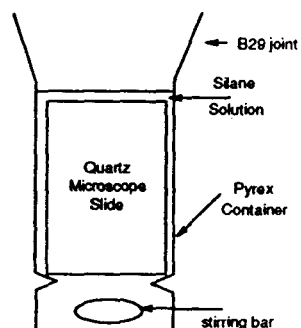
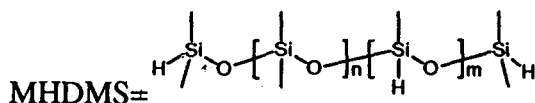


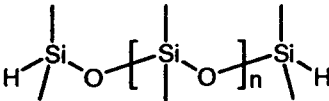
**Figure 17: Modification of Quartz Slides**

The coupling agents used to modify the quartz surfaces are listed in Table 2; average values of contact angle measured all over each slide (8-10 positions) are provided.

**Table 2: Chemical modification of quartz slides surface examined in fouling experiments.**

	Modifying agent	Slide	C.A.	St. dev.
	Vinyltriethoxysilane 1	1-D	66.8	1.8
Fe <sup>3+</sup> /		1-UV	66.5	1.8
humic acid	2-(Phenyldimethylsilyl)ethyltriethoxysilane	2-D	74.0	2.2
	2	2-UV	72.7	1.8
	<i>N</i> -Dodecyltrichlorosilane 3 <sup>a</sup>	3-D	99.6	1.3
		3-UV	97.0	0.5
Fe <sup>3+</sup> / HSA	Octadecyltrichlorosilane 4 <sup>b</sup>	4-D	97.0	1.1
		4-UV	97.6	0.7
	VTES-MHDMS (30-35%, 25-30cSt.) 5 <sup>a</sup>	5-D	105.2	1.3
	MHDMS≡	5-UV	106.0	1.1



Fe <sup>+3</sup> / HSA/ humic acid	Teflon <sup>®</sup> <b>6</b>	<b>6-D</b>	90.3	8.8
		<b>6-UV</b>	90.1	9.2
	VTES + PDMS-2H <sup>a</sup> n ≈ 6 (2-3 cSt.) (HSiMe <sub>2</sub> (OSiMe <sub>2</sub> ) <sub>n</sub> SiMe <sub>2</sub> H <b>7</b> )	<b>7-D</b>	95.8	2.4
	PDMS-2H = 	<b>7-UV</b>	96.3	3.4
Fe <sup>+3</sup> / Ca <sup>+2</sup> / HSA	VTES + PDMS-2H <sup>a</sup> n ≈ 80 (100 cSt.) <b>8</b>	<b>8-D</b>	97.2	3.4
		<b>8-UV</b>	103.3	1.6
	VTES + PDMS-2H <sup>a</sup> n ≈ 230 (500 cSt.) <b>9</b>	<b>9-D</b>	97.1	0.9
		<b>9-UV</b>	95.8	1.4
	Hydrosilylated squalene <b>10</b>	<b>10-D</b>	99.2	0.6
Fe <sup>+3</sup> /		<b>10-UV</b>	98.7	1.1
Ca <sup>+2</sup> / HSA / humic acid	Diphenylmethylchlorosilane <b>11</b> <sup>a</sup>	<b>11-D</b>	69.8	0.8
		<b>11-UV</b>	71.1	1.6
	<i>N</i> -Dodecyltriethoxysilane <b>12</b> <sup>a</sup>	<b>12-D</b>	97.6	1.5
		<b>12-UV</b>	97.0	1.7
	Tridecafluoro-1,1,2,2-tetrahydrooctyl- 1-triethoxysilane <b>13</b> <sup>a</sup>	<b>13-D</b>	95.2	0.8
		<b>13-UV</b>	93.5	1.12
	Bis(trimethylsiloxy)-methyl-(3-triethoxy- silylpropyl)silane <b>14</b>	<b>14-D</b>	84.8	3.8
		<b>14-UV</b>	85.9	4.6
	VTES + PDMS-2H <sup>a</sup> n ≈ 230 (500 cSt.) <b>9A</b>	<b>9A-D</b>	102.9	2.1
		<b>9A-UV</b>	101.9	1.2

<sup>a</sup> Gelest. <sup>b</sup> Aldrich

### 3.3.3. Fouling experiments

For a complete description of the fouling reactor system, see the accompanying paper in this issue.<sup>2</sup> A series of different solutions containing typical foulants found in wastewater were used to foul different sets of slides (Table 3). In all cases, a modified slide exposed to UV light was paired with a partner slide in the same relative position of the reactor, but in the dark (“dark” slides). With solutions containing both protein and iron, it was

necessary to use lower concentrations; otherwise, rapid, excessive fouling occurred making comparisons between experiments impossible. Approximately each 24 hours for several days, the slides were removed from the reactor, allowed to drain for 5 min, and the transmittances at 254 nm were measured. The results may be found in Figure 19- Figure 22 (thick lines represent “dark” slides, thin lines, UV-exposed slides). A list of the mixtures of foulants applied to each modified surface is given in Table 2.

**Table 3: Chemical composition of fouling solutions in fouling experiments with modified slides.**

Fouling agents	Fe <sup>+3</sup> mg/mL	Ca <sup>+2</sup> mg/mL	Humic acid mg/mL	HSA mg/mL
Fe <sup>+3</sup> / HSA	10	0	0	100
Fe <sup>+3</sup> / humic acid	10	0	50	0
Fe <sup>+3</sup> / HSA / humic acid	5	0	50	50
Fe <sup>+3</sup> / Ca <sup>+2</sup> / HSA	5	100	0	50
Fe <sup>+3</sup> / Ca <sup>+2</sup> / HSA / humic acid	5	100	50	50

#### 3.3.4. Cleaning of Fouled Slides

Selected slides from the Fe<sup>+3</sup>/HSA experiment were cleaned by abrasion with water. This process involved the exposure of half of the slide to a high-speed stream of water while the other half was protected from the water so it could act as an internal reference for the fouling deposit. The slides were mounted and fixed on a device to face the nozzle of a glass tube connected to a water supply that was adjusted to provide a stream of water of  $\approx 1.83$  m/s velocity. The water stream was directed at an angle to the surface of  $\sim 45^\circ$  and the targeted area was exposed for about 4 s to the stream; the

exposure was repeated 4 times. The slide was allowed to drain until fluid water was not visible on the surface and then measured for UV transmittance as indicated previously.

### **3.3.5. Optical Microscopy**

Images of some of the fouled slides were obtained using an optical microscope (Carl Zeiss Axiovert 25 CA, Empix Imaging Inc.). After removal from the reactor, selected slides were kept in a capped glass container until they were characterized (~3-4 weeks). Visual inspection showed many had cracked during drying. The microscope images were obtained in the polarized inverse (reflected) mode in the dark field, unless otherwise specified. The details are provided in the accompanying paper.<sup>2</sup>

### **3.3.6. X-ray Photoelectron Spectroscopy (XPS) of Fouled Surfaces**

Selected fouled surfaces were characterized by XPS (Leybold MAX 200 XPS). Slides were broken/cut into pieces less than 1 cm<sup>2</sup>. Unmonochromatized Al K<sub>α</sub> (15 kV and 25 mA) X-ray radiation was used as the excitation source. Features in the resultant low resolution spectra due to excitation from the weaker X-ray satellite lines, which are also present in the non-monochromatic source, were subtracted by use of an algorithm supplied with the instrument.<sup>22</sup> Atomic percentages of the elements present were derived from spectra run in a low-resolution mode (pass energy=192 eV), which were normalized to unit transmission of the electron spectrometer by means of a routine provided by the manufacturer.<sup>23</sup> The sensitivity factors used (O 1s = 0.78, N 1s = 0.54, C 1s = 0.34, Si 2p =0.40) were empirically derived by Leybold for the normalized spectra. Binding energies and peak areas were obtained by the use of the standard provided with the spectrometer.

The energy scale of the spectrometer was calibrated to the Cu  $2p_{3/2}$  (932.7 eV) and Cu 3p (75.1 eV) peaks, respectively, and the binding energy scale was then shifted to place the C 1s feature present at 285.0 eV.<sup>24</sup> Large-area analysis (2x4 mm or 4x7 mm) was performed so that exposure of the samples to the X-ray would be minimized while sufficient signal to noise ratios could be obtained for the spectral features.

### 3.4. Results

#### 3.4.1. Surface Modification and Fouling Experiments

Three classes of hydrophobic surfaces were prepared on the quartz slides: alkyl, aryl/alkyl or alkenylsilanes; fluoroalkylsilanes; and silicones. While all of these are low energy surfaces, their behavior, in surfactants for example, is quite distinct. Thus, it was of interest to establish if the magnitude of the fouling and, additionally, the ease of cleaning the different fouled surfaces were functions of surface properties of the modifying materials.

The application of the coupling agents was performed using standard techniques. Deposition of these silane agents was performed in acetone.<sup>25</sup> Soxhlet extraction with cyclohexane was used to remove ungrafted material following drying in the oven. Frequently, different control over surface modification is exhibited when trichloro- rather than trialkoxysilanes are used.<sup>26</sup> However, the degree of multilayer deposition was not determined in these cases. Instead, rapid proof of modification was obtained by contact angle goniometry. Two different reactions were used to build up silicone-modified surfaces. First, vinyltrialkoxysilane was grafted onto the quartz surface from acetone.

Second, hydrogen-terminated silicones were linked to the surface using Pt-catalyzed hydrosilylation (Scheme 3).<sup>27</sup>

Representative examples of the hydrophobic surfaces were exposed to different mixtures of foulants in an aqueous stream. The solutions passed over a series of quartz slides at about 140 mL/min ( $3.3 \times 10^{-3}$  m/s linear velocity) over approximately one week.<sup>2</sup> The reactor utilized was split into two streams such that one set of quartz slides was exposed to UV light (primarily 254 nm) while an analogous set of slides remained in the dark (Figure 7). Approximately every 24 hours, the transmission at 254 nm through each slide was monitored in a UV-vis spectrometer.

In the accompanying paper,<sup>2</sup> it was demonstrated that mixtures of protein (human serum albumin) and iron ( $\text{Fe}^{3+}$ ) led to the most severe fouling on naked quartz surfaces. The addition of  $\text{Ca}^{2+}$  exacerbated the fouling while humic acid had little effect. It was important to assess if the fouling patterns exhibited by these different mixtures of foulants on hydrophobic surfaces were comparable to the observations on bare quartz. Thus, a series of different hydrophobic coatings was challenged with different mixtures of the four foulants in both UV-exposed and dark domains to permit comparison of the fouling behaviors of these surfaces.

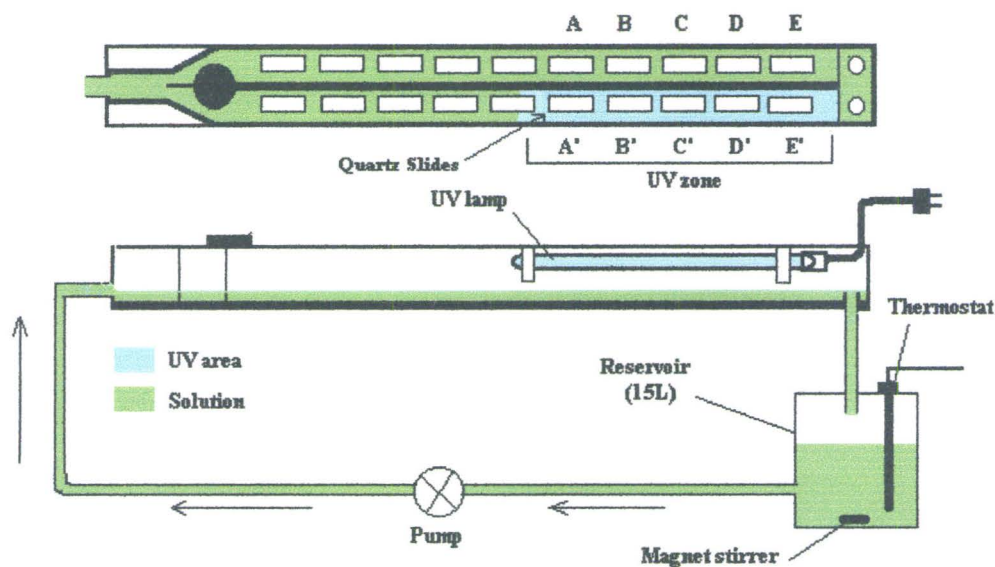
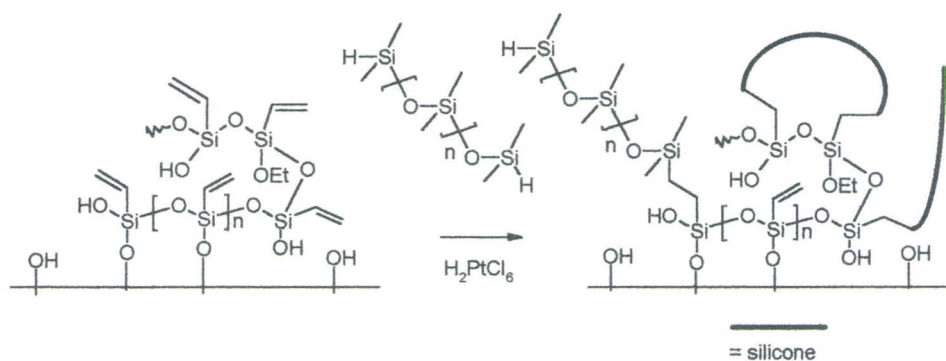


**Figure 18: Fouling Reactor**



**Scheme 3: Crosslinking polydimethylsiloxane by hydrosilylation on functionalized quartz surface with vinyltriethoxysilane**

Little difference in fouling by  $\text{Fe}^{3+}$  and humic acid could be discerned between bare quartz and surfaces modified by vinyltriethoxysilane **1** or 2-(phenyldimethylsilyl) ethyltriethoxysilane **2** (Figure 19), two compounds of relatively low hydrophilicity. The effect of UV light on the fouling efficiency was not very pronounced with this fouling mixture. If anything, the hydrophobic surfaces were more severely fouled than quartz

alone. This experiment provided the first clue that simple hydrophobic surfaces are not sufficient to ameliorate fouling in these systems.

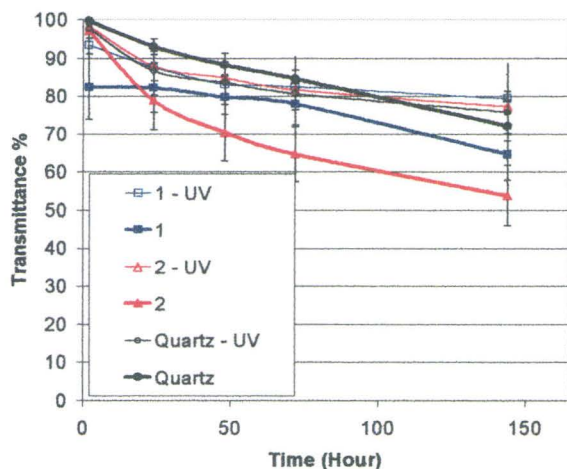


**Figure 19: Transmittance% versus time for fouling by  $\text{Fe}^{3+}$  (10 mg/L), and humic Acid (50 mg/L) in the absence and presence of UV Light (254 nm).**

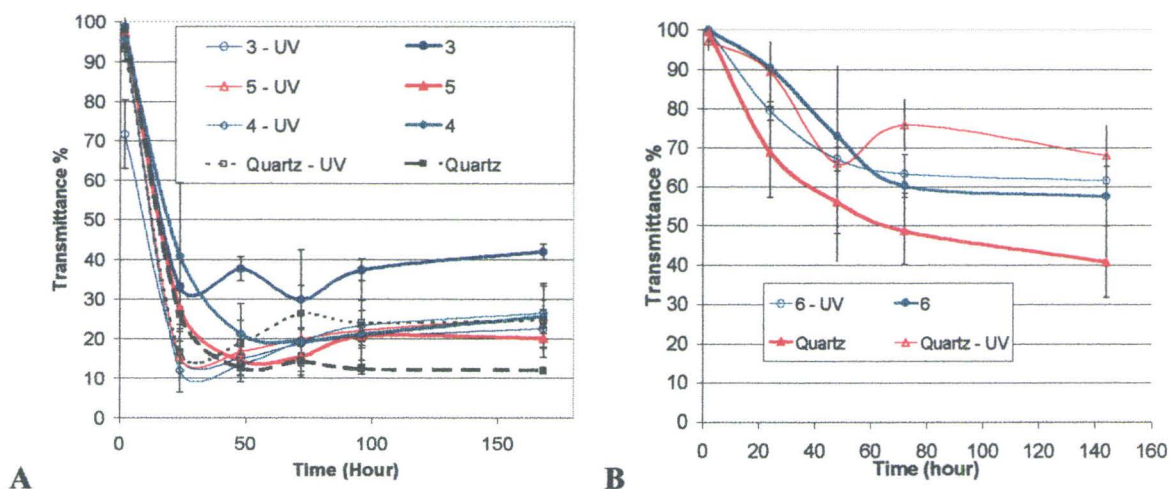


**Figure 20: Transmittance % versus Time for Fouling of A: 3-5-modified slides by  $\text{Fe}^{+3}$  (10 mg/L), HSA (100 mg/L), and B: 6-modified slides by  $\text{Fe}^{+3}$  (5 mg/L), HSA (50 mg/L), humic acid (50 mg/L) in the absence and presence of UV (254 nm)**

Little difference (Figure 20A) could also be discerned in the fouling behavior by  $\text{Fe}^{3+}$  / HSA mixtures on bare quartz, and quartz modified by dodecyltrichlorosilane 3, octadecyltrichlorosilane 4, or highly crosslinked silicone 5 (MW about 2000,

approximately 10 Si-H groups/chain). The alkyl groups, on perfect surfaces, are known to form brushes or complex interlayers that might be expected to form a repellent hydrophobic layer.<sup>28,29</sup> However, only the 3-D surface showed a significant and improved difference in fouling behavior to unmodified quartz. Even Teflon<sup>®</sup> 6, one of the lowest energy surfaces known,<sup>30</sup> was fouled (Figure 20B) by Fe<sup>+3</sup>/ HSA/ humic acid to a comparable level to the simple alkanes, silicone and unmodified surfaces (Figure 20A).

A series of silicone elastomers, which differed only in molecular weight, were grafted onto quartz slides. After deposition of vinyltriethoxysilane on the surface, hydride-terminated silicones of approximate molecular weights of 4507, 6000 8 and 17000 9, respectively, were bound by platinum-catalyzed hydrosilylation to the surface. These materials, which should vary considerably in thickness and “softness”, were exposed to a fouling solution of Fe<sup>+3</sup>, HSA and Ca<sup>+2</sup> (5 mg/L, 50 mg/L and 100 mg/L, respectively). As described above, these slides too were fouled at comparable levels to the unmodified quartz surface (Figure 21A).

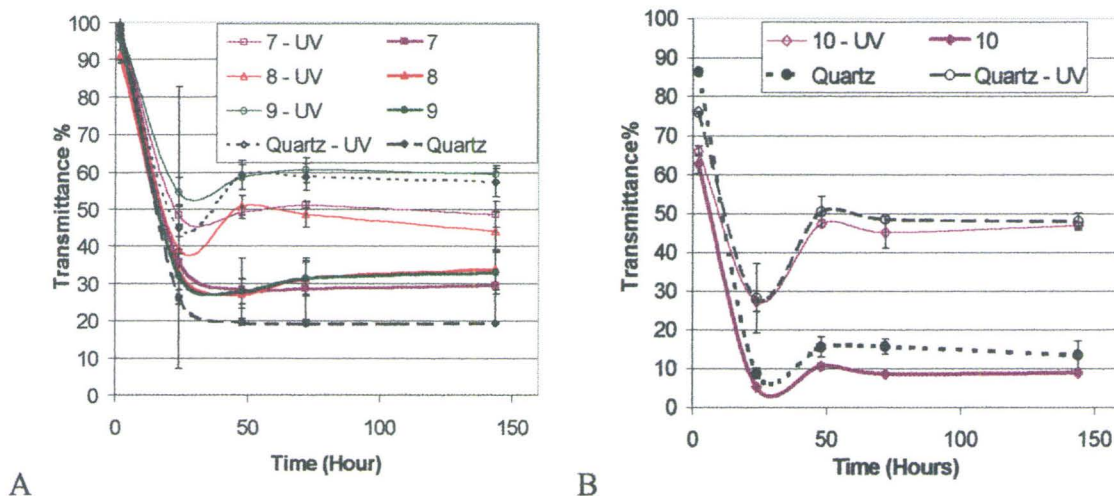
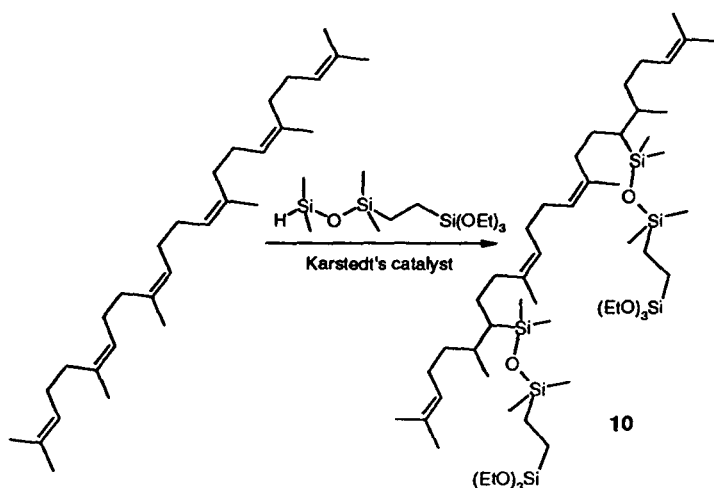


**Figure 21: Transmittance% versus time for fouling by  $\text{Fe}^{3+}$  (5 mg/L), HSA (50 mg/L),  $\text{Ca}^{2+}$  (100 mg/L) in the absence and presence of UV (254 nm). A: 7-9, quartz; B: 10, quartz.**

A novel coupling agent **10** was prepared from squalene (Scheme 4).<sup>21</sup> Of essentially hydrophobic character, the material possesses residual double bonds that are susceptible to oxidation. It displayed a broad UV-absorbance peak in the range 245-200 nm. Indeed, the reduction in transmittance resulting from the coupling agent layer was much greater than for the other coatings (*vide infra*, down to 65% from the 90% of an unmodified quartz slide) such that the normalization procedure generally used was compromised in this case.

This squalene derivative was screened for its antifouling activity against the quaternary mixture of  $\text{Fe}^{3+}$ ,  $\text{Ca}^{2+}$ , humic acid and HSA (5 mg/L, 50 mg/L, 50 mg/L and 100 mg/L, respectively). As shown in Figure 21B, the behavior of this surface completely paralleled that of the hydrophilic quartz. As with previous systems, fouling was more significant problem in the dark.



#### 3.4.1.1. Scheme 4: Hydrosilylation of squalene using Synthesis of 1,1,3,3-Tetramethyl-1((2-triethoxysilyl)ethyl)disiloxane

Other representative examples of the coatings described above were exposed to the same quaternary fouling mixture. Thus, surfaces modified with the monofunctional diphenylmethylchlorosilane **11**, dodecyltriethoxysilane **12**,  $\text{F}_3\text{C}(\text{CF}_2)_5(\text{CH}_2)_2\text{Si}(\text{OEt})_3$  **13**, the small trisiloxane **14** and the high molecular weight silicone elastomer **9A**, were examined for their ease of fouling. As seen in other systems, there was always more fouling in the dark than the UV region. However, different combinations of foulants deposited on the quartz and modified surfaces with similar efficacy. If anything, fouling of the hydrophobic systems under these conditions was worse, not better, than unmodified quartz.

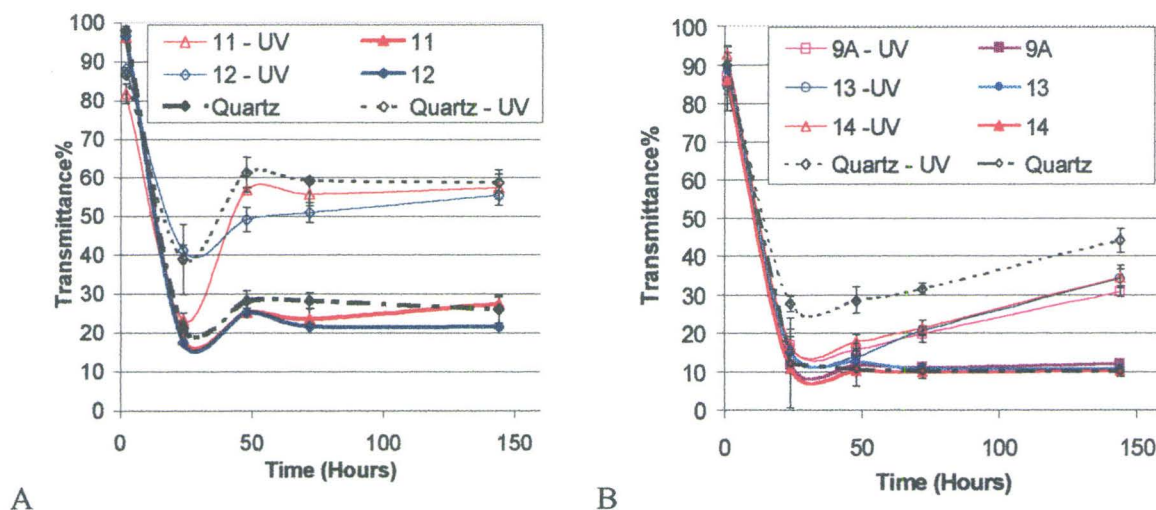


**Figure 22: Modified slides tested in  $\text{Fe}^{+3}$  (5 mg/L) /  $\text{Ca}^{+2}$  (100 mg/L) / Humic acid (50 mg/L) / HSA (50 mg/L) solution. A: 11,12,quartz; B: 9A, 13, 14, quartz.**

### 3.4.2. Surface Characterization of Fouled Slides

While it is clear that the fouling reagents contributed to decreased optical transmittance to various degrees, the actual nature of the fouling layer cannot be established from UV transmittance at 254 nm (nor conclusively from UV-visible spectroscopy, which were also recorded, data not shown). Two additional experimental techniques, optical microscopy and XPS, were used to shed some light on the nature of the fouling layer.

Using dark field optical microscopy, images of several fouled slides were obtained, including both modified and unmodified slides. Starting with unmodified quartz slides exposed to UV, it may be seen that iron/HSA solutions form films with transparent (dark areas) and translucent areas (Quartz - UV). By contrast, the analogous “dark” slide (Quartz) shows a heavy homogeneous deposit (Figure 23); no cracks in the fouling layers are seen in either film. Modified slides 3-D, 5-D, 4-D and 5-UV all exhibit cracks in the

deposited fouling layer (Figure 24, Figure 25). The cracks circled in images of slide 3-D show that these laminae were actually one unit prior to cracking. For a given fouling mixture the size of the cracks depends upon the nature of the modifying layer, as seen in Figure 25. The data are strongly suggestive that the forces of film shrinkage exceed the forces of adhesion between the deposited layer and the modified quartz surface. They further suggest that the presence of UV light can change the nature of the fouling layer and the magnitude of its adhesion to the surface (Figure 24 *versus* Figure 25).

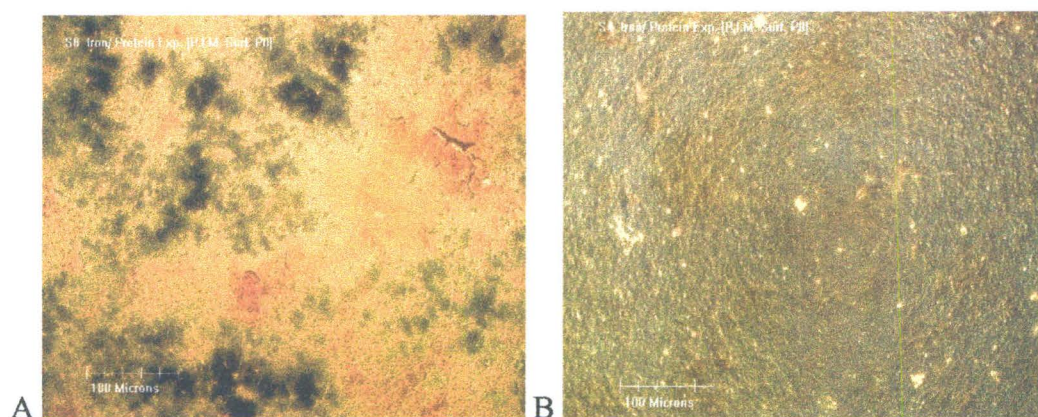


**Figure 23: Micrographs of partially dried fouled films (Fe/ HSA) A: Quartz – UV; B: Quartz.**

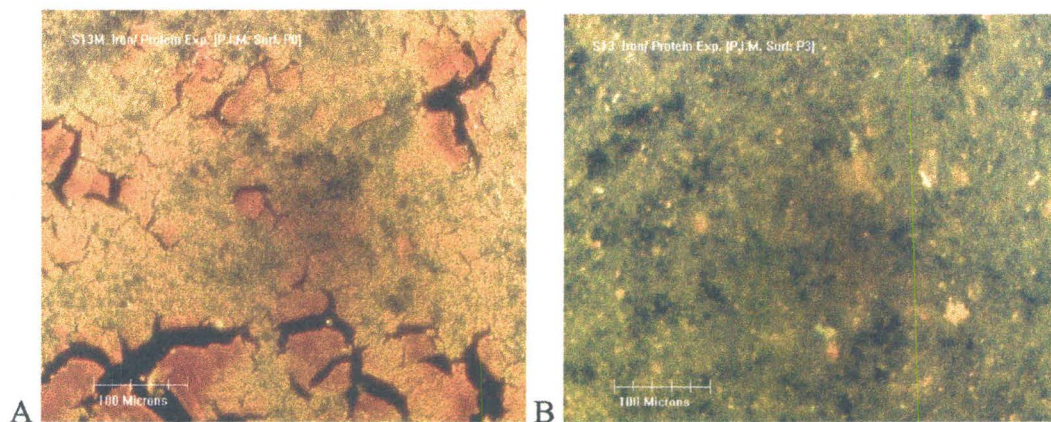


**Figure 24: Micrographs of partially dried fouled films (Fe<sup>+3</sup>/ HSA) A: 5-UV; B: 5-UV.**

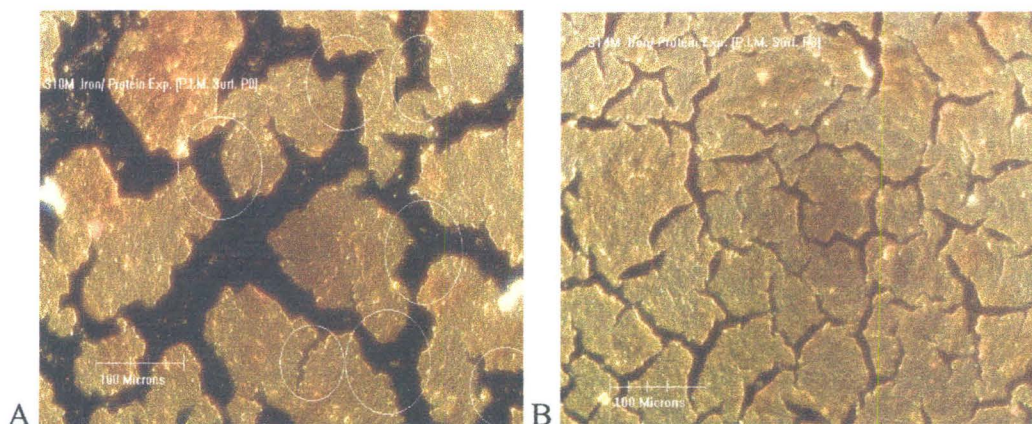


**Figure 25: Micrographs of partially dried fouled films ( $\text{Fe}^{+3}$ / HSA) A: 3-D; B: 5-D.**

The magnitude of fouling is much less severe in fouling from the  $\text{Fe}^{+3}$  (10 mg/L) / humic acid (50 mg/L) mixture (Figure 19). The nature of the fouling is also very different from the protein/HSA solutions shown above. Here, rather than coherent films, domains of small deposited aggregates are seen (Figure 26). While fouling from the UV zone is much lighter, the particulate nature of the fouling is readily seen for both UV and dark slides.

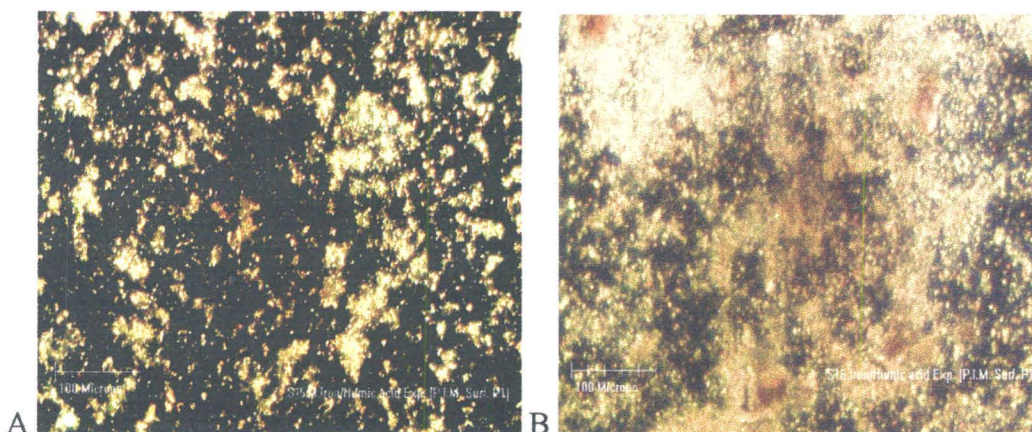


**Figure 26: A: Slides fouled by  $\text{Fe}^{3+}$  and humic acid. A: 2-UV; B: 2-D.**

A partial chemical analysis of the fouling deposits was undertaken using X-ray photoelectron spectroscopy (XPS) for slides fouled with the quaternary mixture

(iron/protein/humic acid/calcium, Figure 27). These data show clearly a higher silicon ratio for the (un)modified slides in the UV zone (Quartz, 10-UV, 11-UV, 13-UV) compared to the twins in the dark zone. This high silicon ratio is consistent with low deposition levels of foulants on the surface; XPS is directly measuring the quartz.

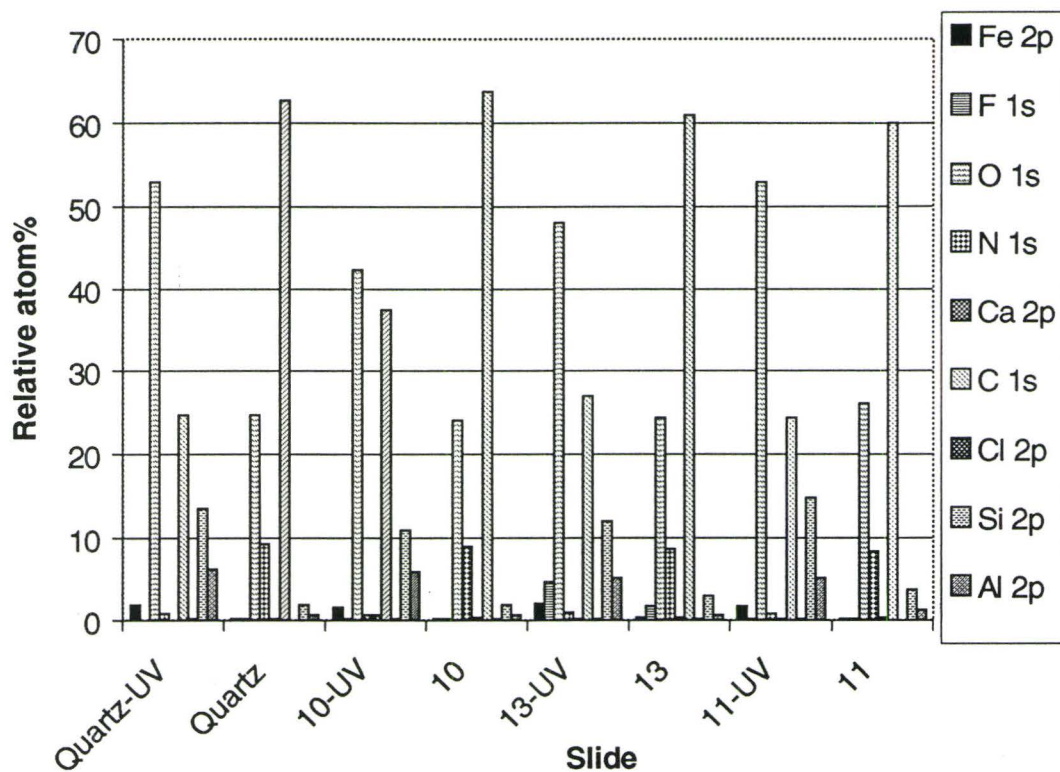


**Figure 27:** Low resolution XPS data of several slides fouled by  $\text{Fe}^{3+}/\text{Ca}^{2+}$ /humic acid/HSA.

In order to obtain a clearer elemental profile of the fouling layer, the contribution from  $\text{SiO}_2$  was excluded in each case and the remaining composition normalized to 100% (Figure 14). It is apparent that such a normalization introduces an error because there is Si/O content in the coupling agent and furthermore because the carbon levels are rather high for typical biopolymers. However, the similar magnitude of Si and O atom% prior to

normalization in the group of UV and dark slides, respectively, is indicative that this is a relatively minor error.

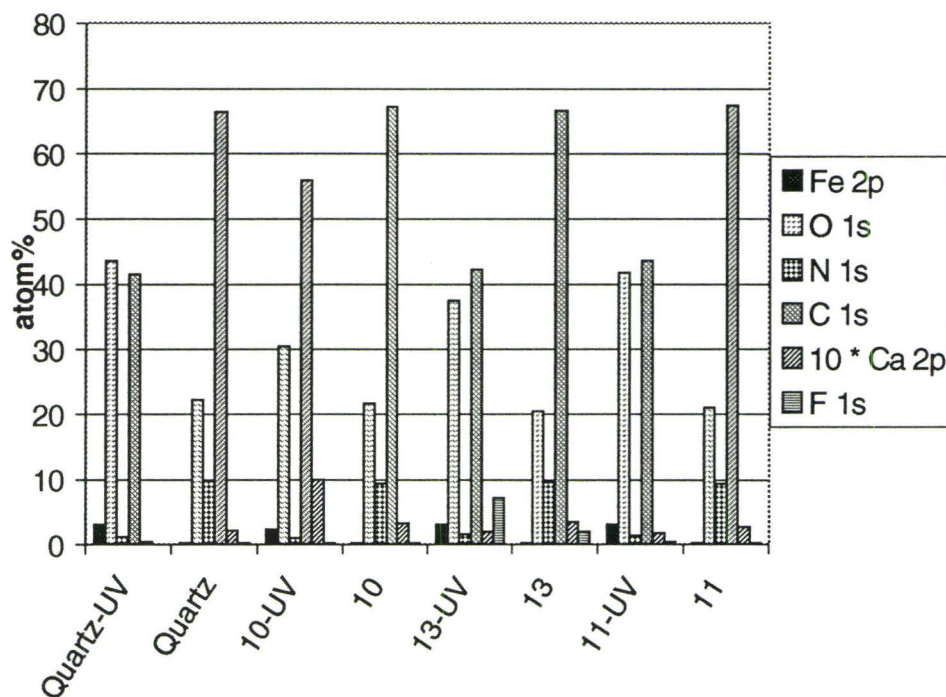


**Figure 28: XPS data excluding SiO<sub>2</sub> (quartz). Calcium values are shown 10 times actual value.**

Several trends are now readily apparent. The magnitude and nature of fouling on the dark slides are very different than the UV slides: for the remainder of this paper, we consider these two groups independently.

Protein deposition (nitrogen) is approximately 5 times higher in the dark slides. The O:N:C atom% contributions in HSA are *ca.* 21, 12, 67, respectively,<sup>31</sup> very close to the observed ratio in the dark slides, suggesting most of the fouling is due to protein. By contrast, the UV-opaque foulant Fe<sup>3+</sup> is present in much higher quantities in the UV slides. Very little protein is present on the surface of the UV slide as shown by the near

absence of nitrogen. Instead, oxygenated hydrocarbons are present in C:O atom% ratios appropriate for humic acids. Aluminum was also found in a higher ratio in the UV zone (a possible source of aluminum is the reactor itself; some parts are fabricated from aluminum and aluminum coupons were placed in some of the reactor positions). Calcium was found on fouled slides in the dark in higher ratios than on those fouled in the UV exposed slides. This is consistent with the incorporation of  $\text{Ca}^{+2}$  in the fouling deposit as an integral part of its structure (see below), rather than acting as individual foulant. Moreover, the XPS results clearly show a higher calcium ratio than iron on fouled slides in the dark (note: the fouling solution concentration ratio was  $(\text{Fe}^{3+}:\text{Ca}^{2+} 1:20)$ ).

#### **3.4.3. Cleaning of Fouled Slides**

In an attempt to establish if the fouled layers adhered to a lower degree to hydrophobic surfaces,<sup>11</sup> both quartz and modified slides were subjected to cleaning with a high pressure stream of water; half of each slide was left unexposed to the water so it could act as an internal reference for the fouling deposit. Results of the washing revealed that modified slides 3-D, 5-D, 4-D and 5-UV were partially cleaned by this process (improved transmittance ~ 5-10%). None of unmodified slides were improved by the same process (Figure 29). These experiments suggest that while the dark slides are more heavily fouled, the fouled layers adhere less well to the hydrophobically-modified surfaces than to the quartz. The observation that two of the three slides exposed to UV light do not yield the fouling layer under these conditions is further indication that the entire fouling process is different in the presence of UV light.

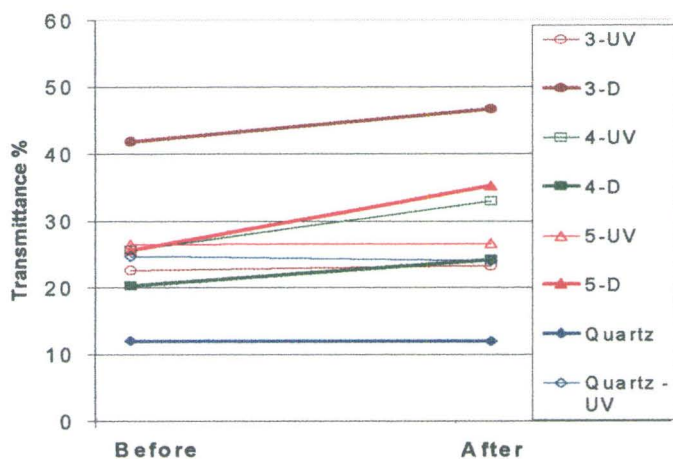


**Figure 29: Effect of the cleaning process on slide transmittance in  $\text{Fe}^{+3}$  (10 mg/L) / HSA (100 mg/L)**

### 3.5. Discussion

Several factors affect the magnitude and nature of the fouling on the quartz and modified quartz slides. These include the mixtures of foulants to which the surfaces were exposed, time of exposure, age of solution, presence of UV light and flow rate. Surprisingly, the nature of the surface modifying layer affected neither the amount of fouling layer formed as a function of the foulants present (Figure 19-Figure 22), its elemental composition (Figure 27, Figure 14), nor the type of film formed on the surface (Figure 23-Figure 26). Thus, rather than reiterate the previous discussion<sup>2</sup> involving these factors, we focus instead on the only observed difference between the behaviors of the quartz and modified quartz slides; adhesion.

#### 3.5.1. Temporal Dependence of Fouling: Interfoulant Adhesion

Both unmodified and modified slides exhibited two different fouling profiles; either i) there was a continuous decrease in transmittance to some minimum, after which no further fouling was noted, or, ii) following a decrease in transmittance, there was an

improvement to a new plateau (e.g., quartz *versus* 8-UV, Figure 21A). UV slides were more likely to show the transmittance recovery process and to a greater extent. Both modified and unmodified slides followed the latter profile to *very similar extents* after 24-48 hours, if the foulants included both protein and iron.

An explanation for the effect of UV light involves the photoablation of organic foulants on the surface. This would not only change the hydrophobic/hydrophilic balance of the surface, but will break down organic polymers into smaller, soluble fragments and disrupt the fouling matrix. The departure of such fragments, with metals complexed in some cases, readily explains for the observed temporal dependence of the transmittance (Figure 19, Figure 22). In addition, as noted in the accompanying paper,<sup>2</sup> this change can be ascribed to a change in the properties with the iron in particular over time by visual inspection: iron aggregates formed in solution may actually help abrade the surface and clean it.

### **3.5.2. Cleaning and Drying: Fouling Layer/Surface Adhesion**

Washing slides with a pressurized jet of water (much higher pressure than typical reactor flows) led to a minor (~5-10%) improvement in the transmittance of modified “dark” 3-D, 5-D and 4-D slides. Of the complementary UV slides, only 5-UV showed improved transmittance (Figure 29). Neither dark nor UV-exposed bare quartz slides could be cleaned by the same process. Thus, as expected in the case of hydrophobic surfaces, the adhesion of the fouling layer to the surface is less tenacious, although this lower adhesion is only noted under fairly vigorous flow conditions.

Optical microscopy was used to gain some additional information on the behavior of fouling layer. The images showed coherent films on quartz both in the UV and the dark. The layer on the UV slide was thinner and less well developed, with translucent and transparent sectors. On drying, no cracks formed, suggesting the adhesion between the fouling layer and the underlying quartz involves comparable or greater force to the interfoulant adhesion: a coherent, metal-crosslinked organic polymer layer is formed, which binds tenaciously to the quartz even after shrinkage due to drying (Figure 23).

Images of the hydrophobically-modified slides, after exposure to the same fouling mixtures, showed much different features. As already noted, fouling is always lighter in the UV-exposed slide. On drying, cracks propagate on both the lightly fouled UV slide and the heavily fouled dark slide, (Figure 24, Figure 25). The shrinkage forces that accompany the drying of water swollen polymers<sup>32,33</sup> (proteins and humic acids) are clearly greater than the adhesive forces of the fouling layer to the underlying hydrophobically modified surface. The laminae are very defined (see circles in Figure 25).

The process is schematically shown in Figure 30. After the fouling layer builds up to some critical thickness (1→3), crack propagation is initiated as the films start to shrink, ultimately leading to slides with good overall transmittance (4→6). This process does not require exhaustive drying (see experimental) and may proceed to some degree even during the fouling process under water. Cracks were always associated with areas of thick fouled layers: this is one reason that UV slides crack less; they are less heavily fouled than their dark counterparts.

**Proposed scheme for cracking process over fouled modified slide**

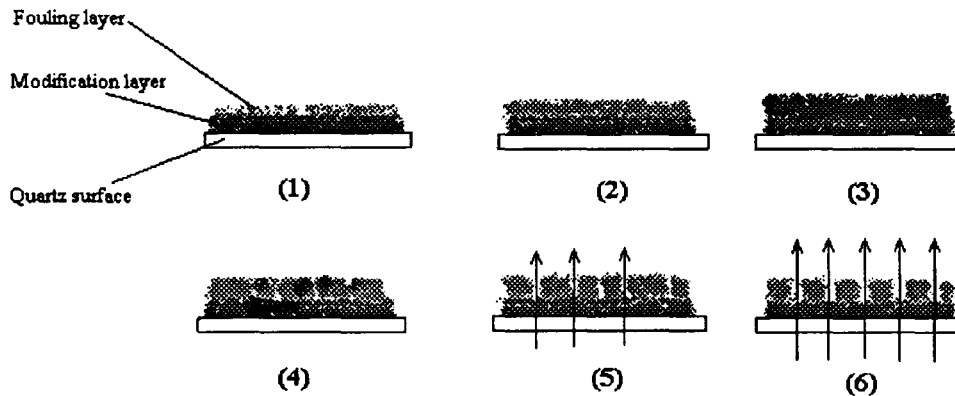


**Figure 30**

**3.5.3. Implications of these Studies on Fouling of UV-Reactors**

It was anticipated, based on extensive studies of marine fouling, that low surface energy coatings would mitigate the problems of fouling on quartz sleeves of UV lamps used for water disinfection. However, the presence of hydrophobic coatings was at best only a very minor factor in determining the magnitude and nature of fouling. The most profound variable was the presence of UV light, which reduced the level of the fouling overall, particularly by proteins. UV did not, however, suppress fouling by iron. Rather, the UV slides were more heavily fouled by iron.

Hydrophobic surface coatings did reduce the degree of adhesion of the fouling layer to the underlying quartz. This is an important observation, as it suggests that such coatings would facilitate removal of the fouling layer from the external surface of the sleeve by mechanical or chemical means. The long-term performance of these coatings, however, which will be exposed to intense UV irradiation, need to be assessed.

### 3.6. Conclusions

A wide variety of different silane agents were used to modify quartz surfaces in the expectation that reduced fouling would occur on a low energy surface. As with unmodified quartz surfaces, the hydrophobic surfaces generally fouled more severely in the dark than when exposed to UV light. However, the magnitude of the fouling of a variety of mixtures of different composition containing one or more of  $\text{Fe}^{3+}$ ,  $\text{Ca}^{2+}$ , humic acid and HSA was either the same or slightly worse with the hydrophobic surfaces than with the unmodified quartz. The major fouling species on dark slides were protein, humic acid and iron derivatives; on UV slides, iron complexed to humic acid or other non-nitrogenous materials were the main constituents found, as shown by XPS. This was the same behavior as on unmodified quartz surfaces. Cleaning of the hydrophobic surfaces was more facile in most cases than the unmodified quartz, indicating that the silane coupling agent did result in reduced adhesion of the fouling layer. This hypothesis was further reinforced by the lack of coherence, after drying, of the fouled films on hydrophobic surfaces; modified surfaces showed extensive film cracking. Thus, surface modification can improve the ability of quartz surface to be cleaned mechanically or chemically, extending their utility in UV disinfection systems. Hydrophobic coatings do not, however, change the fouling propensity of the quartz surface to typical wastewater foulants.

### 3.7. Acknowledgment

We acknowledge with gratitude financial support for this work from Trojan Technologies and Materials and Manufacturing Ontario. We further thank Trojan

Technologies for providing access to fouling reactors of three different geometries and to their instrumentation, including the optical microscope. Finally, we express our gratitude to Rana Sohdi, University of Toronto for the XPS measurements and for assistance with their interpretation.

### 3.8. References

- <sup>1</sup> Oliver, B. and Carey, J., *J. Water Pollution Control Fed.* 48, 2619 (1976).
- <sup>2</sup> Preceding chapter in this issue.
- <sup>3</sup> Vesser, J., “Adhesion and removal of particles I” in *Fouling Science and Technology*, edited by Melo, L. F., Kluwer Academic Publishers: Dordrecht, 87-104 (1988).
- <sup>4</sup> Hottinger, K. J., “Surface Bound Biocides – A Novel Possibility To Prevent Biofouling” in *Fouling Science and Technology*, edited by Melo, L. F., Kluwer Academic Publishers: Dordrecht, 233-239 (1988).
- <sup>5</sup> Panchal, C. B. and Knudsen, J. G., *Adv. Heat Transfer* 31, 431 (1998).
- <sup>6</sup> Bott, T. R., “Crystallization Fouling: Basic Science And Models” in *Fouling Science and Technology*, edited by Melo, L. F., Kluwer Academic Publishers: Dordrecht, 251-260 (1988).
- <sup>7</sup> Kent, C. A., “Biological Fouling: Based Science And Models” in *Fouling Science and Technology*, edited by Melo, L. F., Kluwer Academic Publishers: Dordrecht, 207-222 (1988).
- <sup>8</sup> Lappin-Scott, H. M. and Costerton, J. W., *Biofouling* 1, 323 (1989).

- <sup>9</sup> Kent, C. A. and Juddridge, J. E., "Microbial Fouling In Heat Transfer Surfaces in Cooling Water Systems" in *Harwell Report AERE-R 10065*, Harwell, U.K. (1981).
- <sup>10</sup> Hottinger, K. J., "Surface Bound Biocides – A Novel Possibility To Prevent Biofouling" in *Fouling Science and Technology*, edited by Melo, L. F., Kluwer Academic Publishers: Dordrecht, 233-239 (1988).
- <sup>11</sup> Swain, G. W., Nelson, W. G. and Preedeekanit, S., *Biofouling* 12, 257 (1998).
- <sup>12</sup> Swain, G. W., Nelson, W.G. and Preedeekanit, S., *Biofouling* 10, 187 (1996).
- <sup>13</sup> Nevell, T. G., Edwards D. P., Davis, A. J. and Pullin, R. A., *Biofouling* 10, 199 (1996).
- <sup>14</sup> Edwards, D. P., Nevell, T. G., Plunkett, B. A. and Ochiltree, B. C., *Int. Biodeterioration Biodegradation* 349 (1994).
- <sup>15</sup> Stein, J., Truby, K., Wood, C. D., Wiebe, D., Montemarano, J., Holm, E., Wendt, D., Smith, C., Meyer, A., Swain, G., Kavanagh, C., Kovach, B. and Lapota, D., *Polym. Prepr. (Am. Chem. Soc., Div. Polym. Chem.)* 42, 236 (2001); Dalton, H. M., Stein, J. and March, P. E., *Biofouling* 15, 83 (2000); Dalton, H. M.; Stein, J. and March, P. E., *Biofouling* 15, 83 (2000).
- <sup>16</sup> Kerr, A., Hodgkiess, T., Cowling, M. J., Beveridge, C. M., Smith, M. J. and Parr, A. C. S., *J. App. Microbio.* 58, 1067 (1998).
- <sup>17</sup> Armstrong, E., Boyd, K. G. and Burgess, J. G., *Biotechnol. Annu. Rev.* 6, 221 (2000).
- <sup>18</sup> Alzieu, C., *Ecotoxicology* 9, 71 (2000); Ten Hallers-Tjabbes, C. C., *Environ. Technol.* 18, 1265 (1997); De Mora, S. J. and Pelletier, E., *Environ. Technol.* 18, 1169 (1997).

- <sup>19</sup> Characklis, W. G., *Biofouling Biocorros. Ind. Water Syst.* (Proc. Int. Workshop Ind. Biofouling Biocorros.) 7 (1991); Characklis, W. G., *Biotechnol. Bioeng.* 23, 1923 (1981).
- <sup>20</sup> Meyer, A. E., Baier, R. E. and King, R. W., *Can. J. Chem. Eng.* 66, 55 (1988).
- <sup>21</sup> Brook, M. A.; Ragheb, A., *J. Adhesion*, submitted.
- <sup>22</sup> Van Attekum, P. M. T. and Trooster J. M. J., *Electron. Spectrosc. Relat. Phenom.* 11, 363 (1977).
- <sup>23</sup> Berresheim, K., Mattern-Klossen, M. and Wilmers, M., *Fresenius J. Anal. Chem.* 341, 121 (1991).
- <sup>24</sup> Seah, M. P., *Surf. Interface Anal.* 14, 488 (1989).
- <sup>25</sup> Brook, M. A., Ketelson, H. A. M., Pelton, R. H. and Heng, Y. M., *Chem. Mater.* 8, 2195 (1996); Ketelson, H. A. M., Brook, M. A. and Pelton, R. H., *Chem. Mater.* 7, 1376 (1995); Ketelson, H. A. M., Brook, M. A. and Pelton, R. H., *Polym. Adv. Technol.* 6, 335 (1995).
- <sup>26</sup> Brook, M. A., *Silicon in Organic, Organometallic and Polymer Chemistry*, John Wiley & Sons: New York, Chap. 10, 309-339 (2000).
- <sup>27</sup> Brook, M. A., *Silicon in Organic, Organometallic and Polymer Chemistry*, John Wiley & Sons: New York, Chap. 12, 401-413 (2000).
- <sup>28</sup> Netzer, L., *J. Am. Chem. Soc.* 105, 674 (1983); Kleisner, R. J., Koeck, B. H., Phillips, M. R., Wieland, J. A., Gutow, J. H., Boiadjev, V. and Tysoe, W. T., *Thin Solid Films*

- 381, 10 (2001); Fadeev, A. Y. and McCarthy, T. J., *Langmuir* 16, 7268 (2000); Huang, Z., Wang, P.-C., MacDiarmid, A. G., Xia, Y. and Whitesides, G., *Langmuir*, 13, 6480 (1997).
- <sup>29</sup> Al-Moussawi, H., Drown, E. K. and Drzel, L. T., *Polym. Compos.* 14, 195 (1993).
- <sup>30</sup> Owen, M. J., "Surface Chemistry and Applications" in *Siloxane Polymers*, edited by Clarson, S. J. and Semlyen, J. A., PTR Prentice Hall: Englewood Cliffs, NJ, Chap. 7, 309-372, (1993).
- <sup>31</sup> Extrapolated from: Bartzoka, V., Brook, M. A. and McDermott, M. R., *Langmuir* 14, 1892 (1998).
- <sup>32</sup> Costetron, W. J., Gessey, G. G. and Cheng, K. G., *Sci. Amer.* 238, 86 (1978).
- <sup>33</sup> Sutherland, I. W., "Polysaccharides in the adhesion of marine and freshwater bacteria" in *Microbial Adhesion to Surfaces*, edited by Berkeley, R. C. W., Lynch, J. M., Melling, G., Rutter, P. R., and Vincent, B., Chichester, Horwood, 329 (1980); Zhang, T. C. and Bishop, P. L., *Water Sci. Technol.* 29, 335 (1994); Strathmann, M., Griebe, T. and Flemming, H.-C., *Appl. Microbiol. Biotechnol.* 54, 231 (2000).

#### **4. Conclusions and Future Work**

Fouling is a serious problem that accompanies the process of wastewater disinfection by UV light; fouling causes dramatic loss of UV transmission through quartz and an attendant decrease in disinfection efficiency. In order to understand the chemistry of the quartz surface under fouling conditions, it was necessary to build a model fouling system on a laboratory scale to study fouling processes under controlled conditions and to examine each individual factor that affects the process. This objective was achieved, as a specific reactor was built and examined with several solution compositions that mimic the wastewater treatment UV disinfection system. The role of UV light, fouling solution composition, flow rate and age of the fouling solution on fouling were the factors of the process studied in this thesis.

The examination of the fouling layer on quartz of four prototypical foulants found in wastewater surfaces indicated that the interaction of proteins with multivalent metals, particularly iron, is the most significant fouling problem on quartz in UV wastewater disinfection systems. The presence of UV light during the fouling process was shown to reduce the magnitude of fouling and, more interestingly, to change the nature of the fouling layer; the deposition of the foulant became much less coherent in the presence of UV. Flow rate was also proven to be an important factor in fouling. The dependence of flow rate on fouling follows a parabolic function, suggesting the importance of avoiding

certain, intermediate flow rate values where the process is optimized. Finally, the age of the fouling solution was also shown to be important in the efficiency of the fouling process. It was demonstrated that older solutions foul quartz much less severely.

In an attempt to utilize surface modification to mitigate fouling, a wide variety of different silane agents were used to modify quartz surfaces with the expectation that reduced fouling would occur on a low energy surface. However, as with unmodified quartz surfaces, the hydrophobic surfaces generally fouled more severely in the dark than when exposed to UV light: there was little change in the fouling pattern as a function of surface modification.

XPS analyses have shown that the constitution of fouling layer on the modified slides was similar to that on the unmodified slides: the major fouling species on dark slides were protein, humic acid and iron derivatives; on UV slides, iron complexed to humic acid or other non-nitrogenous materials were the main constituents found. These results indicate that surface modification in a matter of fact did not affect the build up of the fouling layer in term of composition. However, it was shown in this work that cleaning of the hydrophobic surfaces was more facile in most cases than the unmodified quartz, indicating that the silane coupling agent did actually result in reduced adhesion of the fouling layer. This indicates that surface modification can improve the ability of quartz surfaces to be cleaned mechanically or chemically, and this would extend their utility in UV disinfection systems.

The findings in this work also suggest that by combining surface modification with suitable choice of flow rate, fouling mitigation would be more feasible, especially if

coupled with aging of the solution. We think that future research should focus on this direction, and also on putting new hydrophilic, flexible, responsive groups on the quartz surface that have even less adhesion with the fouling layer.

## 5. Appendix: Oxidizable Coupling Agents: Introduction of Surface Functionality<sup>1</sup>

### 5.1. Abstract

Alkylalkoxysilanes ( $\text{RSi}(\text{OR}')_3$ ) are frequently used to convert inorganic, siliceous surfaces into organic surfaces, the chemistry of which is dominated by the R group. There remains a need for silane coupling agents that are responsive to various types of stimuli, following which the hydrophobicity and the functionality of the surface change. In this paper, the synthesis and grafting to glass or quartz of silane coupling agents that are susceptible/responsive to oxidation is described. Hydrosilylation of the inexpensive polyolefin squalene occurred efficiently once or twice with the silane  $\text{HSiMe}_2(\text{CH}_2)_3\text{Si}(\text{OEt})_3$  to give a silane coupling agent possessing several alkene groups (the efficiency of the hydrosilylation of squalene with other hydrosilanes was highly structure dependent). Once grafted to a silica surface using traditional means, the coupling agent was oxidized in two different ways. First, epoxidation using soluble peracids led to polyepoxides that could be further modified by standard epoxide chemistry. Second, ozonolysis with gaseous  $\text{O}_3$  led to the ozonides, which could be decomposed to give either the aldehyde and ketone, or ketone and carboxylic acid groups, bound to the surface. The epoxides and carbonyl groups were characterized by the addition and condensation, respectively, of aromatic amines. These studies

demonstrate the ready portability of organic chemistry to silica (or related) surfaces using judiciously chosen silane coupling agents and the possibility of controlling surface adhesion by post-grafting oxidation.

## 5.2. Introduction

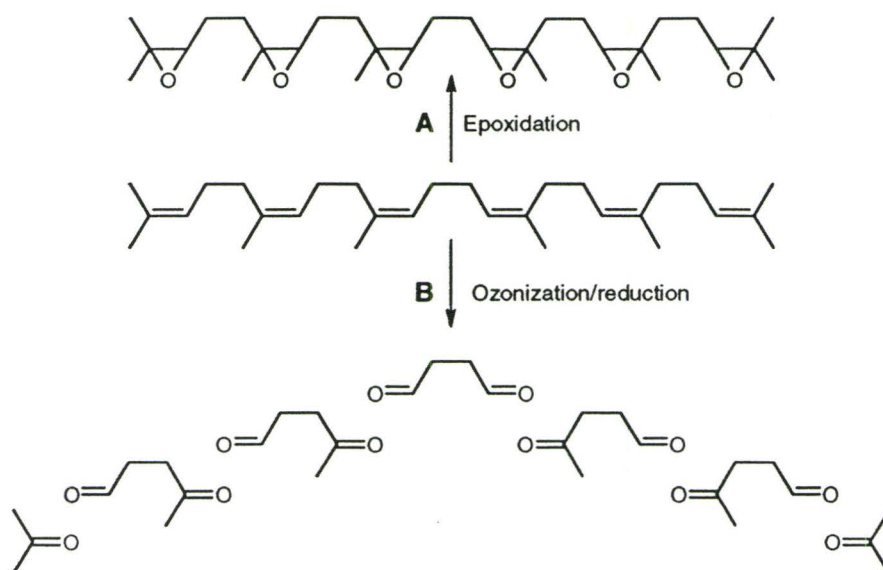
Silane coupling agents are widely used to change surface properties and promote the adhesion of substances to modified surfaces. For example, one of the major uses of silane coupling agents is the surface modification of fibreglass. The glass-resin composites are very strong, but the loss in laminate strength following prolonged exposure to moisture is problematic<sup>2</sup> unless the glass is first sized with silane coupling agents. Such changes lead to a reduction in moisture sensitivity and an enhanced adhesion of the resin to the glass fibres.

Generally, the best silane coupling agents in composites are those where the organofunctional group on silicon can efficiently react with thermosetting resins during curing.<sup>3</sup> In such systems, the coupling agent acts as a bidirectional glue between the surface and the matrix. Improved adhesion can result even when the surface is modified with agents that have no residual organofunctional groups.

Coupling agents that are responsive to specific stimuli are rare. The advantages that such compounds would give are related to the ability to change, on demand, the surface energy of the surface and thus the effective adhesion of materials to the modified surface. Our attention was drawn to the work of Puskas, which demonstrated the efficiency of epoxidized squalene as a highly functional crosslinkers (Scheme 5A).<sup>4</sup> It is apparent that

the hydrophobicity of the epoxy compound is very different to that of the starting squalene. Furthermore, the squalene could be expected to be readily oxidized using ozone<sup>5</sup> (Scheme 5B), which provides yet different hydrophobicity and access to new functional groups.

The objective of the work described below was to determine if groups possessing a sensitivity to oxidation could be grafted to siliceous surfaces. The approach utilized to prepare such oxidation-sensitive materials involved the modification of squalene. Thus, the hydrosilylation of squalene by a series of hydrosilanes was examined. The resulting coupling agents, and other coupling agents both commercial and synthesized by us, were grafted to quartz and glass surfaces. The fouling studies described elsewhere in this thesis were used to assess the magnitude in changes of the surface chemistry. In addition, in the case of the squalene-derived coupling agent, oxidative studies using ozone and peracids were undertaken. The physical and chemical changes that accompany these transformations were established.



**Scheme 5: Oxidation reactions of squalene.**

### 5.3. Experimental Section

#### 5.3.1. Materials

Quartz Slides (PSI<sup>®</sup> Supplies) of at least 85% UV transmittance at 254 nm; allyltriethoxysilane (Gelest), bis(trimethylsiloxy)methylsilane (Gelest), vinyltriethoxysilane (Gelest), vinyltrimethoxysilane (Gelest), 1,1,3,3-tetramethyldisiloxane (Gelest), methylhydrogen,dimethylsiloxane copolymer

$$\left( \text{Si} \begin{array}{c} | \\ \text{---} \\ | \end{array} \text{O} \left[ \text{Si} \begin{array}{c} | \\ \text{---} \\ | \end{array} \text{O} \right]_n \left[ \text{Si} \begin{array}{c} | \\ \text{---} \\ | \\ \text{H} \end{array} \text{O} \right]_m \text{Si} \begin{array}{c} | \\ \text{---} \\ | \end{array} \right)$$
 $m = 30\text{-}35\%$ , viscosity: 25-30 cSt) (Gelest), polymethylhydrosiloxane homopolymer (viscosity: 15-25 cSt.) (Gelest), PDMS-2H

$$\left( \text{HSiMe}_2(\text{OSiMe}_2)_n\text{SiMe}_2\text{H}, \begin{array}{c} \text{H} \\ | \\ \text{Si} \begin{array}{c} | \\ \text{---} \\ | \end{array} \text{O} \left[ \text{Si} \begin{array}{c} | \\ \text{---} \\ | \end{array} \text{O} \right]_n \text{Si} \begin{array}{c} | \\ \text{---} \\ | \\ \text{H} \end{array} \end{array} \right)$$
 $n \approx 6$  (2-3 cSt.),  $n \approx 80$  (100 cSt.),  $n \approx 230$  (500 cSt.), Gelest), anhydrous magnesium sulphate (BDH), platinumdivinyltetra-

methylidisiloxane complex (Karstedt's catalyst, Gelest), Teflon<sup>®</sup> AF 1601S (Dupont), cyclohexane (Caledon), pentane (Caledon), and squalene (Aldrich) were used as received.

### 5.3.2. Instrumentation

<sup>1</sup>H NMR and <sup>13</sup>C NMR spectra were recorded on Bruker AC-200 and AV-200 (at 200 MHz for protons and 50.3 MHz for carbon, respectively) Fourier transform spectrometers, respectively. <sup>29</sup>Si NMR spectra were recorded on a Bruker AV-300 spectrometer (at 59.6 MHz for silicon). Chemical shifts are recorded with respect to CDCl<sub>3</sub> as an internal standard and set at 7.24 ppm and 77 ppm for <sup>1</sup>H NMR and <sup>13</sup>C NMR, respectively. Coupling constants (for <sup>1</sup>H NMR) were recorded in ppm. The abbreviations s = single, d = doublet, t = triplet, q = quartet, dd = doublet of doublet, m = multiplet, are used to report the spectra.

Electron impact (EI) and chemical ionization (CI, NH<sub>3</sub>) mass spectra were recorded at 70 eV with a source temperature of *ca.* 200 °C on a Finnigan 4500 Mass Spectrometer. Electrospray ionization mass spectroscopy was performed using a Micromass Quattro LC.

Infrared spectra were recorded using BIO RAD FTS-40 Fourier spectrometer and UV transmittance was measured using Varian Cary-300 and Cary-50 Spectrophotometers, respectively.

An argon plasma glow discharge system from Picotron<sup>™</sup> (Park Dental Research Corp.) was used to clean the glass and quartz slides. Static (advanced) contact angles of a sessile

drop of deionized distilled water were measured using a NRLCA goniometer (model 100-00) (Ramé-Hart Inc.).

GC-MS analysis was carried out using a Hewlett-Packard model 5890 series II gas chromatograph equipped with DB-17 capillary column (30 m x 0.25 mm i.d. x 0.15  $\mu$ m film) (J&W Scientific). The detection system was a Hewlett-Packard model 5971A mass selective detector operated in full scan mode. The temperature gradient was from 50  $^{\circ}$ C to 200  $^{\circ}$ C with rates of 5  $^{\circ}$ C/min and injector temperature of 200  $^{\circ}$ C.

### 5.3.3. Preparation of Coupling Agents

#### 5.3.3.1. Synthesis of 2-(Phenyldimethylsilyl)ethyltriethoxysilane

In a 25 ml round bottomed flask was placed vinyltriethoxysilane (5.7 g, 0.30 mol) and Karstedt's catalyst (1 drop). The temperature was set to 0  $^{\circ}$ C before phenyldimethylsilane (4.5 ml, 4.14g, 0.03M) was added; the reaction was left overnight in a dry nitrogen environment at room temperature. Pure product was collected through vacuum distillation at 125 $^{\circ}$ C/2 mm Hg (yield: 7.53g, 81%).

$^1$ H NMR ( $\text{CDCl}_3$ ):  $\delta$  = 0.25 (s, 6H, Si ( $\text{CH}_3$ )<sub>2</sub>); 0.54 (m, 2H,  $\text{CH}_2\text{CH}_2\text{Si}(\text{OEt})_3$ ); 0.77 (m, 2H,  $\text{Si}_2\text{CH}_2\text{CH}_2\text{Si}(\text{OEt})_3$ ); 1.20 (t, 9H,  $J$  = 7.0 Hz,  $\text{CH}_3\text{CH}_2\text{O}$ ); 3.78 (q, 6H,  $J$  = 7.0 Hz,  $\text{CH}_3\text{CH}_2\text{O}$ ); 7.32 (m, 3H, ([2,4,6]- $\text{C}_6\text{H}_5$ )); 7.49 (m, 2H, [3,5]- $\text{C}_6\text{H}_5$ );  $^{13}\text{C}$  NMR ( $\text{CDCl}_3$ ):  $\delta$  = -3.7 (Si $\text{CH}_3$ ); 2.6 (Si $\text{CH}_2\text{CH}_2\text{Si}(\text{CH}_3)_2\text{Ph}$ ); 6.8 (Si $\text{CH}_2\text{CH}_2\text{Si}(\text{CH}_3)_2\text{Ph}$ ); 18.2 ( $\text{CH}_3\text{CH}_2\text{O}$ ); 58.4 ( $\text{CH}_3\text{CH}_2\text{O}$ ); 128.8 ([4]- $\text{C}_6\text{H}_5$ ); 133.6 ([2,6]- $\text{C}_6\text{H}_5$ ); 139.1 ([3,5]- $\text{C}_6\text{H}_5$ ).  $^{29}\text{Si}$  NMR:  $\delta$  = -46.1 (Si( $\text{OCH}_2\text{CH}_3$ )<sub>3</sub>); -1.8 (Si( $\text{CH}_3$ )<sub>2</sub>(Ph)); IR:  $\nu$  ( $\text{cm}^{-1}$ ) 3071, 3052, 2975, 2924, 2889, 1428, 1390, 1250, 1167, 1140, 1109, 1081, 957, 839, 813, 780, 727; MS

(EI):  $m/z = 311$  ( $M^+ - \text{CH}_3$ , 67); 249 ( $M^+ - \text{Ph}$ , 52); 163 ( $[\text{Si}(\text{OEt})_3]^+$ , 29); 135 ( $[(\text{CH}_3)_2\text{SiPh}]^+$ , 100).

### 5.3.3.2. Synthesis of bis(trimethylsiloxy)-methyl-(3-triethoxysilylpropyl)silane

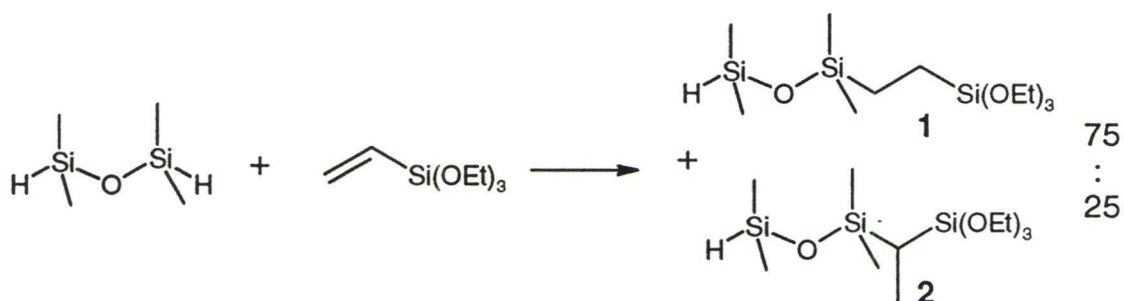
In a 25 ml round bottomed flask bis(trimethylsiloxy)methylsilane (3 g, 135 mol) was mixed with allyltriethoxysilane (2.756 g, 0.135mol). The temperature was adjusted to 0 °C before the addition of Karstedt's catalyst (1 drop). The reaction left stirring for ½ h at 0 °C, then left overnight at room temperature with stirring under nitrogen. The crude product was vacuum distilled at 100 °C/1mm Hg to give a clear colorless liquid (yield: 3.9 g, 68%).

$^1\text{H}$  NMR ( $\text{CDCl}_3$ ):  $\delta = -0.03$  (s, 3H,  $\text{CH}_3$ ); 0.06 (s, 18H, 6  $\text{CH}_3$ ); 0.58 (m, 2H,  $\text{CH}_2\text{CH}_2\text{CH}_2\text{Si}(\text{OEt})_3$ ); 0.62 (m, 2H,  $\text{CH}_2\text{CH}_2\text{CH}_2\text{Si}(\text{OEt})_3$ ); 1.20 (t, 9H,  $J = 7.0$  Hz,  $\text{CH}_3\text{CH}_2\text{O}$ ), 1.46 (m, 2H,  $\text{CH}_2\text{CH}_2\text{CH}_2$ ); 3.81 (q, 6H,  $J = 7.0$  Hz,  $\text{CH}_3\text{CH}_2\text{O}$ );  $^{13}\text{C}$  NMR ( $\text{CDCl}_3$ ):  $\delta = 0.3$  ( $\text{SiCH}_3$ ); 1.8 ( $\text{OSi}(\text{CH}_3)_3$ ); 14.4 ( $\text{CH}_2\text{CH}_2\text{CH}_2\text{Si}(\text{CH}_3)$ ); 16.6 ( $\text{CH}_2\text{CH}_2\text{CH}_2\text{Si}(\text{CH}_3)$ ); 18.3 ( $\text{CH}_3\text{CH}_2\text{O}$ ); 21.8 ( $\text{SiCH}_2\text{CH}_2\text{CH}_2\text{Si}$ ), 58.2 ( $\text{CH}_3\text{CH}_2\text{O}$ );  $^{29}\text{Si}$  NMR:  $\delta = -46.1$  ( $\text{CH}_2\text{CH}_2\text{CH}_2\text{Si}(\text{OEt})_3$ ); -22.4 ( $\text{Si}(\text{OSi}(\text{CH}_3)_3)_2(\text{CH}_3)$ ); 6.3 ( $\text{OSi}(\text{CH}_3)_3$ ); IR:  $\nu$  ( $\text{cm}^{-1}$ ) 2974, 2962, 2929, 1411, 1257, 1168, 1106, 1082, 959, 864, 843, 782, 756.; MS (EI):  $m/z = 411$  ( $M^+ - \text{CH}_3$ , 6); 353 ( $M^+ - (\text{CH}_3)_3\text{Si}$ , 15); 337 ( $M^+ - (\text{CH}_3)_3\text{SiO}$ , 9); 233 ( $[\text{SiCH}_2\text{CH}_2\text{CH}_2\text{Si}(\text{OEt})_3]^+$ , 7); 221 ( $M^+ - [\text{CH}_2\text{CH}_2\text{CH}_2\text{Si}(\text{OEt})_3]^+$ , 82); 163 ( $[\text{Si}(\text{OEt})_3]^+$ , 62); 73 ( $[(\text{CH}_3)_3\text{Si}]^+$ , 100).

### 5.3.3.3. Synthesis of 1,1,3,3-Tetramethyl-1((2-triethoxysilyl)ethyl)disiloxane

In a 100 mL round bottomed flask 1,1,3,3-tetramethyldisiloxane (10.72 g, 0.08 mol) was dissolved in dried pentane (30 mL, dried over anhydrous magnesium sulphate). After cooling to 0 °C, Karstedt's catalyst (~2 drops) was added to the solution and then vinyltriethoxysilane (3.8 g, 0.02 mol) was added dropwise over ½ h under a nitrogen atmosphere. After 30 min, the reaction was allowed to warm to room temperature and left overnight. The crude mixture was rotary evaporated to remove the solvent and the excess of reagent, then the product was collected through vacuum distillation at 75-76 °C/1 mm Hg (yield: 5.28 g, 81.5%).

GC-analysis indicated that the product was actually a mixture of two compounds (25% -  $R_t = 16.8$  min) and (75% -  $R_t = 17.448$  min). GC-MS indicated that the two compounds are isomers. From  $^1\text{H}$  NMR analysis, the two products were identified as the regioisomers **15** (75%) and **16** (25%). The distilled mixture was used directly in the subsequent reactions.



**Scheme 6: Hydrosilylation of vinyltriethoxysilane with 1, 1, 2, 2 tetramethyl-disiloxane**

## 15

$^1\text{H}$  NMR ( $\text{CDCl}_3$ ):  $\delta = 0.017$  (s, 6H,  $\text{Si}(\text{CH}_3)_2\text{CH}_2\text{CH}_2\text{Si}(\text{OEt})_3$ ); 0.129 (d, 6H,  $J = 2.8$  Hz,  $\text{H}(\text{CH}_3)_2\text{SiOSi}$ ); 0.528 (s, 4H,  $\text{Si}(\text{CH}_3)_2\text{CH}_2\text{CH}_2\text{Si}(\text{OEt})_3$ ); 1.202 (t, 9H,  $J = 7.0$  Hz,  $\text{O}(\text{CH}_3)_2\text{SiCH}_2\text{CH}_2\text{Si}(\text{OCH}_2\text{CH}_3)_3$ ); 3.794 (q, 6H,  $J = 7.0$  Hz,  $\text{SiCH}_2\text{CH}_2\text{Si}(\text{OCH}_2\text{CH}_3)_3$ ); 4.650 (m, 1H,  $H\text{-Si}$ ).  $^{13}\text{C}$  NMR ( $\text{CDCl}_3$ ):  $\delta = -0.7$  ( $\text{HSi}(\text{CH}_3)_2\text{OSi}$ ); 0.8  $\text{Si}(\text{CH}_3)_2\text{CH}_2\text{CH}_2\text{Si}(\text{OEt})_3$ ; 5.9  $\text{Si}(\text{CH}_3)_2\text{CH}_2\text{CH}_2\text{Si}(\text{OEt})_3$ ; 9.0  $\text{Si}(\text{CH}_3)_2\text{CH}_2\text{CH}_2\text{Si}(\text{OEt})_3$ ; 18.3 ( $\text{CH}_3\text{CH}_2\text{O}$ ); 58.4 ( $\text{CH}_3\text{CH}_2\text{O}$ ).  $^{29}\text{Si}$  NMR:  $\delta = -45.4$  ( $\text{SiCH}_2\text{CH}_2\text{Si}(\text{OEt})_3$ ); -7.1 ( $\text{HSi}(\text{CH}_3)_2\text{OSi}$ ); 10.1  $\text{Si}(\text{CH}_3)_2\text{CH}_2\text{CH}_2\text{Si}(\text{OEt})_3$ .

$\text{H}(\text{CH}_3)_2\text{SiOSi}(\text{CH}_3)_2\text{CH}(\text{CH}_3)\text{Si}(\text{OEt})_3$ .

## 16

$^1\text{H}$  NMR ( $\text{CDCl}_3$ ):  $\delta = 0.097$  (d, 6H,  $J = 1.9$  Hz,  $\text{H}(\text{CH}_3)_2\text{SiOSi}(\text{CH}_3)_2\text{CH}(\text{CH}_3)\text{Si}(\text{OEt})_3$ ); 0.154 (s, 6H,  $\text{OSi}(\text{CH}_3)_2\text{CH}(\text{CH}_3)\text{Si}(\text{OEt})_3$ ); 0.009-0.15 (m, 1H,  $\text{OSi}(\text{CH}_3)_2\text{CH}(\text{CH}_3)\text{Si}(\text{OEt})_3$ ); 1.047 (d, 3H,  $J = 7.5$  Hz,  $\text{OSi}(\text{CH}_3)_2\text{CH}(\text{CH}_3)\text{Si}(\text{OEt})_3$ ); 1.182 (t, 9H,  $J = 7.0$  Hz,  $\text{SiCH}(\text{CH}_3)\text{Si}(\text{OCH}_2\text{CH}_3)_3$ ); 3.787 (q, 6H,  $J = 7.0$  Hz,  $\text{SiCH}(\text{CH}_3)\text{Si}(\text{OCH}_2\text{CH}_3)_3$ );  $^{13}\text{C}$  NMR ( $\text{CDCl}_3$ ):  $\delta = -0.7$  ( $\text{HSi}(\text{CH}_3)_2\text{Si}$ ); -0.2 ( $\text{SiCH}(\text{CH}_3)\text{Si}$ ); 1.7 ( $\text{OSi}(\text{CH}_3)_2\text{CH}(\text{CH}_3)\text{Si}$ ); 7.6 ( $\text{SiCH}(\text{CH}_3)\text{Si}$ ); 18.3 ( $\text{CH}_3\text{CH}_2\text{O}$ ); 58.4 ( $\text{CH}_3\text{CH}_2\text{O}$ ).  $^{29}\text{Si}$  NMR:  $\delta = -46.4$  ( $\text{SiCH}_2\text{CH}_2\text{Si}(\text{OEt})_3$ ); -7.9 ( $\text{HSi}(\text{CH}_3)_2\text{OSi}$ ); 9.7 ( $\text{OSi}(\text{CH}_3)_2\text{CH}(\text{CH}_3)\text{Si}(\text{OEt})_3$ ); IR:  $\nu$  ( $\text{cm}^{-1}$ ) 2975, 2927, 2888, 2121, 1408, 1390, 1255, 1167, 1144, 1106, 1082, 958, 912, 840, 813, 785; MS (EI):  $m/z = 323$  ( $\text{M}^+ - 1$ , 10); 309 ( $\text{M}^+ - \text{CH}_3$ , 38); 279 ( $\text{M}^+ - \text{OCH}_2\text{CH}_3$ , 100); 249 ( $\text{M}^+ - \text{H}(\text{CH}_3)_2\text{SiO}$ , 48).

#### 5.3.3.4. Synthesis of Methyl(2-triethoxysilyl-ethyl)siloxane Homopolymer

In a 10 ml round bottomed flask, polymethylhydrosiloxane homopolymer (1.0 g, viscosity: 15-25 cSt., Mw ~ 1500-1900, calculated by  $^1\text{H}$  NMR to have ~28-29 Si-H bonds/molecule on average) was mixed with vinyltriethoxysilane (2.91g, 0.015 mol). After cooling to 0 °C, Karstedt's catalyst (one drop) dissolved in cyclohexane (1 ml) was added. The mixture was brought to room temperature after 10 min and stirred overnight under nitrogen at room temperature. The Pt catalyst was removed by adsorption on activated charcoal that was added to the solution of the product in dry hexane, followed by filtration through Celite.

$^1\text{H}$  NMR spectrum revealed that on average ~ 96% of the Si-H bonds had reacted. The spectrum also suggests a major product resulted from anti-Markovnikov addition (78%)

$^1\text{H}$  NMR ( $\text{CDCl}_3$ ):  $\delta = 0.060 - 0.128$  (m, calc. ~ 6-7H,  $\text{OSi}(\text{CH}_3)_2\text{CH}(\text{CH}_3)\text{Si}(\text{OEt})_3$ );  $0.060 - 0.128$  (s, ~105H,  $(\text{CH}_3)\text{Si}$ ,  $(\text{CH}_3)_3\text{Si}$ ),  $0.512$  (s, ~88H,  $\text{OSi}(\text{CH}_3)\text{CH}_2\text{CH}_2\text{Si}(\text{OEt})_3$ );  $1.04$  (d, calc.~18 - 24H,  $\text{OSi}(\text{CH}_3)_2\text{CH}(\text{CH}_3)\text{Si}(\text{OEt})_3$ );  $1.176$  (t, ~254H,  $J = 6.9$  Hz,  $\text{Si}(\text{OCH}_2\text{CH}_3)_3$ );  $3.747$  (q, ~169H,  $J = 6.9$  Hz,  $\text{Si}(\text{OCH}_2\text{CH}_3)_3$ );  $4.669$  (m, ~1H,  $H\text{-Si}$ ).

#### 5.3.3.5. Synthesis of Methyl(2-triethoxysilyl-ethyl)dimethylsiloxane

##### Copolymer (30-35%):

In a 25 ml round bottomed flask, 4.0 g of methylhydrogen,dimethylsiloxane copolymer (30-35% SiH, viscosity: 25-30 cSt., Mw ~ 1900-2000, calculated by  $^1\text{H}$  NMR to have ~8 Si-H bonds/molecule on average) was mixed with vinyltriethoxysilane (3.05 g, 0.016

mol). After cooling to 0 °C Karstedt's catalyst (one drop) was added. After 2 h, the mixture was brought to room temperature and left overnight under nitrogen. The Pt catalyst was removed by adsorption over activated charcoal that was added to the solution of the product in dry pentane, followed by filtration through Celite powder.

<sup>1</sup>H NMR spectrum revealed that on average ~7.5 of 8 of the Si-H bonds had reacted. The spectrum also revealed the major product resulted from anti-Markovnikov addition (80%).

<sup>1</sup>H NMR (CDCl<sub>3</sub>): δ = 0.044 - 0.112 (m, 1H, OSi(CH<sub>3</sub>)<sub>2</sub>CH(CH<sub>3</sub>)Si(OEt)<sub>3</sub>); 0.044 - 0.112 (s, ~150H, (CH<sub>3</sub>)Si, (CH<sub>3</sub>)<sub>2</sub>Si, (CH<sub>3</sub>)<sub>3</sub>Si), 0.518 (s, ~24H, OSi(CH<sub>3</sub>)CH<sub>2</sub>CH<sub>2</sub>Si(OEt)<sub>3</sub>); 1.190 (t, ~67H, *J* = 6.9 Hz, Si(OCH<sub>2</sub>CH<sub>3</sub>)<sub>3</sub>); 3.782 (q, ~45H, *J* = 6.9 Hz, Si(OCH<sub>2</sub>CH<sub>3</sub>)<sub>3</sub>); 4.669 (m, ~1H, *H*-Si).

### 5.3.3.6. Hydrosilylation of Squalene

#### 5.3.3.6.1. By HMe<sub>2</sub>SiOSiMe<sub>3</sub>

In a 50 ml round bottomed flask squalene (13.86 g, 0.00244 mol) was mixed pentamethyldisiloxane (5.0 g, .00244 mol) and Karstedt's catalyst (2 drops); the oil bath temperature was set to 75 °C. The reaction mixture was stirred with heating under nitrogen for 4 h, after which <sup>1</sup>H NMR indicated complete consumption of Si-H and the appearance of a new multiplet CH<sub>2</sub> peak (δ = 0.86 ppm). The product was transferred to a 100 ml round bottomed flask and dissolved in dried pentane (~ 25 ml), following which activated charcoal (~3 g) was added and the mixture was stirred for 3 h to adsorb the Pt

catalyst. After the solids were removed by filtration over Celite, the solution was rotary evaporated to remove pentane and the oily product was collected.

The  $^1\text{H}$  NMR spectrum of the product indicated that, on average, the reaction product comprised a 1:1-adduct of the two starting materials. The integration of the  $H-C=C$  peak of squalene at  $\delta=5.08$  ppm had dropped in intensity from 6H to  $\sim 5\text{H}$ . Moreover, a new  $\text{CH}_2$  peak at  $\delta = 0.86$  ppm appeared as a result of the hydrosilylation of the double bond. The  $^1\text{H}$  NMR also revealed the presence of the methylsiloxy groups. Since all 6 double bonds are, in principle, capable of reacting with silane compounds, several structural and regioisomers are possible constituents of a 1:1-adduct. Electrospray ionization mass spectrometry revealed the formation of mono-, di- and tri-hydrosilylated squalene as well as unreacted squalene.

For 1/3 and 1/6 ratios of squalene/pentamethyldisiloxane: squalene was mixed with the appropriate amount of silane and the same procedure noted above was followed. According to the  $^1\text{H}$  NMR spectrum of the product, an average of 3  $\text{C}=\text{C}$  bonds reacted with the silane in the case of 1:3 ratio. With the 1/6 ratio, the reaction did not go to completion, but indicated over 5.5  $\text{C}=\text{C}$  bonds had reacted (92% conversion) on average.

IR:  $\nu$  ( $\text{cm}^{-1}$ ) 2969, 2925, 1660, 1445, 1386, 1255, 1139, 1106, 1082, 960, 840, 789; MS-ESI: ( $\text{AgNO}_3$   $1 \times 10^{-5}$  M in  $\text{MeCN}/\text{Cl}_2\text{CH}_2$  (2:1)  $m/z = 963.7$  ( $\text{M}^+[\text{854 Squalene:}3\text{xHSiMe}_2\text{OSiMe}_3] + \text{Ag}^+[\text{109.5}]$ ); 961.7 ( $\text{M}^+[\text{854}] + \text{Ag}^+[\text{107.5}]$ ); 815.6 ( $\text{M}^+[\text{706 Squalene:}2\text{xHSiMe}_2\text{OSiMe}_3] + \text{Ag}^+[\text{109.5}]$ ); 813.5 ( $\text{M}^+[\text{706}] + \text{Ag}^+[\text{107.5}]$ ); 667.4 ( $\text{M}^+[\text{558 Squalene: HSiMe}_2\text{OSiMe}_3] + \text{Ag}^+[\text{109.5}]$ ); 665.4 ( $\text{M}^+[\text{558}] + \text{Ag}^+[\text{107.5}]$ ); 519.4 ( $\text{M}^+[\text{410 squalene}] + \text{Ag}^+[\text{109.5}]$ ); 517 ( $\text{M}^+[\text{410}] + \text{Ag}^+[\text{107.5}]$ ).

### 5.3.3.6.2. By $\text{HSi(OEt)}_3$

In 10 ml round bottomed flask squalene (3.0 g, 0.00732 mol) was mixed with triethoxysilane (1.2 g, 0.0073 mol) and Karstedt's catalyst (1 drop) was added; the oil bath temperature was set to 70 °C. The reaction mixture was stirred with heating under nitrogen for 24 h, after which  $^1\text{H}$  NMR indicated almost complete consumption of Si-H without the appearance of the expected multiplet  $\text{CH}_2$  peak as found in previous experiments ( $\delta = 0.86$  ppm). The reaction was repeated with higher amounts of catalyst without success.

### 5.3.3.6.3. By $\text{HMe}_2\text{SiO(CH}_2)_3\text{Si(OEt)}_3$ 17

To a 5 ml round bottomed flask was added squalene (2.05g, 0.005 mol) and **15/16** (75/25 mixture, 1.62 g, 0.005 mol). Karstedt's catalyst (one drop) was added and the oil bath temperature was set to 85 °C. The reaction mixture was stirred with heating under nitrogen for 4 h, after which  $^1\text{H}$  NMR indicated a complete consumption of Si-H and the appearance of a new  $\text{CH}_2$  peak ( $\delta = 0.85$  ppm). The product was dissolved in dried pentane (~ 10 ml), following which activated charcoal (~1 g) was added and the mixture was stirred for 2 h to adsorb the Pt catalyst. After the solids were removed by filtration over Celite, the solution was rotary evaporated to remove pentane and the oily product was collected (yield: 3.1g, 85%).

The  $^1\text{H}$  NMR spectrum of the product indicated that, on average, the reaction product comprised a 1:1-adduct of the two starting materials. The integration of the  $\text{H-C=C}$  peak of squalene at  $\delta=5.08$  ppm has dropped in intensity from ~ 6H to ~ 4.8H. Also, a new  $\text{CH}_2$  peak at  $\delta = 0.85$  ppm appeared as a consequence of the hydrosilylation of the double

bond. Similarly, the  $^1\text{H}$  NMR spectrum revealed the presence of the triethoxysilyl group. As all 6 double bonds are, in principle, capable of reacting with silane compounds, several structural and regioisomers are possible constituents of a 1:1-adduct.

IR:  $\nu$  ( $\text{cm}^{-1}$ ) 2969, 2925, 1660(weak), 1445, 1386, 1255, 1167, 1139, 1106, 1082, 960, 840, 789; UV:  $\lambda_{\text{max}1}$  = 206,  $\epsilon$  = 31988  $\text{mol}^{-1} \text{cm}^{-1}$  and  $\lambda_{\text{max}2}$  = 240,  $\epsilon$  = 10915  $\text{mol}^{-1} \text{cm}^{-1}$   
MS-ESI: ( $\text{AgNO}_3$  in MeCN  $5 \times 10^{-4}$  M)  $m/z$  = 841.5 ( $\text{M}^+ - 15[734] + \text{Ag}^+[107.5]$ ); 843.5 ( $\text{M}^+ - 15[734] + \text{Ag}^+[109.5]$ ); 517.5 (squalene [410] +  $\text{Ag}^+[107.5]$ ); 519.5 (squalene [410] +  $\text{Ag}^+[109.5]$ ).

#### 5.3.3.6.4. Oxidation Experiments: Reactions on 18-grafted quartz slides.

Compound **18** was grafted to quartz slides following the procedure noted below. The contact angle shifted from  $2^\circ$  for unmodified quartz to  $\sim 99^\circ$ ; the UV absorbance at 254 nm had dropped from 90% to 63% indicating successful grafting of squalene to the surface.

##### 5.3.3.6.4.1. Ozonization

The grafted slide was put in the vessel used for introduction of the coupling agent and ozone gas was applied through a glass hollow tube probed to the lower portion of the tube. The reaction was left for 3 h. UV measurements showed an increase in the absorbance at 254 nm from 63% to 88% (Figure 32).

##### 5.3.3.6.4.2. Reduction and coupling with DNPH:

In the same reaction vessel, glacial acetic acid (30 ml) was added to dichloromethane (30 ml) and zinc metal (1.5 g, 22.9 mmol) was added and the mixture was stirred for 5

min before the ozonide-containing slide was added to the tube. The reaction was left at room temperature for 15 min before the slide was removed, rinsed thoroughly with water and acetone then let aside to dry. The ozonized, then reduced slide was directly transferred to another tube containing dinitrophenylhydrazine DNPH solution (50 ml ethanol, 11 ml water, 5 ml conc. sulfuric acid and 1.4 g DNPH). The reaction was left for 30 min before the slide was removed, rinsed with ethanol, acetone and then Soxhlet extracted with acetone for 2 days. The UV spectrum showed a decrease of transmittance at 365 nm (56%), the typical DNP-hydrazone absorbance (Figure 33), which is similar to the absorbance profile of DNPH.

#### **5.3.4. Modification of the slides – Application of the coupling agent.**

The quartz slides were thoroughly cleaned before use. The slides were initially soaked in a 5M hydrochloric acid solution for at least 2 days then cleaned thoroughly with distilled water and acetone, followed by a 20 min cleaning period using an argon plasma, just before the launch of the experiment. The slides were then removed from the plasma cleaning system, contact angles were recorded, then slides were removed to a clean glass container and transferred to an oven where they were heated for 30 minutes at 110 °C, before being transferred to the modification apparatus. Contact angles measured for the clean slides were in the range of 2-3°.

The modification apparatus was built of Pyrex tube that was specially designed to fit the slide in it, with magnetic stirrer bar beneath to permit stirring during the modification process. The tube, which contains the quartz slide, was attached to a condenser and a solution of the silane coupling agent in acetone (~ 4 % in weight) was refluxed at 56 °C

for 24 h. The slide was then removed, rinsed with acetone, and put into oven at 110 °C for 3 h before it was subjected to Soxhlet extraction using cyclohexane.

A variety of commercially available and synthesized silane coupling agents were grafted to quartz and/or glass surfaces (**Table 4**). Further details are provided in the accompanying papers.<sup>6,7</sup>

**Table 4 Commercial and synthesized silane coupling agents used in quartz and glass surface modification.**

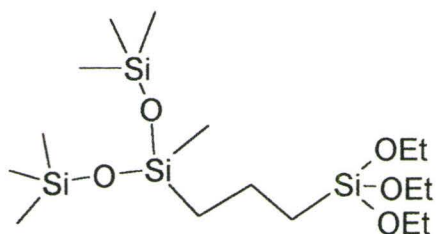
Exp. #	Modifying agent	Type <sup>a</sup>	Contact Angle	
			Avg.	St. dev.
1	Bis(trimethylsiloxy)-methyl-(3-triethoxysilyl Propyl)silane	Q	84.8	3.82
		Q	85.9	4.56
2	2-(phenyldimethylsilyl)ethyltriethoxysilane	Q	74	2.2
		Q	72.7	1.8
3	5.3.4.1. hydrosilylated squalene	Q	99.2	0.63
		Q	98.7	1.06
4	methyl(2-triethoxysilyl-ethyl)dimethyl siloxane copolymer (30-35%)	Q	105.2	1.3
		Q	106	1.07
5	methyl(2-triethoxysilyl-ethyl)siloxane homopolymer	Q	78.1	2.09
		Q	78.4	1.67

6	1) VTES	Q	75	3.07
		Q	75.8	2.31
	2) PDMS-2H (2-3 cSt.)	Q	95.8	2.38
		Q	96.3	3.37
7	1) VTES	Q	76	0.93
		Q	77.3	1.91
	2) PDMS-2H (100 cSt.)	Q	97.2	3.38
		Q	103.3	1.58
9	1) VTES	Q	79.9	1.97
		Q	75.8	2.62
	2) PDMS-2H (500 cSt.)	Q	97.1	0.88
		Q	95.8	1.4

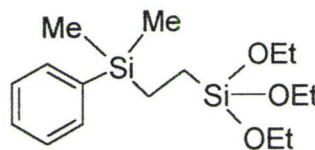
<sup>a</sup> Q – quartz.

#### 5.4. Results

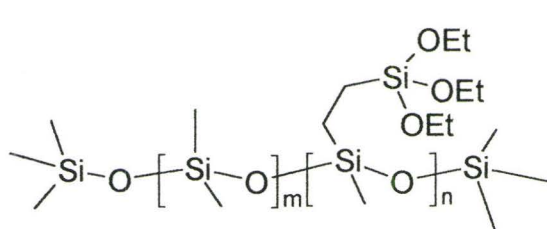
The fouling studies described elsewhere in this thesis required the preparation of a series of hydrophobic coupling agents: many possible interesting compounds were simply not commercially available. For most of these compounds, the syntheses involved the straightforward hydrosilylation of either allyl- or vinyl-triethoxysilane with an appropriate hydrosilane. The compounds prepared, with yields, are given in **Scheme 7**.



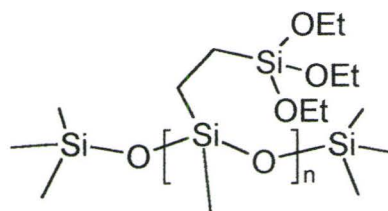
bis(trimethylsiloxy)-methyl-(3-triethoxysilyl propyl)silane ( 68%)



2-(phenyldimethylsilyl)ethyl triethoxysilane



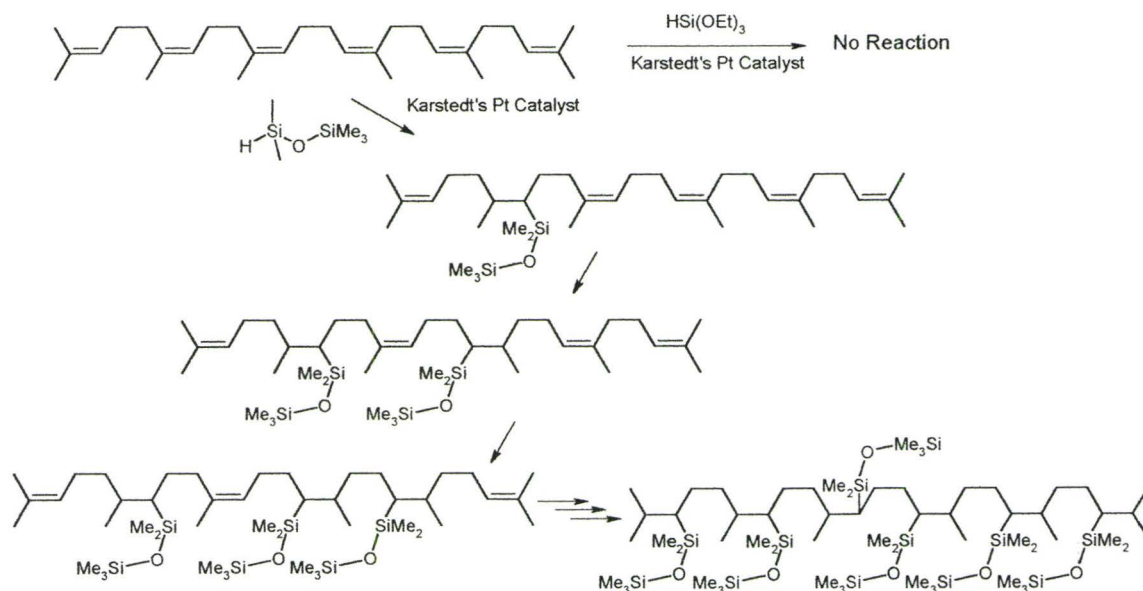
methyl(2-triethoxysilyl-ethyl)dimethyl siloxane copolymer (30-35%), (80%)



methyl(2-triethoxysilyl-ethyl) siloxane homopolymer (78%)

### Scheme 7: Synthesized silane coupling agents.

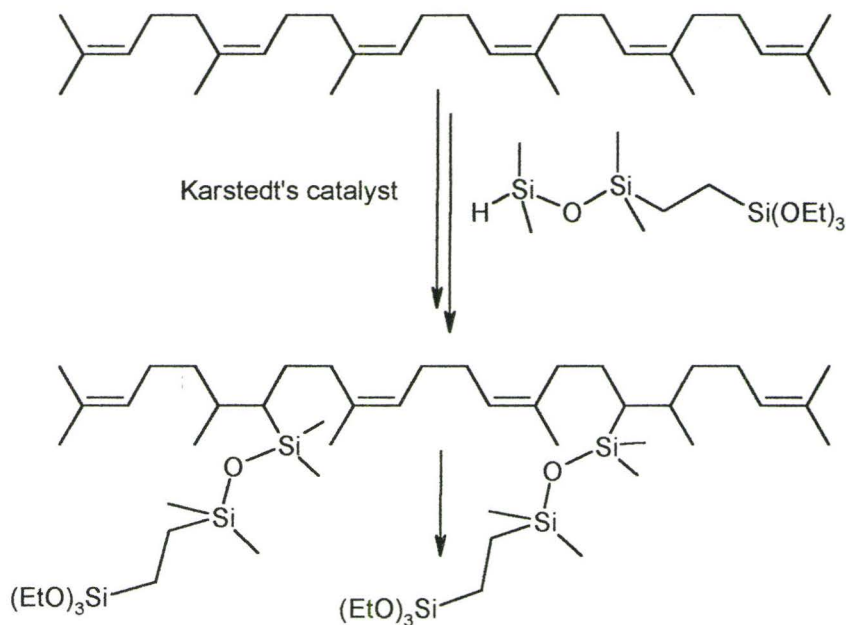
Much more work was involved in the preparation of coupling agents based on squalene: these compounds should be sensitive to oxidation. Preliminary studies with the model compound,  $\text{HSiMe}_2\text{OSiMe}_3$  showed that on average, from one up to all six alkenes on the squalene could be hydrosilylated (Scheme 8). Not all the yields for these conversions were determined. These experiments simply proved that the hydrosilylation of internal bonds could be performed (see discussion section).



**Scheme 8: Hydrosilylation of squalene using pentamethyldisiloxane.**

Pentamethyldisiloxane does not, of course, possess the functional groups necessary for binding to a glass/quartz surface. Initial attempts to hydrosilylate squalene with  $\text{HSi}(\text{OEt})_3$  were completely unsuccessful (Scheme 8). There was no evidence for formation of any squalene-derived products; starting materials were recovered. Therefore, a new coupling agent combining the characteristics of both triethoxysilane and pentamethyldisiloxane was prepared. In addition to the normally favoured addition of the silyl group to the terminal position **15**, significant quantities (*ca.* 25%) of the internal regioisomer **16** were obtained (Scheme 6). The mixture of isomers was used to hydrosilylate squalene leading, on average, to the incorporation of one or two silyl groups into the chain **18** (Scheme 9, only one isomer shown). Attempts to incorporate more groups by pushing the reaction thermally were unsuccessful. The  $^1\text{H}$  NMR data is consistent with hydrosilylation with the regiochemistry shown. Doublets of integration

3H accompanied the hydrosilylation ( $\text{RH}(\text{R}'_3\text{Si})\text{C}-\text{CHMe}$ ), rather than the alternative methyl singlets, which would be expected in the other regioisomer ( $\text{RH}_2\text{C}-\text{C}(\text{SiR}'_3)\text{Me}$ ).

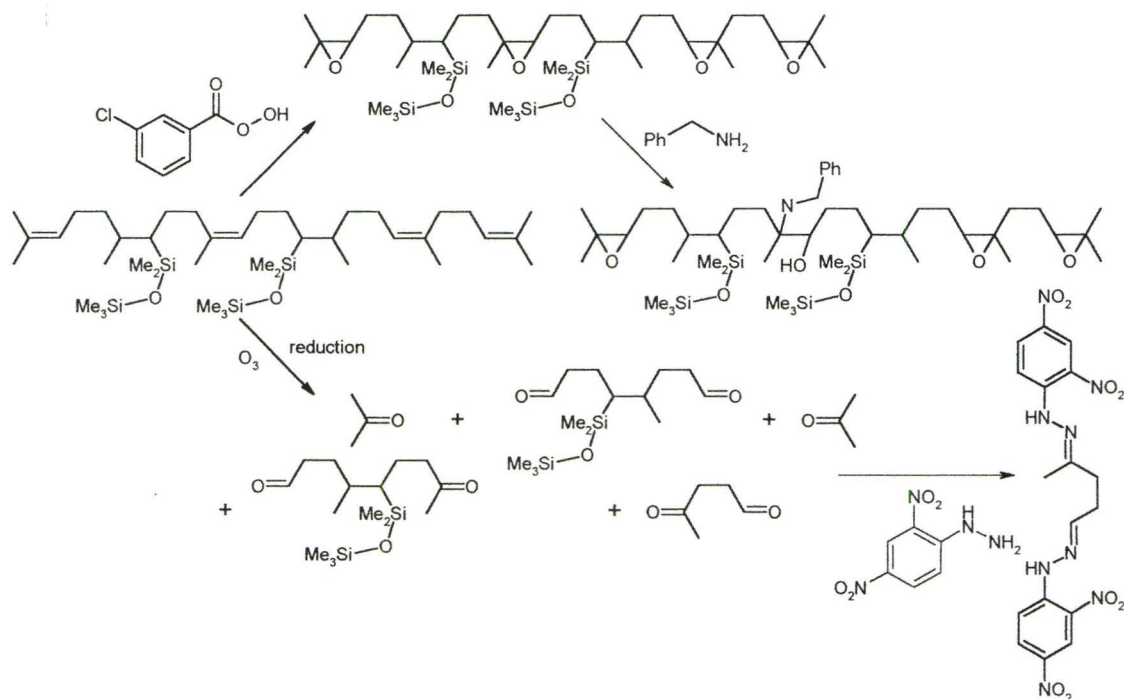


**Scheme 9: Hydrosilylation of squalene using 1,1,3,3-Tetramethyl-1((2-triethoxysilyl) ethyl) disiloxane.**

Prior to grafting this new coupling agent **18** to glass or quartz, its oxidative sensitivity had to be established. Thus, both squalene and **18** were subjected to oxidation by peracetic or *m*-chloroperbenzoic acid and ozone, respectively. In both cases, oxidation efficiently occurred. Formation of the ozonide from either squalene or **18** was highly exothermic (the introduction of  $\text{O}_3$  had to be carefully regulated to suppress overheating of the reaction flask).

Once the compounds had been oxidized, proof of their reactivity to nitrogen nucleophiles was necessary. The reaction between fluorescent amines and the polyepoxide remains for

future work. However, the ozonides underwent workup with zinc and acetic acid, to produce mixtures of aldehydes and ketones. These could be detected directly by NMR and also by formation of dinitrophenylhydrazones. To date, we have used these data to qualitatively prove the formation of carbonyls from the alkenes (Scheme 10). In future work, we shall quantify the product mixture and further assess the structures of the products that, by inference, will allow the determination of the hydrosilylation regiochemistry.



**Scheme 10: Oxidation for introducing new functionality to squalene molecule.**

The formation of the hydrazone can be quantified by UV spectroscopy. Comparison of the UV spectra between dinitrophenylhydrazine and the resulting hydrazones from the

squalene reduction process just described show the characteristic red shift, indicative of formation of the hydrazone (Figure 31).

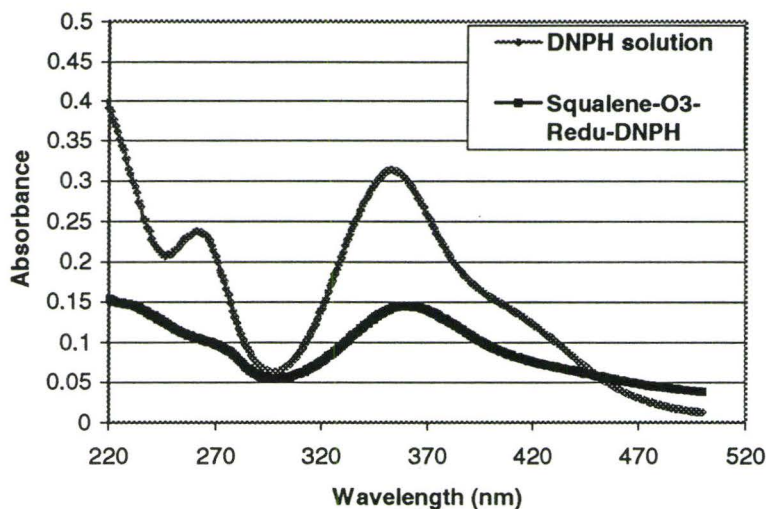


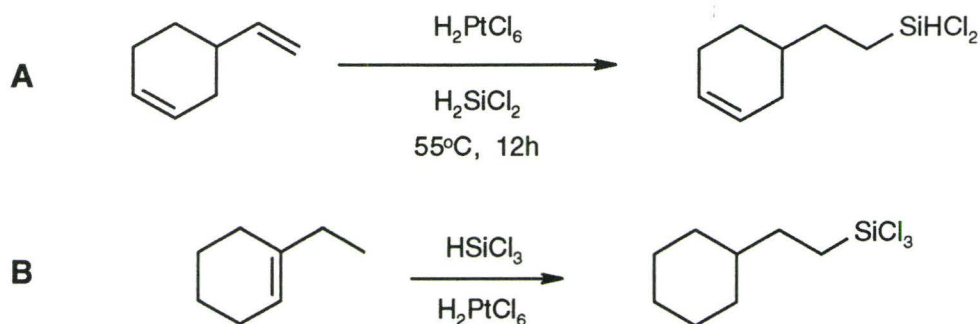
**Figure 31: UV spectra of dinitrophenylhydrazine, and squalene after ozonization/reduction by Zn/HOAc and dinitrophenylhydrazine.**

Having demonstrated that the oxidation reactions are not suppressed by the presence of the silyl groups, **18** was grafted to quartz by methods described elsewhere (Scheme 11).<sup>7</sup> The quartz slides were submitted to the same series of ozonization and condensation reactions that had been done in solution. While no quantitation has yet been done, qualitatively the reaction occurred efficiently as could be judged by the changes in UV transmittance through the quartz slide (Figure 32). Our future objectives include better quantitation of the residual aldehyde/ketone groups on the surface and to use these functional groups to graft other materials to the surface.



### 5.5. Discussion

Hydrosilylations normally occur, with platinum catalysts at least, at the least hindered site alkene. This preference was observed, essentially exclusively, for the coupling agents shown in **Scheme 7**. In practical terms, it is normally very difficult to hydrosilylate internal double bonds (Scheme 12A). The mechanism of the reaction is such that double bond migration can occur along the alkene chain, moving the  $\pi$  bond to the terminus, at which point hydrosilylation occurs (Scheme 12B).<sup>8</sup>



**Scheme 12: Internal bond in hydrosilylation.**

Thus, the efficient hydrosilylation of the internal bonds of squalene was unexpected: it should be noted that fairly vigorous conditions were used for the hydrosilylation (the temperature has to be increased from *ca.* 0 °C to 75 °C). It is not clear which of the double bonds reacted most efficiently. In addition to hydrosilylation, it is apparent that double bond migration was simultaneously occurring. The UV of the hydrosilylated mixture showed a new, red-shifted absorbance at 240 nm consistent with a diene (Figure 33). Thus, in addition to hydrosilylation of the compound, dienyl units are formed (Scheme 13).

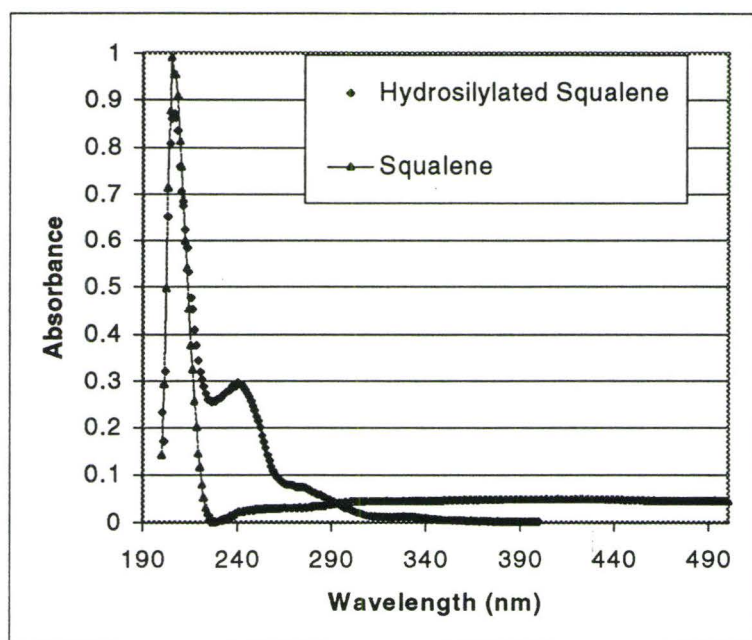
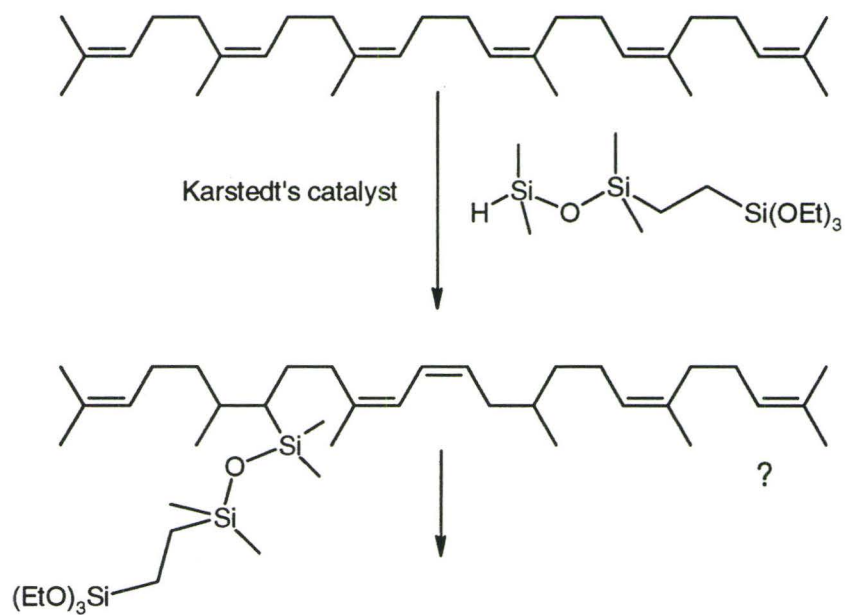


**Figure 33:** UV spectra of A: squalene and B: 18 showing presence of diene fragments in the latter material.



**Scheme 13:** Diene formation in squalene hydrosilylation reaction.

The alkoxy silane groups introduced to **18** remained surface active. It was possible using standard conditions to graft the coupling agent to the surface. Such compounds could not be removed by extraction, and their presence on the surface was confirmed both by contact angle and by UV spectroscopy, as noted in Figure 32. The residual double bonds, either in solution or once bound to the surface, behaved exactly as expected for such compounds. Facile conversion by peracids and  $O_3$ , respectively, to the oligoepoxide or oligoozonide occurred as shown by NMR. In the case of the ozonide, further conversion to carbonyl groups and then hydrazones occurred unexceptionally.

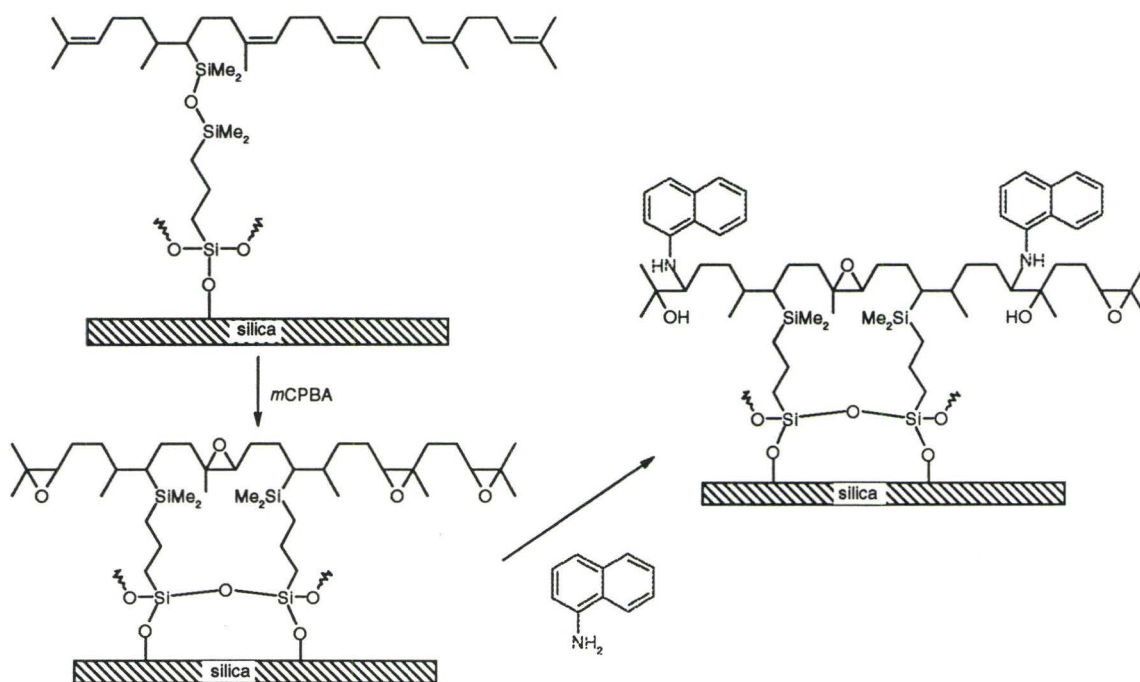
It should be noted that liquid and gaseous oxidation reagents were used in these studies; solid reagents could also be utilized. This flexibility in the phase of oxidizing agent that are acceptable to the reaction could provide advantageous. For instance, composites reinforced by silica stabilized by the squalene-derived coupling agent could be decomposed by ozonization:  $O_3$  can permeate through solid organic matrices. Such possibilities need to be examined in the future.

These experiments demonstrate that oxygen-sensitive moieties can be grafted to siliceous surfaces. They further show that the hydrophobic nature can be modified both to increase surface energy and to provide new synthetic opportunities via the introduction of new groups by reaction with epoxides, carbonyl groups or carboxylic acids. Such conversions will form part of our future endeavours in this research.

## 5.6. Future Work

One of the foci of this thesis was the possible utility of modified surfaces to mitigate fouling in wastewater reactors. As shown in Chapter 3, like other hydrophobic surfaces, the squalene-derived compound did not improve fouling performance, but aided in cleaning. The issue of the photobehaviour of the coupling agent was not addressed. As noted, dienyl groups are present in the coupling agent. Further, simple alkenes are known to undergo UV-induced photodimerization reactions. However, the ability to crosslink/dimerize surface alkenyl and dienyl moieties by exposure to intense UV-irradiation will form a future experimental direction for this research.

Although ozonides were shown to be susceptible to conversion to carbonyl groups, which could then be functionalized, further synthetic conversions were not attempted with the epoxides. Future research will remedy this by first demonstrating that ring-opening polymerization and ring-opening functionalization by other groups will occur with epoxy-squalene derivatives (Scheme 14). These modifications will first be attempted and quantified with small molecules and then, for both ozonide and epoxide, with polymeric systems.



**Scheme 14: Amine reaction with an epoxidized squalene-modified surface.**

### 5.7. Conclusions

Silane coupling agents with many different structures are readily prepared by the hydrosilylation of vinyl-substituted organic compounds. Squalene, a natural hexaene, can be converted to a coupling agent by hydrosilylating the internal double bonds. Accompanying this addition, is the internal rearrangement of double bonds to form dienes. Once grafted to the surface, the residual double bonds can be converted by oxidation into carbonyl groups, carboxylic acids or epoxides. This not only changes the surface activity of the coating, but provides handles for further synthetic modification.

## 5.8. References

- <sup>1</sup> Brook, M. A.; Ragheb, A., First presented at the Conference of the Adhesion Society, Williamsburg, Virginia, Feb. 2001, Abstract 373.
- <sup>2</sup> Plueddemann, E. P., *Silane Coupling Agents*, Plenum Press: New York, Chap. 1, 2 (1991).
- <sup>3</sup> Plueddemann, E. P., *Silane Coupling Agents*, Plenum Press: New York, Chap. 6, p. 153 (1991).
- <sup>4</sup> Puskas, J. E., Pattern, W., Wetmore, P. M., and Krukonis, V. *Polym. Mater. Sci. Eng.* 80, 429 (1999); Puskas, J. E., Pattern, W., Wetmore, P. M., and Krukonis, V. *Rubber Chem. Technol.* 72, 559 (1999); Puskas, J. E., Brister, L. B., Michel, A. J., Lanzendorfer, M. G., Jamieson, D., and Pattern, W. G. *Polym. Sci., Part A: Polym. Chem.* 38, 444 (2000).
- <sup>5</sup> Herman, S., *US patent* 5,093,326 (1992).
- <sup>6</sup> Brook, M. A., Ketelson, H. A. M., and Ragheb, A. The Role of UV Light in the Fouling of Quartz Sleeves Used in Water Disinfection, *Biofouling*, submitted.
- <sup>7</sup> Brook, M. A., Ketelson, H. A. M., and Ragheb, A. Role of Hydrophobic Coatings on Quartz Sleeves in the Mitigation of Fouling by Wastewater Streams, *Biofouling*, submitted.
- <sup>8</sup> Brook, M. A. *Silicon in Organic, Organometallic, and Polymer Chemistry*, Wiley: New York, Chap. 12.8, 401-413 (2000).

## **6. Anticipated publication and co-authors**

### **Chapter 2:**

#### **The Role of UV Light in the Fouling of Quartz Sleeves Used in Water Disinfection**

Michael A. Brook,<sup>\*</sup> Janinne Crowley, Howard A. M. Ketelson<sup>#</sup> and Amro M. Ragheb

<sup>\*</sup>Department of Chemistry, McMaster University, 1280 Main St. W., Hamilton, ON  
Canada L8S 4M1

<sup>#</sup> Trojan Technologies 3020 Gore Rd., London, Ontario Canada N5V 4T7.

To be submitted to *Biofouling*.

### **Chapter 3:**

#### **The Role of Hydrophobic Coatings on Quartz Sleeves in the Mitigation of Fouling by Wastewater Streams**

Michael A. Brook<sup>\*</sup> Janinne Crowley, Howard A. M. Ketelson<sup>#</sup> and Amro M. Ragheb

<sup>\*</sup>Department of Chemistry, McMaster University, 1280 Main St. W., Hamilton, ON  
Canada L8S 4M1

<sup>#</sup> Trojan Technologies 3020 Gore Rd., London, Ontario Canada N5V 4T7.

To be submitted to *Biofouling*.

**Appendix 1:****Oxidizable Coupling Agents: Introduction of Surface Functionality**

Michael A. Brook\* and Amro M. Ragheb

\*Department of Chemistry, McMaster University, 1280 Main St. W., Hamilton, ON

Canada L8S 4M1

**Roles of Co-authors**

Howard Ketelson (Trojan Technologies, current address: Alcon Laboratories, 6201 South Freeway, R8-7 Mailcode, Fort Worth, Texas 76134, USA) was our contact at Trojan Technologies, the industrial partner for this research. He participated in discussions on the progress and direction of the project.

Janinne Crowley was a summer student May-August 2000. Under my supervision, she performed fouling experiments in the reactor including preparing fouling solutions, fouling the slides and measuring loss of transmittance of the slides. Her data is incorporated, in part, in Chap. 2 and 3.